



universität  
wien

# MASTERARBEIT

„Dissecting the role of fibroblastic reticular cells in  
the tumour draining lymph node and their  
contribution to tumour progression“

verfasst von

Lisa Haas, BSc

angestrebter akademischer Grad

Master of Science (MSc)

Wien, 2015

Studienkennzahl lt. Studienblatt:

A 066 834

Studienrichtung lt. Studienblatt:

Masterstudium Molekulare Biologie

Betreut von:

Univ.-Prof. Mag. Dr. Pavel Kovarik





## Acknowledgments

I would like to use this opportunity to thank everyone who supported me throughout this master thesis. First and foremost I would like to thank Dr. Pavel Kovarik for being a helpful supervisor, for being always contactable and for supporting me with answers to my questions.

Furthermore I would like to dearly thank all the people in my lab, for providing such a productive and friendly environment and for making work in the lab a pleasure. I would like to express my biggest thanks to Jacqui, for offering me the chance to work and learn in her lab and get in touch with a research field that has absolutely thrilled me. Without her this entire work would have never been possible, as she was always a big help and her door was always open for me. She is an exemplary PI and I can't be grateful enough for all the things I was able to learn from her.

I also want to thank Angi for being a great supervisor and always so helpful and supportive. She made it a pleasure for me to be part of her project and I will truly miss this time.

Furthermore I need to thank Jen, Matt and most of all Luisa for their everlasting patience and support in the lab, for all their great little tips and tricks and for always cheering me up.

Working together with all of them was a great experience for me and I will always be happy to recall it.

My biggest thanks goes to my parents, who made all this possible for me. Without them I would never have been able to finish my studies and achieve my goal and I am deeply grateful for that. But I do not only need to thank them for enabling me to study, but also for being always at the end of the phone and backing me up in times of need. They have always been my greatest help.

Last but not least I would like to thank David for being part of this adventure. He was always an amazing support, my biggest motivator and there were days where I would have gone crazy without him.

# Table of contents

<b>Acknowledgments.....</b>	<b>3</b>
<b>Abstract.....</b>	<b>7</b>
<b>Kurzfassung.....</b>	<b>9</b>
<b>1. Introduction.....</b>	<b>11</b>
1.1 The lymphatic system.....	12
1.2 Lymph node architecture and function .....	13
1.3 Stromal cells residing in the lymph nodes.....	15
1.4 Fibroblastic reticular cells .....	16
1.5 Lymphatics in cancer .....	20
1.6 Tumour draining lymph nodes.....	21
1.7 Podoplanin .....	23
1.8 Interleukin-7.....	25
<b>2. Aims.....</b>	<b>26</b>
<b>3. Results .....</b>	<b>28</b>
3.1 Isolated C57BL/6 p53 <sup>ER/ER</sup> FRCs closely resemble primary cells.....	28
3.2 Tumour conditioned media is capable of inducing gene expression changes in FRCs.....	30
3.3 Treatment with TCM changes protein levels of PDPN and IL-7.....	31
3.4 Treatment with TCM does not induce morphologic or proliferative changes in FRCs.....	32
3.5 Migration potential is not changed upon treatment with TCM .....	34
3.6 TCM treatment induces an “activated state” in FRCs.....	35
3.7 TCM treatment increases Collagen formation by FRCs .....	38
3.8 TCM treatment increases permeability in FRCs.....	40
3.9 TCM treatment impacts mitochondrial dynamics and resistance to oxidative stress.....	43
3.10 FRCs treated with TCM are not significantly diminished in their potential to support immune cells.....	48
3.11 FRCs take up exosomes secreted by B16 F10 melanoma cells.....	49
3.12 Exosomes do not induce changes in PDPN and IL-7 mRNA levels .....	52
3.13 Cytokine expression profiles of TCM and tumour lysates are highly different.....	53
<b>4. Discussion.....</b>	<b>56</b>
4.1 FRCs pretreated with TCM display an activated phenotype .....	57
4.2 Permeability of FRCs increases upon TCM treatment.....	60

4.3 TCM treatment reduces IL-7 secretion by FRCs .....	61
4.4 Model advantages and limitations .....	62
4.5 Conclusions and future directions .....	65
<b>5. Material and Methods.....</b>	<b>67</b>
5.1 Cell culture.....	67
5.1.1 Melanoma cell lines.....	67
5.1.2 Fibroblastic reticular cells .....	67
5.1.3 Isolation and culture of mouse derived lymph node stromal cells .....	67
5.1.4 Isolation of mouse derived splenocytes .....	68
5.1.5 Cell passage.....	68
5.1.6 Cryopreservation.....	68
5.1.7 Tumour conditioned medium (TCM) and control medium (CON) production.....	69
5.1.8 3D cultures of FRCs.....	69
5.1.9 Transfection.....	69
5.2 RNA Work.....	70
5.2.1 RNA isolation.....	70
5.2.2 cDNA synthesis .....	70
5.2.3 RT-qPCR.....	70
5.3 DNA work.....	71
5.3.1 Polymerase chain reaction (PCR) .....	71
5.3.2 Agarose gel electrophoresis.....	71
5.3.3 PCR purification.....	72
5.3.4 Restriction digest.....	72
5.3.5 Gel extraction.....	72
5.3.6 Ligation .....	72
5.3.7 Transformation into chemical competent bacteria.....	72
5.3.8 Plasmid Preparations.....	73
5.4 Protein work.....	73
5.4.1 Fluorescent immunocytochemistry (Fluorescent- ICC) .....	73
5.4.2 Flow cytometry analysis.....	74
5.4.3 AnnexinV staining .....	74
5.4.4 Mitochondrial Flow Cytometry staining .....	74
5.4.5 Sodium dodecyl sulphate polyacrylamide gel electrophoresis (SDS- PAGE) and Western Blot .....	75
5.4.6 Enzyme-linked-immunosorbent assay (ELISA).....	76

5.4.7 Cytokine Array.....	76
5.5 Exosome purification.....	76
5.6 Functional assays .....	77
5.6.1 Cell titre blue proliferation assay.....	77
5.6.2 Permeability assay.....	77
5.6.3 Adhesion assay .....	78
5.6.4 Scratch assay.....	78
5.6.5 Splenocyte survival assay .....	78
5.6.6 Contractility assay .....	78
5.6.7 Oxidative stress assay .....	79
5.7 Statistics .....	79
5.8 Mice .....	79
<b>6. References .....</b>	<b>80</b>
<b>7. Abbreviations.....</b>	<b>95</b>
<b>8. Appendix.....</b>	<b>97</b>
8.1 Primer sequences.....	97
8.2 Antibodies.....	97
8.3 TaqMan Assays.....	98
8.4 Plasmid Maps.....	99
8.5 Cytokine array.....	100
<b>9. Curriculum Vitae .....</b>	<b>102</b>

## Abstract

Metastasis through the lymphatic system is the major route of dissemination for many cancer types, yet little is known about the underlying mechanisms. However, recent studies indicated drastic changes in the lymph nodes that drain tumours and reported that under influence of these tumours the nodes become partially immune suppressed. Developing a therapeutic strategy to reverse these suppressive mechanisms and interrupt the chain of cancer progression is a major goal of the field.

Although the knowledge about immune cell populations in the tumour draining node is increasing, changes occurring in non-haematopoietic, stromal cell populations are less understood. Here we investigate the remodelling occurring in fibroblastic reticular cells, lymph node myofibroblasts that are critical to the architecture and function of the node, following drainage using a simple *in vitro* model.

We provide evidence that culturing FRCs in tumour cell conditioned medium alters their gene expression programme and induces phenotypical changes. We report an upregulation of Podoplanin, a transmembrane protein influencing contractility and interactions between distinct immune cells, and downregulation of Interleukin-7, a potent immunomodulatory cytokine required for survival of T-cells, B-cells and dendritic cells.

The work performed here shows that upon culture in tumour conditioned medium FRCs gain an activated phenotype, reflected by increased contraction of collagen gels, faster adhesion and higher expression levels of extracellular matrix molecules. Furthermore we show an increase in permeability of FRCs, as junctional molecules are degraded. Tumour conditioned medium treatment moreover increase mitochondrial mass and activity and enhances the resistance to reactive oxygen species. Taken together we see these as signs for occurrence of a process similar to fibroblast activation in cancer, where the draining tumour prepares the lymph node prior to arrival of cancer cells. FRCs thereby obtain an activated phenotype and express higher levels of Collagen I, which might allow attachment of cancer cells and formation of nodal metastasis. The increase in permeability and the downregulation of cytokines regulating immune cell

survival might be additional mechanisms to impair function of the node and provide an advantage for the tumour. This illustrates how the tumour might influence stromal cell populations in the node to “prepare the soil” prior to arrival of the first cancer cells.

## Kurzfassung

Obwohl viele Krebsarten durch das lymphatische System metastasieren, ist wenig über die zugrunde liegenden Mechanismen bekannt. Neuere Studien haben jedoch gezeigt, dass sich in Lymphknoten, die unter dem Einfluss von Tumoren stehen, die Effektivität der Immunzellen stark verringert. Daher ist es von höchster Priorität eine Therapie zu entwickeln, die diese Unterdrückung des Immunsystems aufhebt und dabei den Krebs am Metastasieren und der Bildung von Sekundärtumoren hindert.

Das Wissen über die Veränderung von Immunzellpopulationen im Lymphknoten steigt stetig, wesentlich weniger ist jedoch über die nicht-immun Zellpopulationen bekannt. Diese Arbeit untersucht die Veränderungen in „Fibroblastic reticular cells“, nicht-hämatopoetischen Myofibroblasten im Lymphknoten, die dessen Funktion und Struktur stark beeinflussen. Dabei wird ein einfaches *in vitro* Model verwendet, bei dem die Fibroblasten in konditioniertem Medium von Tumorzellen kultiviert werden und danach auf morphologische und Veränderungen der Genexpression untersucht werden.

Durch dieses Modell konnten ein höheres Expressionslevel von Podoplanin, einem Transmembranprotein, das Kontraktion und Interaktion mit Immunzellen kontrolliert, und eine verminderte Expression von Interleukin-7, einem Zytokin das Überleben von T-Zellen, B-Zellen und dendritischen Zellen beeinflusst, erzielt werden.

Weiters zeigt die Studie einen Aktivierungsprozess in „Fibroblastic reticular cells“ auf, wenn diese in Tumorzellmedium kultiviert werden. Dieser Prozess spiegelt sich in erhöhter Kontraktion von Collagen-Gelen und schnellerer Adhäsion, sowie in vermehrter Expression von Proteinen der extrazellulären Matrix wieder. Außerdem konnten wir zeigen, dass Behandlung mit Tumormedium zu erhöhter Permeabilität in FRCs führt, welche vermutlich durch den Abbau von Verbindungsmolekülen zwischen Zellen erreicht wird.

Des Weiteren sind mitochondriale Masse und Morphologie verändert und die Zellen sind resistenter gegen Sauerstoffradikale. Zusammengefasst sehen wir dies als Zeichen eines Aktivierungsprozess wie er schon aus Tumor-assoziierten Fibroblasten bekannt ist. Der Tumor verändert den Phänotyp von FRCs noch bevor die ersten Krebszellen den Lymphknoten erreichen und

verschafft sich dadurch einen Vorteil für die spätere Metastasen Bildung. Wir erstellen die Hypothese, dass die erhöhte Expression von Collagen durch FRCs einen Vorteil für das spätere Anheften der Krebszellen bildet und die Erhöhung der Permeabilität, so wie die verminderte Expression von Zytokinen die Funktion des Lymphknotens einschränkt. Dies repräsentiert einen möglichen Mechanismus wie der Tumor die nicht-Immunzellen des Lymphknotens verändert und sich einen Vorteil für die spätere Invasion verschafft.



## 1. Introduction

The lymphatic system, consisting of a network of lymphatic vessels carrying protein rich fluid called lymph, forms part of the body's circulatory system and is responsible for maintaining fluid homeostasis<sup>1</sup>. To do this, lymphatic vessels collect blood vessel exudates containing waste products, proteins and cells from the interstitial space and subsequently return it to the blood circulation. The lymphatic system also represents a crucial transport route for immune cells and soluble antigens, enabling rapid delivery to lymph nodes, and is necessary for absorption of fatty acids<sup>2</sup>.

Its role in the immune system and transport is tightly regulated, and disruption can result in pathologies such as lymphedema and autoimmunity<sup>3</sup>. Moreover many tumours exploit the lymphatic system to spread and colonize lymph nodes<sup>4,5</sup>, which function as immunological hubs. Lymph node metastasis is an independent indicator of poor patient prognosis in cancer, yet the mechanisms by which metastasis occurs, and how tumour cells are able to avoid destruction once in lymph nodes is not fully understood. It is highly paradox that tumour cells succeed in the colonisation of lymph nodes, the part of our body that is best equipped to fight the disease. Recent studies indicated drastic changes in nodes drained by upstream tumours, including changes in cytokine and chemokine production, increase in immunosuppressive cell populations, insufficient presentation of tumour antigens and therefore creation of systemic tolerance<sup>6</sup>. A better understanding of how those nodes adapt and the investigation of a mechanism to interrupt this immunosuppressive cascade are highly needed to increase the success of anti-tumour immunotherapy.

We would like to investigate the mechanism of tumour induced immune escape by focusing on the role of supporting, non- immune cells in mediating these events. Although stromal cell populations in the lymph node have been extensively investigated in steady-state or infectious conditions<sup>7, 8</sup>, little is known about on going changes in cancer. Since stromal cells have crucial roles for architecture and function of the node, as further elucidated in the following chapters, we strongly believe that characterising their specific

remodelling in the tumour draining node could lead to a highly needed improve in cancer immunotherapy.

### **1.1 The lymphatic system**

The lymphatic system is punctuated by specialised lymphoid organs, which house and maintain immune cells, and allow immune responses to develop. These are commonly divided into three groups; the primary or central lymphoid organs, peripheral or secondary lymphoid organs (SLO) and so called tertiary lymphoid tissues<sup>1</sup>.

Primary lymphoid organs including the foetal liver, red bone marrow and thymus are keystones for the development of a functional immune system. They provide a supportive environment for haematopoiesis, the development of leukocytes. B cells mature within the bone marrow, however T cell maturation occurs in the thymus. Although these lymphocytes become mature, they are still naïve, having not yet encountered antigens required for the initiation of an immune response<sup>1</sup>. This process relies on dynamic interactions between multiple cells types, and therefore SLOs have evolved to bring together all of the necessary components needed for a functional immune response<sup>9,10,11</sup>. These include the lymph nodes, spleen, tonsils, mucosa associated lymphoid tissue and Peyer's Patches. SLOs maximize the chance of an engagement between antigen and cells of the adaptive immune system by providing a network designed to capture antigens and present them to the appropriate immune cells<sup>10</sup>. Multiple methods of antigen passage into SLOs have recently been described. Antigen may be transported by migrating immune cells<sup>11</sup> or via active migration across a mucosal barrier, but can also be carried passively within the lymph<sup>12</sup>.

SLOs are highly compartmentalized with distinct immune cells like dendritic cells (DC), macrophages and lymphocytes localising within different zones of this tissues. To enable this specialised architecture and function, SLOs are supported by a subset of non-hematopoietic stromal cells of mesenchymal origin, which form a physical scaffold, guide immune cells and influence immune homeostasis and function<sup>13, 14,15, 16</sup>. Stromal populations within the lymph node will be discussed in more detail in section 1.3. In contrast to

primary and secondary lymphoid organs, tertiary (or ectopic) lymphoid organs are typically associated with pathological, chronic inflammation e.g. atherosclerosis, cancer and autoimmunity and are highly similar to SLOs in terms of organization, cellularity and chemokine production<sup>17</sup>.

## **1.2 Lymph node architecture and function**

As introduced in the previous section, lymph nodes are highly compartmentalized secondary lymphoid organs. They are surrounded by a fibrous capsule of lymphatic vessels and served by afferent and efferent vessels<sup>1</sup>. The nodes are based at vascular junctions, where they filter the lymph and collect antigens and cells carried within the lymph fluid.

The node itself is divided into the medulla and cortex, and specific populations of hematopoietic and non-hematopoietic cells inhabit each area. The cortex is located underneath the capsule and its outer region contains the B cell follicles<sup>18</sup>, whereas the T cell area is located in the paracortex (Figure 1.1)<sup>10,13</sup>. The lymph node medulla comprises blood vessels, nerves, efferent lymphatics, lymphocytes, medullary cords and medullary sinuses<sup>11</sup>.

Antigens and antigen-presenting cells enter the node across afferent lymphatics<sup>19</sup> and can subsequently be transported deeper into the cortex of the node or can leave the node through the subcapsular sinus and thereafter the efferent lymphatics<sup>20</sup>. In contrast to antigen-presenting cells, lymphocytes migrate across specialized blood vessels called high endothelial venules (HEVs), which are located in the T cell area of the cortex. In 1964 Gowans and colleagues demonstrated the entry of radioactive labelled lymphocytes into the node via HEVs<sup>21</sup>, and we now possess detailed understanding of the complex adhesion cascade controlling entry of cells. This multistep process relies on the expression of a lymphocyte homing receptor L-selectin (CD62-L) and its interaction with mucin-like glycoproteins on HEV walls that allows rolling of lymphocytes along the HEV. The chemokines CCL21, CXCL12 and CXCL13 are thereafter needed for extravasation of lymphocytes from HEVs and correct localisation within the lymph node. Those cytokines are abundantly produced by follicular dendritic cells (FDCs) and fibroblastic



packed B-lymphocytes. T cell areas are located in the paracortex region and contain T cells as well as a network of FRCs. FRCs, FDCs and the other subsets of non-hematopoietic cells in the lymph node will be the focus of the next chapter. The lymph node medulla contains blood vessels, nerves, medullary sinuses and efferent lymphatics. Figure sourced from <sup>29</sup>.

### 1.3 Stromal cells residing in the lymph nodes

Although stromal cells residing in the lymph node only represent a diminutive percentage of all cells in the node<sup>30</sup>, they are nevertheless indispensable for its normal function. They do not only form a scaffold and construct the architecture of the node<sup>19</sup>, but are also crucial for the regulation of hematopoietic cells. Stromal cells provide a backbone for lymphocytes to migrate, guide cells to distinct niches by secretion of immune modulatory chemokines, and interact directly with lymphocytes<sup>31</sup> and dendritic cells.

Moreover, the FRC network formed allows for the rapid transport of low molecular weight antigens and chemokines throughout the node, and has more recently been shown to be capable of inducing T cell tolerance<sup>32</sup> and controlling the proliferation of T cells<sup>15, 33</sup>.

As stromal cell populations are extremely heterogeneous, they are commonly divided into subclasses based on their localization in the node and by the expression of two surface markers, namely CD31 and Podoplanin (PDPN or gp38). FDCs express PDPN, but no CD31 (CD31<sup>-</sup> gp38<sup>+</sup>) and cluster in B cell follicles, where they are needed to form a network where B cells can be activated and search for antigens (Figure 1.2, top left panel). They can be distinguished from other stromal cells by their expression of CD35 and secrete CXCL13 to attract CXCR5 expressing B cells into the follicles<sup>34</sup>. Lymphatic endothelial cells (LECs) express both markers (CD31<sup>+</sup>, gp38<sup>+</sup>) and line afferent and efferent lymphatics (Figure 1.2, top right panel). They are primarily responsible for transport of cells and components from the periphery, and are equipped to fulfil a range of additional functions like the presentation of antigen on MHCI and MHCII molecules<sup>35</sup>, the expression of regulatory receptors and cytokines, and the modulation of dendritic cell function<sup>36</sup>. Blood endothelial cells (BECs), which express CD31, but not PDPN, (CD31<sup>+</sup>, gp38<sup>-</sup>)

comprise HEVs of the lymph node (Figure 1.2, lower right panel). They have been shown to both produce and present CCL19 and CCL21a and thereby promote the recruitment of T cells<sup>11</sup>. Fibroblastic reticular cells (FRCs) expressing PDPN, but not CD31 (CD31<sup>-</sup>gp38<sup>+</sup>) are cells of mesenchymal origin located throughout the T cell zone of the lymph node (Figure 1.2, lower left panel). These cells are reviewed in more detail in chapter 1.4.

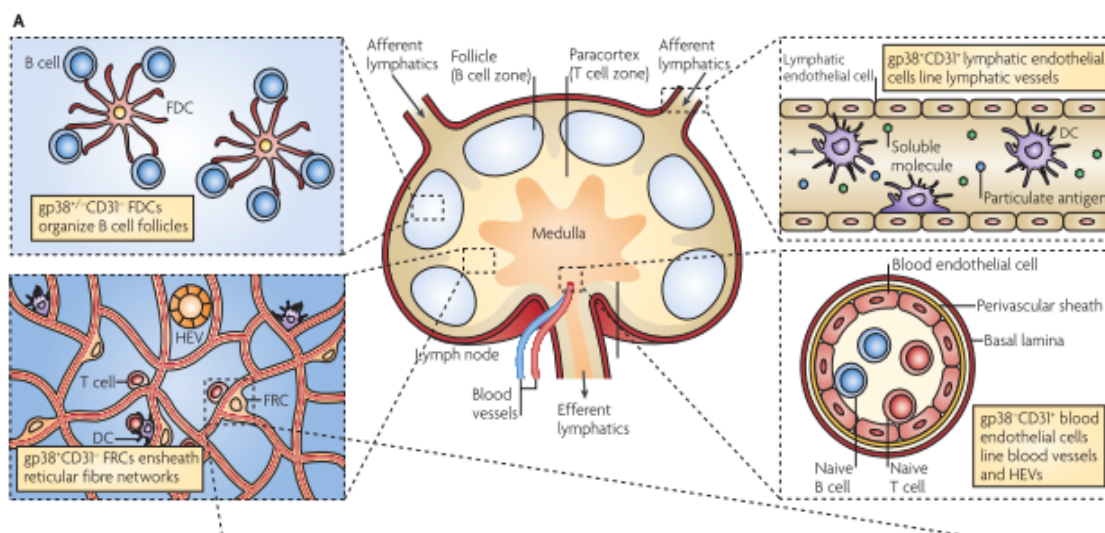


**Figure 1.2 Lymph node stromal cells** The lymph node can be divided into 3 major regions, the medulla, the cortex and the paracortex. Stromal cells residing in these regions are characterized upon their expression of the two surface markers CD31 and gp38 and their localization in the organ. The cortex contains the B cell follicles, in which FDCs (CD31<sup>+</sup>gp38<sup>+</sup>) are needed to organize the structure and interact with B cells. In the T cell zone, which is located in the paracortex, FRCs (CD31<sup>-</sup>gp38<sup>+</sup>) form a dense network to allow trafficking and engagement of DCs and T cells. Afferent and efferent lymphatics serve the node and are lined by a subset of endothelial cells called LECs (CD31<sup>+</sup> gp38<sup>+</sup>) that mediate movement of leukocytes. Blood vessels lead into the medullary region, where they open out into HEVs lined by BECs (CD31<sup>+</sup>gp38<sup>-</sup>). Figure sourced from <sup>11</sup>.

## 1.4 Fibroblastic reticular cells

FRCs are myofibroblasts of mesenchymal origin located in SLOs. Most studies to date have focused on FRCs of the LNs under steady state conditions or in infection, where they account for 20-50% of the non-haematopoietic cells<sup>13, 25</sup>. FRCs express molecules typical for fibroblasts, like  $\alpha$ -smooth muscle actin ( $\alpha$ -sma), vimentin and desmin as well as more

specialised matrix proteins such as ER-TR7. Further distinction from other cell populations can be made by the expression of the two markers PDPN and platelet derived growth factor receptor  $\alpha$  (PDGFR $\alpha$ ) and the lack of CD45 and CD31<sup>30</sup>. FRCs are crucial components of the scaffold that provides strength, yet flexibility to the node and keeps it in a response-ready state. Upon initiation of an adaptive immune response lymph nodes rapidly and transiently expand to accommodate the influx of naïve and proliferating lymphocytes, before returning to normal state. Recently it has been reported that during hyperplasia of the node FRCs become activated, expand rapidly and finally cover a much larger volume for the accommodation of immune cells. As reported by Ying-Yang et.al. FRCs do not only start to proliferate faster, but do also increase in size within 20 hours<sup>7</sup>. The same study also proved that FRC networks from the T cell zone expand into the medullary region upon swelling, but do preserve their architecture and function<sup>7</sup>. Moreover, FRC-derived chemokine signalling orchestrates the correct compartmentalization of T cells and B cells required for proper lymph node function. In the T cell zone FRCs secrete CCL19 and CCL21 to guide trafficking of responsive mature CCR7<sup>+</sup> DCs and naïve CCR7<sup>+</sup>IL-7R<sup>+</sup> T cells throughout the network<sup>25</sup> (Fig 1.3.A). This process maximises the chance of antigen-specific interaction between antigen presenting cells and their cognate T cell. Additionally, FRCs secrete Interleukin-7 (IL-7) and thereby regulate survival of DCs and T cells they encounter<sup>13</sup> (Fig 1.3.A). This was highlighted by studies illustrating that depletion of FRCs reduces numbers of conventional and migratory DCs detected within nodes<sup>37</sup>. FRCs also produce the B cell attractant CXCL13 and the growth factor B cell-activating factor (BAFF), indicating a role in the survival and attraction of B cells<sup>30, 38</sup> (Fig 1.3.B, Fig 1.3.C). More recent *in vivo* studies have shown that reticular cells of the B cell follicles maintain the follicle boundaries and promote survival of B cells<sup>39</sup>.

PDPN, which is extensively reviewed in 1.7, helps to modulate the migration events of DCs coming into contact with FRCs (Fig 1.3.A). Its interaction with C-type lectin domain family 1 member B (CLEC-2) on antigen-carrying DCs is sufficient to induce cytoskeleton changes in DCs thereby regulating their

motility. Podoplanin-CLEC2 interactions extend beyond immune trafficking, and are in fact critical to maintain lymph node structure<sup>40</sup>. FRCs control the integrity and permeability of HEVs through accumulation of CLEC-2<sup>+</sup> platelets contacting PDPN<sup>+</sup> FRCs that surround the HEVs (Fig 1.3.D). This starts a signalling pathway resulting in the secretion of Sphingosine-1-phosphate (S1P) by platelets, which in turn drives VE-Cadherin upregulation in HEVs and reinforces cellular junctions<sup>41</sup>. The reinforcement of cell-cell contact prevents leakage of cellular and non-cellular components into the node, reflected by the fact that high amounts of red blood cells leak into PDPN deficient nodes<sup>40</sup>.

FRCs contribute to physiological immunosuppression referred to as tolerance, whereby they have evolved mechanisms to prevent autoimmunity and tissue damage from the T cells that reside there. FRCs are known to keep the immune system in check via three major pathways: the mediation of tolerance by deletion of CD8<sup>+</sup> T cells<sup>32</sup>, the suppression of proliferation in effector T cells<sup>15</sup> and the promotion of regulatory T cells<sup>42</sup>. Deletional tolerance is mediated by the expression of tissue-specific self-antigens that FRCs can directly present to CD8<sup>+</sup> T cells for the induction of tolerance. This process is known to prevent autoimmunity by deleting auto reactive T cells in animal models<sup>43,44,32</sup>. *In vitro* experiments performed by Lukacs-Kornek<sup>15</sup> and Siegert<sup>33</sup> demonstrated that T cells in contact with FRCs display reduced proliferative capacity. This is mediated by the production of FRC-derived nitric oxide in response to Interferon- $\gamma$  (IFN- $\gamma$ )<sup>15</sup>. This could be a fundamental process to prevent T cells from becoming effective within the node and might in turn be needed to prevent damage to the node's infrastructure through expanding T cells. Although the exact mechanism has yet to be established, independent studies showed that lymph node stromal cells are capable of T<sub>Reg</sub> cell induction, indicating another highly important immunosuppressive function<sup>45,46</sup>.

The effects of FRCs extend far beyond the lymph nodes, and it is now understood that they are required for systemic generation of cellular and humoral immunity. The requirement of mature FRCs was tested in a study,



using Ccl19-Cre-x LTBr<sup>fl/fl</sup> mice. In these mice, CCL19 driven Cre-recombinase leads to directed deletion of lymphotoxin beta receptor specifically within FRCs. This results in immature FRCs and consequently low levels of IL-7, CCL21, CCL19 and PDPN. When infected with lymphocytic choriomeningitis virus which is usually controlled effectively by CD8<sup>+</sup> T cells, mice suffer a 60-70% depletion of T cells, B cells, DCs and macrophages and are therefore incapable of clearing the virus infection<sup>47</sup>. Two other studies using mice with FRC-specific gene deletion gave similar results<sup>37, 39</sup>, and taken together point to the systemic relevance of FRCs in the generation of an immune response.

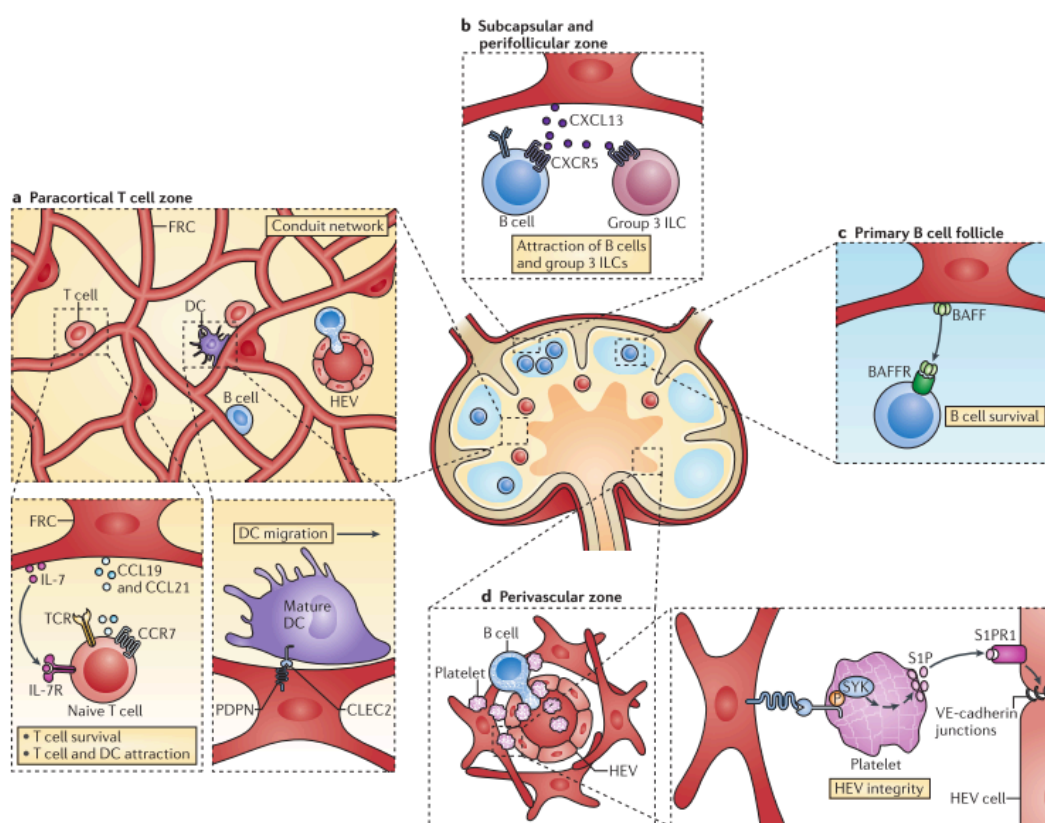


**Figure 1.3 The impact of FRCs in the lymph node.** **A** T cell zone FRCs support the survival of T cells by expressing IL-7 and attract T cells and DCs via CCL19 and CCL21. Besides they express PDPN, interacting with CLEC2 on antigen-bearing DC and thereby control their migration. **B** FRCs in the subcapsular and perifollicular zone express CXCL13 and thereby attract B cells and group 3 innate lymphoid cells (ILC), expressing the receptor CXCR5. **C** Moreover FRCs in primary B cell follicles express BAFF and promote the survival of naïve B cells. **D** FRCs also reinforce cell junctions in HEVs and thereby prevent leakage of unspecific components into the node.

## 1.5 Lymphatics in cancer

The spread of cancer from the primary tumour is referred to as metastasis and the major cause for death in cancer patients<sup>48</sup>. Many tumours utilize the lymphatics for this process, and thus the presence of tumour cells residing in sentinel or regional lymph nodes has become a keystone in the prediction of poor outcome in cancer<sup>49, 50</sup>. The growth and formation of new lymphatics (lymphangiogenesis) as well as the remodelling of pre-existing ones is crucial for metastasis to occur. Lymphangiogenic drivers required for the induction of metastasis identified in recent years include vascular endothelial growth factor A (VEGF-A)<sup>51</sup>, VEGF-C, VEGF-D,<sup>52</sup> fibroblast growth factor 2(FGF2)<sup>53</sup>, platelet derived growth factor B<sup>54</sup>(PDGF-B) and endothelial growth factor (EGF)<sup>55</sup>. Initial lymphatic vessels in and around the tumour have been observed to respond to these stimuli via proliferation and sprouting<sup>56</sup>.

Lymphangiogenesis may occur within the tumour or at the periphery. Although Leu<sup>57</sup> reported almost complete absence of lymphatics in the primary tumour, others<sup>58,56</sup> have shown the formation of new lymphatics within the tumour via lymphangiogenic growth factors. However, the functions of these new lymphatics remain elusive as several studies have indicated that intratumoural lymphatics are not in fact needed for metastasis to occur<sup>58, 59</sup>. Thus, many do not consider the vessels as crucial for the formation of metastasis, but they still represent a potential interface of invasion into the lymphatic system<sup>60</sup>. While the need for intratumoural lymphatics for metastasis remains controversial, lymphatics at the tumour edge *are* widely considered critical for metastasis. The increased number of vessels provides a greater chance for invading tumour cells to escape via passive mechanisms; recent studies have highlighted that active and dynamic changes in lymphatics around the tumour also facilitate metastasis. The increased number of vessels, and their enlargement also translate to enhanced drainage capacity away from the tumour<sup>61</sup>. The resulting biophysical effects can enhance tumour cell shedding, can stimulate the production of chemokines and growth factors providing directional chemical cues and can impact other cells found within the tumour microenvironment resulting in tissue matrix remodelling. All of these factors

rely on lymphatic function and synergise to create a pro-tumour environment<sup>62, 63,64</sup>.

Although remodelling of the lymphatic vessels and associated environment has mostly been reported within the primary tumour, downstream collecting lymphatics and lymph nodes are also beginning to receive attention.

Recent studies focused on collecting lymphatics (vessels that drain the tumour) and reported dynamical remodelling in collecting lymphatics in response to lymphangiogenic growth factors<sup>65, 66</sup>. The presence of growth factors promotes enlargement of collecting lymphatics, which in turn increases the flow rate in the vessels<sup>66, 65</sup> and is crucial for migration of cancer cells to lymph nodes and distant organs<sup>67</sup>. Remodelling also occurs beyond primary tumours in sentinel and regional lymph nodes that have become known as the “lymph vascular niche”<sup>68</sup>. VEGFC and VEGFD produced within primary tumours are capable of modifying blood vessels, HEVs and lymphatic vessels in lymph nodes prior to arrival of metastatic cells and thereby create a favourable environment for tumour cells<sup>69, 70, 47</sup>. This altered environment in the node has been speculated to provide an environment for the survival of tumour cells resistant to chemotherapy or cancer stem cells. The lymphangiogenesis occurring in the node might also influence the immune response to tumour cells and thereby provide the conditions for the expansion of micro metastases<sup>71</sup>.

The work in this thesis has been carried out with malignant melanoma models, which represent the most lethal skin cancer and are prone to metastasize into regional lymph nodes<sup>72, 73</sup>. In melanoma models the migration of cancer cells to regional lymph nodes has been shown to happen via the lymphatic system and not via blood vessels<sup>74</sup>.

## **1.6 Tumour draining lymph nodes**

Tumour-draining lymph nodes (TDLN), which can be found downstream of tumours and undergo fundamental changes due to the presence of a tumour (Fig 1.4.A), play a conflicting role in cancer<sup>6</sup>. Of note is that they are capable

of inducing an anti-tumour response, yet are the first site for metastasis of malignant cells. This implies that TDLNs are also influenced by the immune-suppressive microenvironment created by a tumour.

The immune-dampening microenvironment generated in response to a tumour is likely to be the outcome of a mixture of growth factors, immunosuppressive cytokines and inhibitory cell populations<sup>75</sup>. Tumour cells and macrophages associated with the tumour produce transforming growth factor  $\beta$  (TGF- $\beta$ ), IL-10, IL-6 and monocytes secrete CCL2 and CXCL8, which in turn causes tumour angiogenesis and progression through recruitment of myeloid-derived suppressor cells (MDSC). An accumulation of regulatory T cells in TDLNs has been reported in several cancer models and is correlated with a progression of the disease. Regulatory T cells are capable of limiting the numbers of DCs, CD8<sup>+</sup> and NK cells via granzyme B and perforin secretion<sup>76,77</sup>. Together with MDSC and tolerogenic DCs they suppress the effector function of T cells<sup>78,79,80</sup>. Lower levels of proinflammatory cytokines in the TDLN (IL-12, IFN- $\gamma$ ) result in a low level of T-cell activation and the reduction in numbers of DCs in the TDLN contributes further to the immunosuppressive state<sup>81,82, 80</sup>. Antigen presenting cells in the TDLN show lower levels of maturation signals<sup>81, 80</sup> and often lack co-stimulatory signals leading to insufficient priming of T cells<sup>83</sup>.

The knowledge about immune cell populations in the TDLN is increasing steadily, yet little is known about the alterations occurring in non-hematopoietic cell populations.

Moreover signalling pathways between tumour cells and their surrounding stroma and lymphatics have been extensively investigated<sup>61</sup>, yet hardly anything has been reported about signalling occurring between a tumour and the stromal cells in the downstream lying lymph node. A “priming” of the draining node prior to the arrival of cancer cells to generate a favourable environment has been reported, yet most of these studies focus on the alterations occurring in the immune cell populations. Knowledge about how the tumour alters stromal cell populations to subsequently achieve colonisation of the node is highly needed and might represent an important contribution to the improvement of cancer immunotherapy.

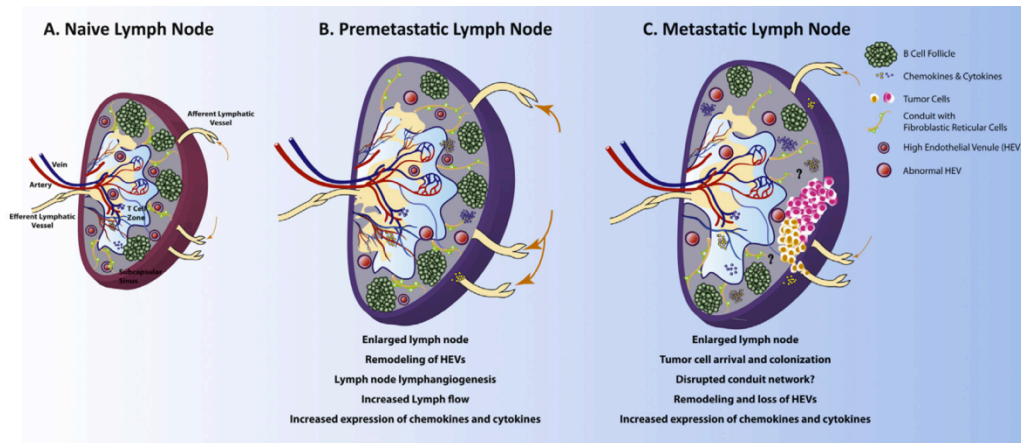


**Figure 1.4 Remodelling of TDLN during development of metastatic disease** Tumour drainage induces fundamental changes in the TDLN prior to arrival of the cancer cells in the node. Lymph nodes enlarge in size, HEVs are remodelled, expression of chemokines and cytokines gets deregulated and immune cell populations are altered. Upon arrival of cancer cells the node undergoes further changes like loss of HEVs, lymphatic vessel regression and disruption of the conduit system. Figure sourced from <sup>6</sup>.

## 1.7 Podoplanin

The investigation of alterations occurring in FRCs in the TDLN proves to be exceedingly complex, as a gene array performed on FRCs out of a TDLN indicated highly altered transcriptional signature (unpublished data, Shields Lab).

The focus of the following thesis lies on the two proteins PDPN and Interleukin-7 (Chapter 1.8) that have been shown to be deregulated and are both crucial for the function of the node.

PDPN has been studied in several different contexts and is therefore known under several different names. In LECs it has been described as E11 antigen<sup>84</sup> and on FRCs and thymic epithelial cells as gp38<sup>85</sup>, but finally it was called Podoplanin due to expression on podocytes. It is a 36-43 kDA mucin-like transmembrane protein with high conservation between different species and expression in humans, rats, mice, dogs and hamster<sup>86, 87</sup>.

PDPN has a huge impact in development, as it is crucial for development of heart, lungs and lymphatic system. This is reflected by the fact that 40% of PDPN<sup>-/-</sup> mice die between days E10 and E16 and the surviving ones die

shortly after birth as they are incapable of inflating their lungs<sup>88</sup>. Moreover PDPN<sup>-/-</sup> mice have hardly any lymph nodes and the few developing ones are disorganized.

PDPN consists of a transmembrane domain, a short cytoplasmic tail and an extracellular domain with many glycosylated residues<sup>89</sup>. The protein co-localizes with ERM family proteins (ezrin, radixin and moesin) that are important connection points between membrane proteins and the cytoskeleton<sup>90</sup>. PDPN also interacts with CD44<sup>91</sup>, which affects functions as migration and adhesion and is often linked to invasive cancers. Furthermore PDPN has been reported to interact with CD9 that acts as a tumour suppressor<sup>92</sup>. Only one receptor for PDPN has been discovered so far, a C-type lectin named CLEC-2 expressed on neutrophils, dendritic cells and platelets<sup>93,94</sup>. The CLEC-2 PDPN axis has recently been identified as the major regulator of contractility of FRCs, as an engagement of PDPN with CLEC-2 on dendritic cells attenuates the contractility resulting in relaxation and reduced stiffness. Therefore in resting conditions where FRCs are unlikely to meet migratory dendritic cells expressing CLEC-2, PDPN acts on the actomyosin machinery and FRCs are able to exert tension. Engagement with CLEC-2 prevents this signalling pathway and has fundamental consequences on the node architecture<sup>95</sup>.

In addition to expression on stromal cell populations in the node, PDPN has been reported on a subset of T cells and macrophages,<sup>96</sup> usually correlated with inflammation or disease. Whereas the exact function in T cells remains elusive, the expression on macrophages has been reported as sufficient to induce platelet aggregation<sup>96</sup>. PDPN also plays a hugely important role in cancer, as it is expressed on lymphatic vessels and therefore a major diagnostic marker for lymphangiogenesis<sup>97, 98</sup>. Of note is that tumour cells themselves upregulate PDPN<sup>99,100</sup>, often on the leading, invasive edge of the tumour where it is involved in invasion, metastasis and epithelial-mesenchymal transition (EMT)<sup>90</sup>.

## 1.8 Interleukin-7

FRCs are known as an abundant source of IL-7, a regulatory cytokine produced by distinct stromal cell types in lymph node, bone marrow and thymus, as well as by hepatocytes<sup>101</sup>, epithelial cells<sup>102</sup> and dendritic cells<sup>103</sup>.

Since IL-7 has been reported to stimulate proliferation of lymphoid cells (NK cells, B cells and T cells) and plays a crucial role in the survival and development of B and T cells<sup>104</sup>, studying its role in the TDLN could prove as highly interesting. Normal lymphocytes do not produce IL-7, yet they are highly dependent on it<sup>104</sup>. The requirement of IL-7 for efficient B cell development was proved by a study using IL7<sup>-/-</sup> mice that reports blockage of B cell formation at the transition from pro-B-cells to pre-B-cells<sup>105</sup>. Apart from the impact on B cell development IL-7 was shown to influence developing T cells in multiple steps. An anti-apoptotic effect of IL-7 on thymocytes was reported<sup>106</sup>; moreover the cytokine contributes to T cell-precursor expansion and is involved in T cell receptor (TCR) rearrangement<sup>107</sup>.

IL-7 also exhibits a profound impact on mature T cells as it controls homeostasis of memory CD8 and naïve T cells<sup>108</sup>. Yet the effects of IL-7 are not limited to B and T cells, but it also influences dendritic cell function and development as studies inhibiting IL-7 production showed a substantial reduction in generation of DCs<sup>109</sup>. The cytokine binds to the IL-7 receptor (IL-7R), which results in a signalling cascade including the phosphatidylinositol 3-kinase (PI3-kinase), Janus kinase/ signal transducer activator of transcription (Jak/STAT) pathway and Src family tyrosine kinases<sup>104</sup>. IL-7R<sup>-/-</sup> mice display profound reductions in thymocyte cellularity and this hypothesizes IL-7R signalling as critical for efficient lymphoid development<sup>110</sup>.

Of note is that IL-7 is also produced by solid tumours and has been found expressed in leukaemia and lymphoma<sup>111</sup>. It has been examined as an immunotherapeutic agent in several settings of cancer and its administration to humans has been reported to expand CD4<sup>+</sup> and CD8<sup>+</sup> T cells, but decrease T<sub>regs</sub><sup>112</sup>. Several features of IL-7 could potentially be exploited for cancer therapy and it could also be used for adoptive immunotherapy. Furthermore IL-7 was reported to improve survival of tumour bearing hosts by increasing tumour specific T cells in independent studies<sup>113,114</sup>.

## 2. Aims

The number of global cancer cases is expected to double by 2030 and therefore improving treatment and survival is a major worldwide goal. To be able to identify new therapeutic targets and develop treatment platforms, we need to understand the processes exploited by the tumour. Here, it is important not to limit the focus to the tumour cells themselves, but to also include their surroundings, the cells that support them and the microenvironment that allows them to metastasize and spread throughout the body. In the process of metastasis lymph nodes have been defined as the “lymph vascular niche”, prepared by the tumour for the arrival of cancer cells and allowing them to survive and form micro metastases.

This thesis focuses on changes that occur to cells of the TDLN prior to the arrival of cancer cells, specifically focusing on fibroblastic reticular cells, a stromal cell population representing 20-50% of the non-hematopoietic cells in the node. The Shields lab has shown that TDLNs increase in size and that stromal populations, specifically within draining nodes expand. Moreover, a gene array of FRCs isolated out of TDLN shows a variety of altered transcription signatures.

Taking the complexity of the TDLN into account and considering the range of stimuli that could induce the changes observed (e.g factors within draining fluid from the tumour or shear stress resulting from increased fluid flow) this thesis aims to dissect this complex model. Specifically we will address the following specific aims/questions

1. Investigation of the question whether merely culturing FRCs in tumour conditioned medium (TCM) from melanoma cells could reproduce changes in the gene array and these are therefore induced by secreted factors from the tumour. Therefore the establishment of a simple *in vitro* treatment model and subsequent screening of FRCs for gene expression changes was a major aim.



2. Determination of resultant functional changes in FRCs upon TCM treatment and relating them to the causing molecular mechanisms.
3. Dissection of factors in the tumour conditioned media (TCM) that induce these changes, e.g. ruling out whether exosomes secreted by tumour cells play a role in this process.

### 3. Results

#### 3.1 Isolated C57BL/6 p53<sup>ER/ER</sup> FRCs closely resemble primary cells

Lymph nodes located immediately downstream of tumours have been reported to remodel, in this process generating an immune dampening environment due to increased immunosuppressive cell populations<sup>6</sup>. Yet little is known about the mechanisms driving these changes or how stromal cell populations are modified in the remodelling process. A gene array performed by Dr. Angela Riedel in the Shields Lab (unpublished data) indicated that FRCs specifically from the TDLN change their gene expression programme dramatically. This model is based on the subcutaneous injection of B16F10 melanoma cells into the shoulder region of C57BL/6 mice and the subsequent analysis of FRCs from individual TDLN after 4 or 11 days. 4 days after injection of tumour cells the gene array indicated 86 genes as up and 95 genes as down regulated on FRCs, after 11 days this number even increased to upregulation of 193 and downregulation of 103 genes.

Aiming to perform *in vitro* verification of this gene array hits, it was necessary to derive a source of FRCs for culture systems.

Stromal cells in the lymph node are characterized upon their lack of expression of the hematopoietic marker CD45 and their distinct expression patterns of CD31 and PDPN (gp38)<sup>11</sup>. Single cell suspensions isolated from lymph nodes of C57BL/6 mice yielded a heterogeneous, adherent primary stromal population, which could be separated from immune cells in suspension by frequent washes. Stromal cells were then stained for CD31 and PDPN to further define the subpopulations and purify CD31<sup>+</sup>PDPN<sup>+</sup> FRCs by fluorescence activated cell sorting (FACS). Yet with this protocol of isolation, FRCs represented only about 15% of the whole stromal population, which itself formed a minor subset of all cells in the lymph node (Fig 3.1.A). The low number of isolated FRCs, significant variation between isolations as well as the stress induced through the sorting process led to insufficient cell numbers necessary to perform the *in vitro* studies. To avoid this, experiments were performed using an immortalized FRC cell line generated “in-house” from p53<sup>ER/ER</sup> C57BL/6 mice. These cells lack functional expression of tumour

suppressor p53 and are therefore suitable for long time culture. They display fibroblast morphology and express the surface marker PDPN as well as vascular cell adhesion molecule 1 (VCAM-1) (Fig 3.1.C), a typical FRC adhesion molecule. p53<sup>ER/ER</sup> FRCs are moreover lacking the expression of the hematopoietic marker CD45, the macrophage marker CD11b and the lymphatic and blood vessel marker CD31 (Fig 3.1B). These results demonstrated the identity of p53<sup>ER/ER</sup> FRCs and their acceptance for the following experiments<sup>115</sup>.

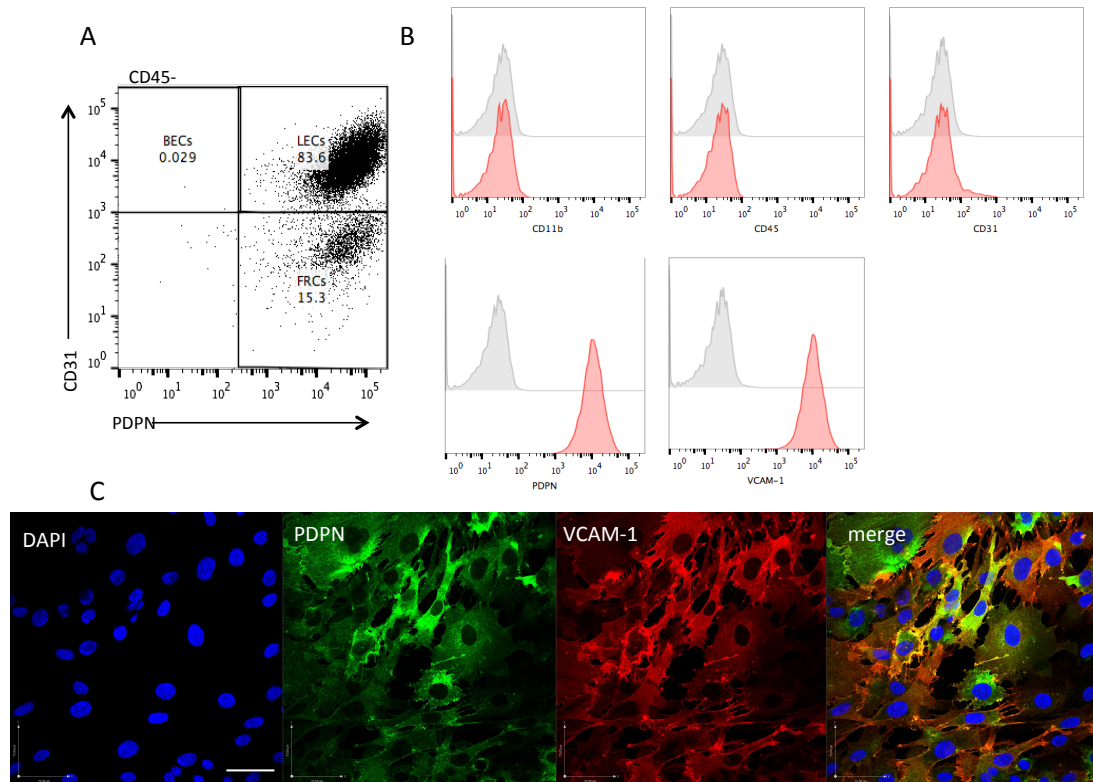


**Fig 3.1. FRC characterisation *in vitro*.**

**A** Representative flow cytometry scatter plot of primary lymph node stromal cells pre-gated on the CD45 negative population showed CD31<sup>+</sup>PDPN<sup>-</sup> BECs, CD31<sup>+</sup>PDPN<sup>+</sup> FRCs and CD31<sup>+</sup>PDPN<sup>+</sup> LECs. **B** Flow cytometric analysis of the p53<sup>ER/ER</sup> FRC cell line illustrated a lack of CD11b, CD45 and CD31, but high levels of PDPN and VCAM-1. Isotype control depicted in grey and indicated antibody in red. **C** Immunofluorescent staining of p53<sup>ER/ER</sup> FRCs confirmed FACS data; PDPN (green) and VCAM-1 (red). Nuclei are labelled in blue. Scale bar represents 73  $\mu$ m.

### 3.2 Tumour conditioned media is capable of inducing gene expression changes in FRCs

*In vivo*, the lymph node is a highly complex, dynamic system and thus multiple factors and interactions could contribute to the reprogramming observed in FRCs. Therefore, to begin to dissect the signals responsible, we raised the question whether merely culturing FRCs in conditioned medium from tumour cells could recapitulate the changes indicated in the gene array. This simple model ignores the impact of other cell populations in the node as well as mechanical conditions like flow or expansion of the node, but is suitable for the identification of genes deregulated by the tumour secretome alone.

Using the experimental model explained in 5.1.7, FRCs were treated with conditioned medium from a B16F10 melanoma cell line (TCM) or conditioned medium from FRCs as control (CON) over indicated time courses and subsequently RNA was extracted to perform qPCR on potential targets deregulated in the gene array. Early time points (24h, 48h) were not sufficient to induce significant changes in the gene expression pattern of tested candidates (data not shown), but after 4 days a significant upregulation of PDPN could be detected, in line with the gene array (Fig 3.2 A). After 7 days of TCM treatment, this was enhanced with PDPN up regulated by  $1.69 \pm 0.07$  (Mean  $\pm$  standard error of mean (SEM)), whereas IL-7 was now significantly down regulated by  $0.55 \pm 0.10$  (Mean  $\pm$  SEM), (Fig 3.2.B). The downregulation of IL-7 could not be detected after 4 days of treatment, and consistent with gene array data requires longer treatment period for initiation. Screening of several other candidate proteins (e.g CD44, Vinculin, CD90) revealed slight, but not significant deregulations *in vitro* and therefore IL-7 and PDPN were chosen as candidates to further explore functional changes induced through TCM treatment. Both factors have high physiological relevance, as they are major functional regulators in the lymph node. IL-7 controls survival and homeostasis of naïve T cells as well as B cell development and its loss or downregulation has been linked to impaired immune function.

Besides managing interactions with DCs, PDPN influences contractility in FRCs and is therefore a major regulator of lymph node architecture and function.

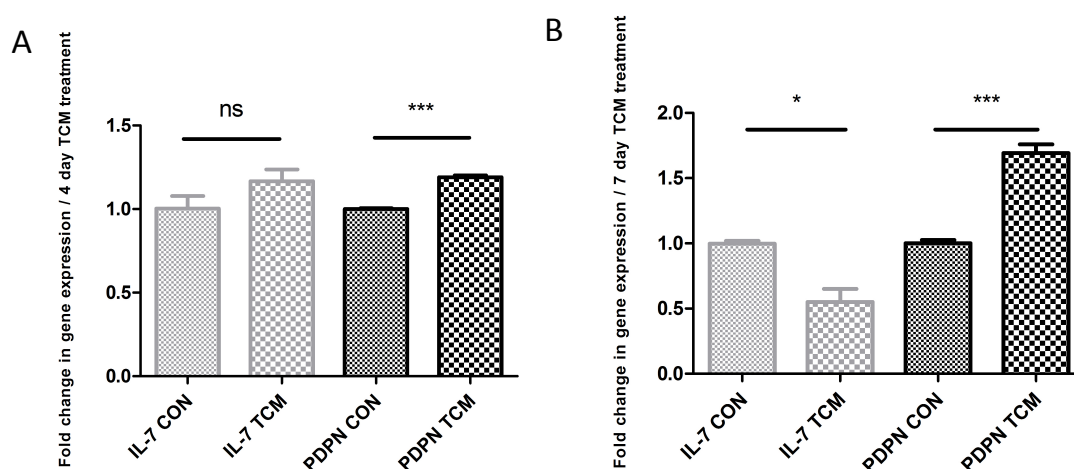


**Fig 3.2 TCM treatment deregulates mRNA levels of PDPN and IL-7**

mRNA expression of IL-7 and PDPN in FRCs was measured **A** after 4 days and **B** after 7 days of TCM treatment and normalized to two housekeeping genes. Data is representative of two independent experiments with each n=3 biological replicates and represented as Mean  $\pm$  SEM. ns not significant, \*p<0.05, \*\*\*p<0.001 (Unpaired t-test)

### 3.3 Treatment with TCM changes protein levels of PDPN and IL-7

Subsequently we aimed to investigate whether the changes in mRNA are translated into deregulated protein levels of PDPN and IL-7. Flow cytometry analysis of cells at day 7 of TCM treatment confirmed a significantly increased surface expression of PDPN (Fig 3.3 A). Downregulation of IL-7 upon TCM treatment was demonstrated by ELISA. Although the level of secreted protein was close to the detection limit of the assay, a significant reduction of > 50% was measured following TCM treatment (Fig 3.3 B). To be fully confident about the downregulation and gain more reliable results cells were treated with Brefeldin A, an inhibitor of protein transport and thereby preventing secretion<sup>116</sup>, for 6 hours on the last day of TCM treatment, lysed and immunoblotting for IL-7 was performed (Fig 3.3 C). Consistent with the ELISA, the western blot also demonstrated downregulation of IL-7 at the protein level.

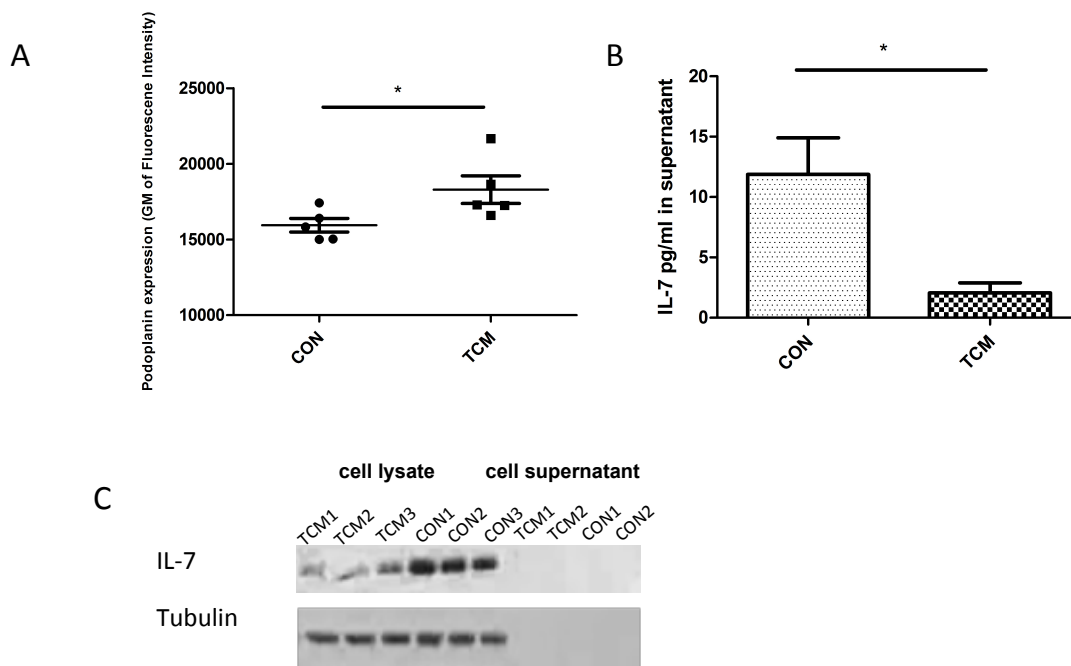


**Fig 3.3 PDPN and IL-7 deregulation on protein level**

**A** PDPN protein levels were measured by flow cytometry after 7 days of TCM treatment. Expression level is displayed as geometric mean (GM) of fluorescence intensity  $\pm$  SEM. Analysis was performed with FlowJo by gating on alive, single cells. Data represents two independent experiments displayed as Mean  $\pm$  SEM with  $n \geq 2$ , \* $p < 0.05$  (Unpaired t-test). **B** Secreted IL-7 was measured by ELISA after 7 days of TCM treatment. Data represents two independent experiments with  $n \geq 2$  and is displayed as Mean  $\pm$  SEM. \* $p < 0.05$  (Unpaired t-test) **C** Western blot confirmation of IL-7 protein levels after 7 days of TCM treatment. FRCs were incubated with Brefeldin A for the final 6h. Loading control;  $\alpha$ -Tubulin. Biological triplicates were analysed per condition.

### 3.4 Treatment with TCM does not induce morphologic or proliferative changes in FRCs

Following verification of TCM-induced up regulation of PDPN and down regulation of IL-7, the next aim was to determine the resultant functional changes. As PDPN, which has been reported to have an effect on proliferation, at least in tumour cells<sup>117</sup>, was deregulated in TCM exposed FRCs (Fig.3.2), and FRCs in tumour draining lymph nodes increased in number (unpublished data, Shields lab), proliferation was measured within 7 days of TCM treatment. No significant effect on proliferation was measured in either cell density used (Fig 3.4.B). The cells were also monitored for

morphological changes, but throughout the study no phenotypic alterations were visible following treatment (Fig 3.4.A).

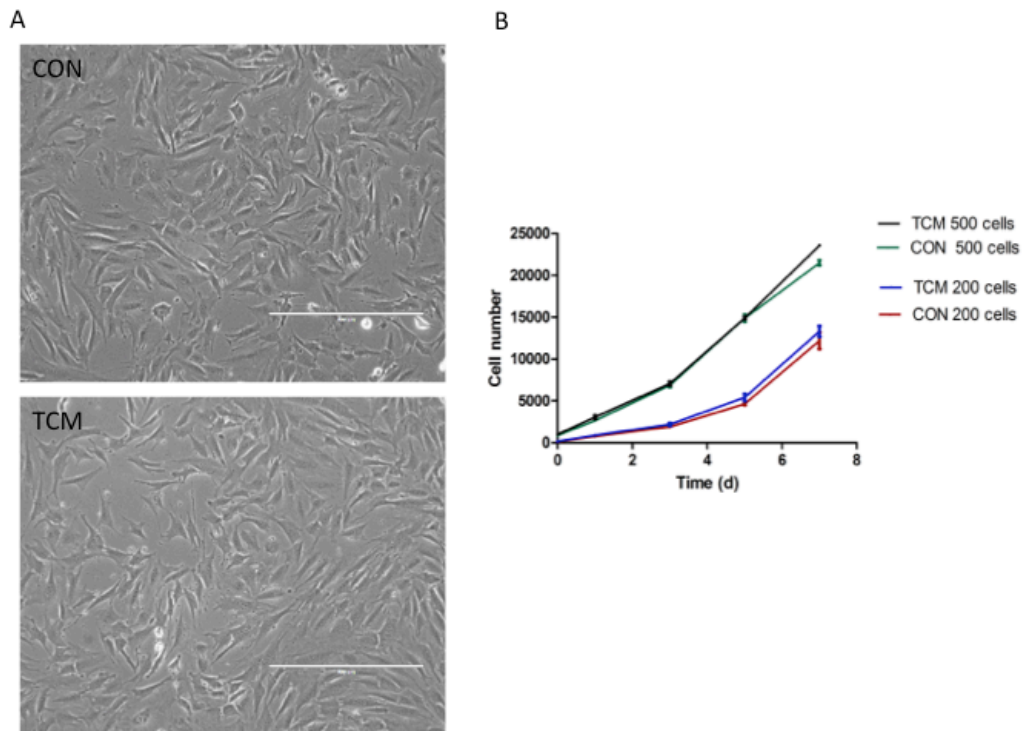


**Fig. 3.4 TCM treatment does not induce morphologic or proliferative changes**

**A** Wide field imaging of FRCs pre-treated with TCM for 7 days did not show a morphological difference compared to control. Scale bar, 400  $\mu$ m. **B** A cell titre blue proliferation assay performed over a time course of 7 days did not show a significant difference between TCM and CON. Technical triplicates were performed and data represents Mean  $\pm$  standard deviation (SD).

### 3.5 Migration potential is not changed upon treatment with TCM

With proliferation not affected, the migratory capacity of FRC after 7 days TCM exposure was investigated via a scratch assay. Again, no direct impact on FRC motility was apparent, with no differences in the ability of the two tested conditions to close the scratch (Fig 3.5).

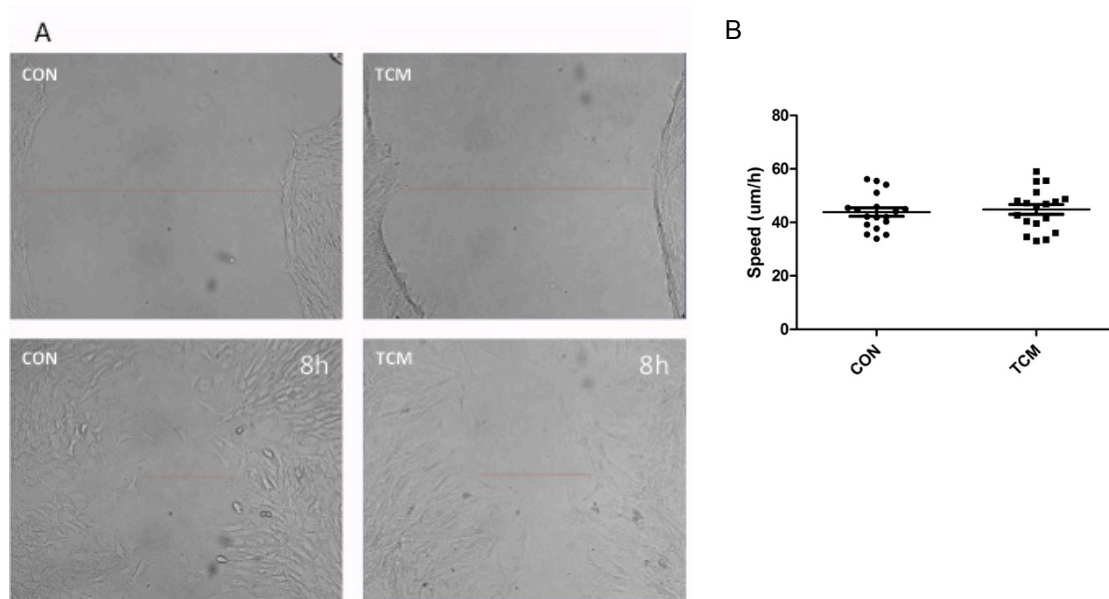


**Fig 3.5 TCM treatment does not influence directed migration**

A confluent monolayer of FRCs treated with either CON or TCM was analysed by a scratch assay over a time course of 24 h and speed of gap closure ( $\mu\text{m/h}$ ) was calculated.

**A** Representative images of the closing scratch at  $t=0$  and after 8 hours. **B** Velocity of gap closure for individual scratches. Data is depicted as Mean  $\pm$  SEM. Assay was performed in technical triplicates and  $n=18$  biological replicates were analysed.



### 3.6 TCM treatment induces an “activated state” in FRCs

As PDPN has been reported to be a mediator of actomyosin mediated contractility in FRCs by several independent studies<sup>95, 118</sup>, we aimed to investigate the impact of TCM treatment in a gel contraction assay. Astarita et al. showed that a knockdown of PDPN in FRCs leads to impaired contraction of collagen gels<sup>95</sup>, thus we hypothesize higher contractility in TCM treated FRCs as they up regulate PDPN. Indeed a significant increase in collagen gel contraction by FRCs pre-treated with TCM was measured compared to CON treated FRCs (Fig 3.6).

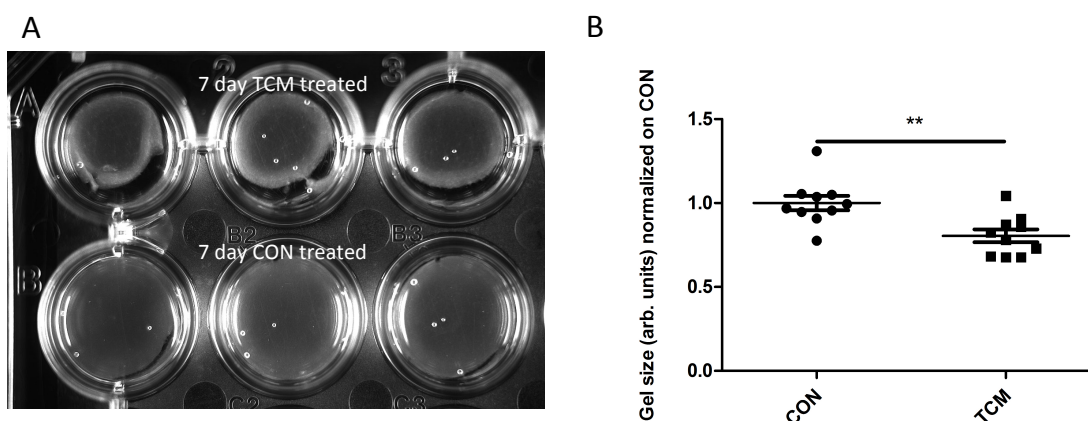
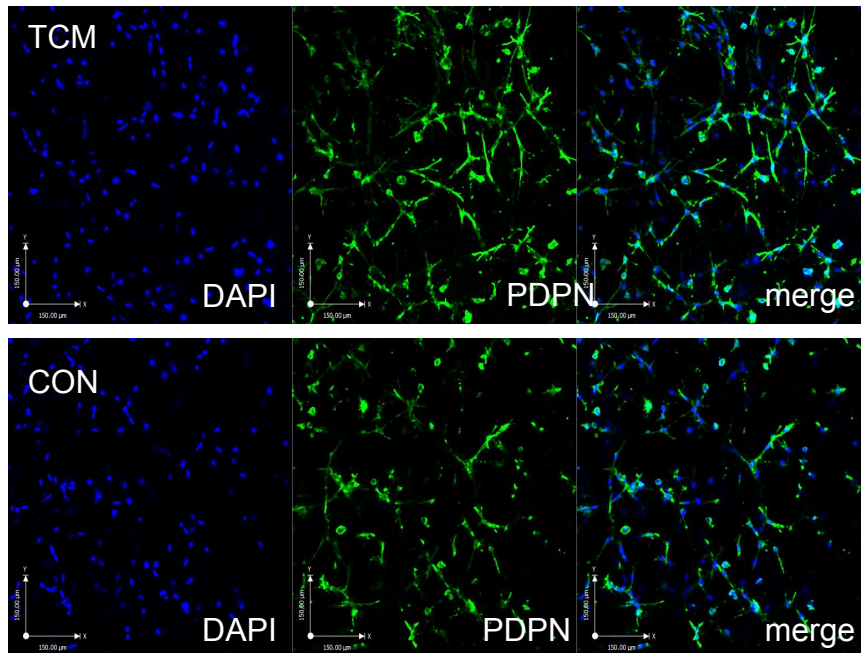


**Fig 3.6 TCM treated FRCs have higher ability to contract collagen gels**

FRCs were pretreated with TCM or CON medium for 7 days and a collagen contraction assay was performed. **A** Representative images of contracted gels after 24h. **B** Size of collagen gels was quantified using ImageJ and subsequently normalized on average size of control gels. Data represents 3 independent experiment with  $n \geq 3$  and is displayed as Mean  $\pm$  SEM. \*\*  $p < 0.01$  (Unpaired t-test)

Contracted collagen gels were then fixed and stained for the markers PDPN and F-Actin. Representative confocal z-stacks illustrate that FRCs pre-treated with TCM expand and form networks throughout the gel at a quicker rate than control (Fig.3.7). This raised the theory that TCM treatment induces an activated and response ready state in FRCs allowing them to spread and therefore contract the gel faster.

A



B

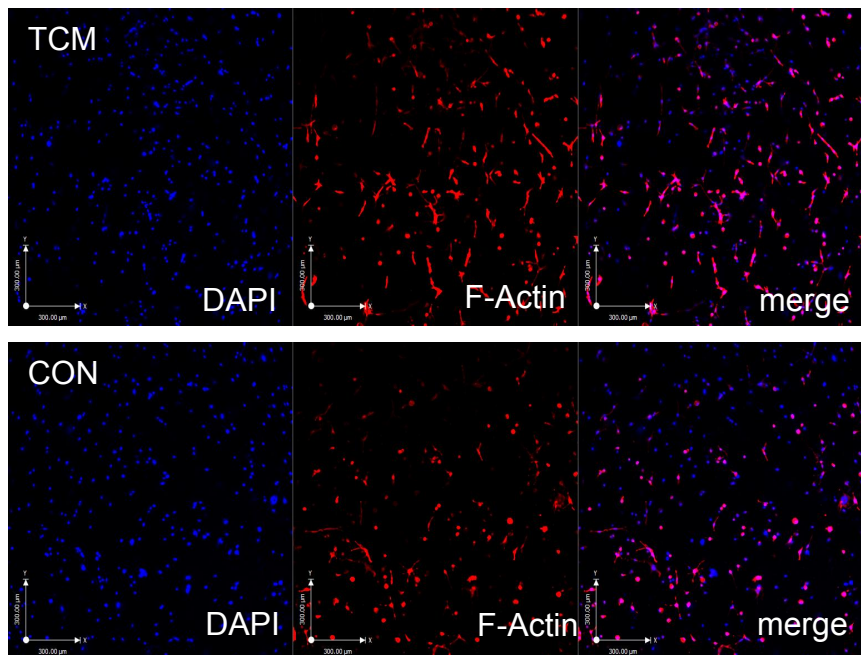


**Fig 3.7 TCM treatment induces rapid FRC network formation within collagen gels.** Contracted collagen gels were fixed 24h after seeding and subsequently stained for **A** PDPN (green) (40x magnification) or **B** F-Actin (red) (20x magnification). Scale bar in A represents 150 μm and in B 300 μm, nuclei are labelled in blue.

As the observed increase in contractility indicated an activation status upon TCM treatment, the effect of TCM treatment on the attachment properties of FRCs was investigated. In line with Tsuneki et.al. observing decreased adhesion in cells deficient for PDPN<sup>8</sup>, we hypothesized that TCM treatment, and consequent PDPN upregulation results in higher adhesive capacity in TCM treated cells. Using an RCTA xCelligence machine adhesion assays were performed over a time course of 2 hours with measurements every 10 minutes and could indeed show that cells pretreated with TCM adhere faster(Fig 3.8).

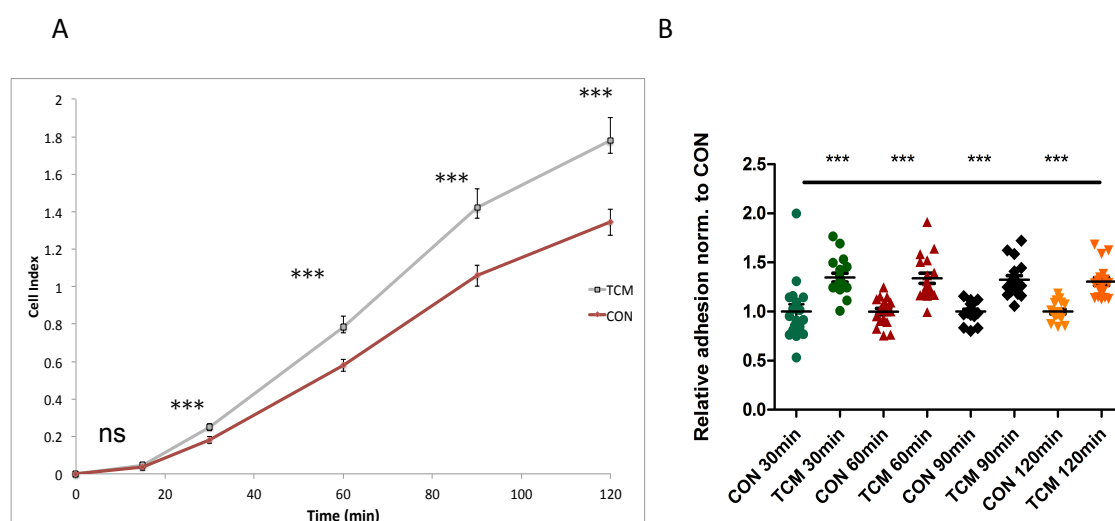


**Fig 3.8 TCM treated FRCs adhere faster**

Adhesion assays were performed over a time course of 120 min with measurements every 10 minutes. Selected measurements were used to perform statistical analysis by usage of a t-test. In **A** data is represented as cell index over time and in **B** selected time points are displayed as relative adhesion changes normalized on average of control cells. Individual measurements are depicted in B. Three independent experiments were performed with n=6 replicates per run. Data is displayed as mean  $\pm$  SEM ns= not significant, \*\*\*  $p < 0.001$ .(Unpaired t-test)

### 3.7 TCM treatment increases Collagen formation by FRCs

Since early experiments indicated an activated status in FRCs upon TCM treatment, resulting in faster attachment and spreading, we aimed to investigate features of this activation status in more detail.

A subpopulation of activated fibroblasts in cancer, so called cancer associated fibroblasts (CAFs), have been identified as important drivers of tumour growth and progression in independent studies <sup>119</sup>.

Therefore we aimed to investigate whether the changes identified in FRCs upon culture in TCM could be the outcome of a similar fibroblast activation signature. Activation of fibroblasts is usually accompanied by increased expression levels of ECM molecules like Collagen or fibronectin, decreased expression of molecules in tight and adherens junctions and overexpression of myofibroblast markers like N-Cadherin (NCAD) and  $\alpha$ -SMA<sup>120</sup>.

Immunoblotting demonstrated an upregulation of Col1 $\alpha$ 2, the pro- $\alpha$ 2 chain of fibrillar type 1 collagen upon culture in TCM (Fig 3.9.A). These results could also be confirmed by immunofluorescent staining of FRCs for type 1 collagen, which revealed an upregulation upon quantification (respective images displayed in 3.9.D) Immunoblotting for other activation markers like N-Cadherin or  $\alpha$ -SMA did not show an upregulation, but in general high levels of both proteins were detected (Fig 3.9.B). This is not further surprising as FRCs are myofibroblasts of mesenchymal origin sharing features with fibroblasts and smooth muscle cells.

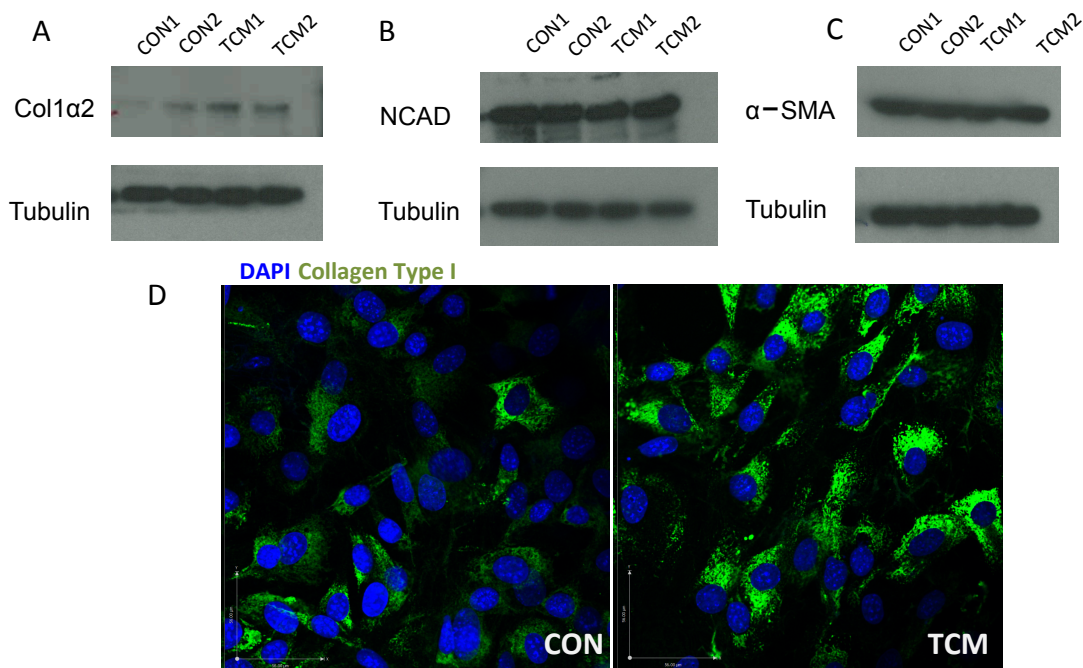


**Fig 3.9 TCM treatment induces upregulation of Collagen type 1**

FRCs were treated for 7 days with CON or TCM and subsequently immunoblotting was performed. An **A** upregulation of Col1α2 but no deregulation of **B** NCAD or **C** α-SMA could be demonstrated by immunoblotting of 40 μg of whole cell lysate. Blotting for α-Tubulin was performed as a loading control. Two independent biological samples were analysed per condition. In **D** representative images of immunofluorescent staining of 7 day TCM or CON treated FRCs for Collagen Type I are displayed. Nuclei are labelled in blue, scale bar represents 56 μm.

Factors such as EGF, FGF, TGFβ or Wnt have been identified as drivers of fibroblast activation<sup>120</sup> and ELISAs previously performed in the lab demonstrated high expression levels of TGFβ (2 ng/ml) within TCM. Based on this finding we tested whether TGFβ in TCM could contribute to these characteristics.

Cells were treated with 5 ng/ml TGFβ for 6 h, 24 h and 72h, lysed and subsequently immunoblotted for Col1α2 and β-Catenin. Western blots revealed downregulation of β-Catenin and increased Col1α2 in response to TGFβ treatment. These were consistent with blots obtained with TCM treatment, showing an exaggerated response likely due to the higher

concentrations used here than those found in TCM (Fig.3.10). The downregulation of  $\beta$ -Catenin observed upon TCM treatment will be the focus of the following section 3.8.

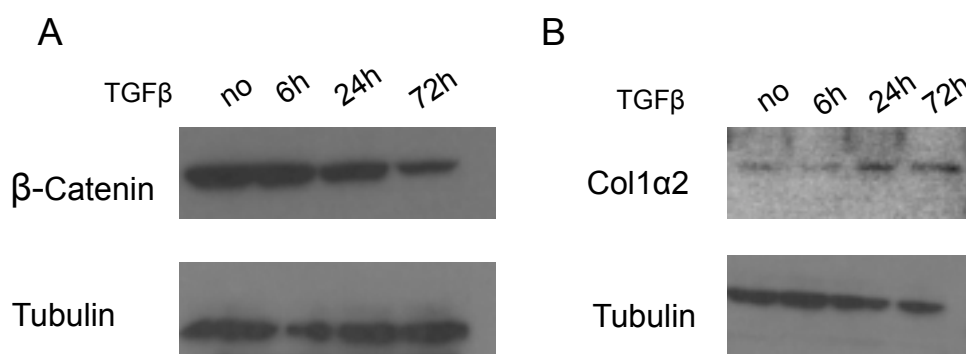


**Fig 3.10 TGF $\beta$  induces downregulation of  $\beta$  -Catenin and increases Col1 $\alpha$ 2 levels**

FRCs were treated with 5 ng/ml TGF $\beta$  for indicated time points and subsequently immunoblotting was performed. In **A** a downregulation of  $\beta$  -Catenin after 24 and 72h could be identified and in **B** an increase in expression of Col1 $\alpha$ 2 over time could be demonstrated by immunoblotting of 40  $\mu$ g of whole cell lysate. Blotting for  $\alpha$ -Tubulin was performed as a loading control. Two independent biological samples were analysed per condition.

### 3.8 TCM treatment increases permeability in FRCs

In the lymph node FRCs form a system consisting of small tubules called conduits that allow the transport of low molecular weight molecules (< 70 kDA) into the node. This size limit is tightly regulated and its deregulation might therefore severely impair the function of the node and present an advantage for the tumour. Based on this theory we aimed to investigate permeability in FRCs using an assay described in 5.6.2.

Permeability was assessed over a time course of 22 h and to confirm the presence of a confluent monolayer, cells were stained with a live-dye prior to starting the assay. This study indicated significantly higher permeability in FRCs pre-treated with TCM than in control treated FRCs (Fig 3.11). It is also of note that the significance of the gained results was increasing over time and highest significance was reached after 22 hours ( $p < 0.001$ ). This indicated a reliable result, since little gaps between cells that could have existed at the

beginning of the assay would have been closed by then, taking the rapid speed of gap closure reported in 3.8 into consideration.

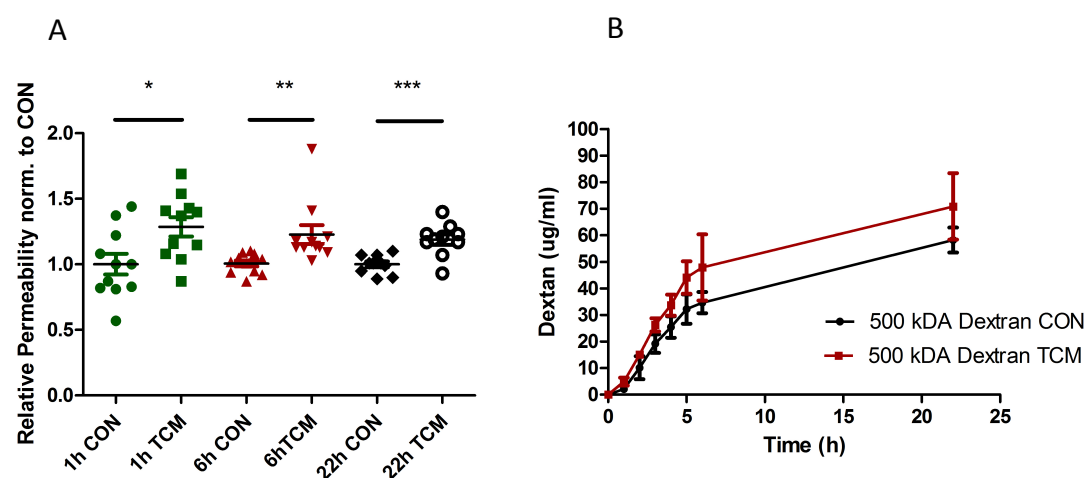


**Fig 3.11 TCM treatment increases the permeability of a confluent FRCs monolayer**

**A** Permeability was investigated over a time span of 22h and measurements taken at 1h, 6h and 22h are displayed in this graph as relative permeability changes normalized on the average of control. Three independent experiments were performed with  $n \geq 3$ . Data is displayed at Mean  $\pm$  SEM. **B** A 22h measurement curve from a single experiment is displayed in  $\mu\text{g/ml}$  dextran. Protein was normalized based on a dextran standard curve and  $n=4$  technical replicates were analysed per condition. Data is displayed as Mean  $\pm$  SD. \* $p < 0.05$  \*\* $p < 0.01$  \*\*\* $p < 0.001$  (Unpaired t-test)

Enhanced permeability in tumour draining lymph node FRCs may translate to increased capacity and rates of transport of small molecules i.e. antigen or chemokines within lymph nodes via the conduit system. Those macromolecules could cross FRCs via either transcellular or paracellular means. Transcellular transport describes a process where molecules travel through the cell body, whereas paracellular transport describes the transfer through intercellular space between cells<sup>121</sup>. As real time PCRs for aquaporin, an integral membrane protein forming pores<sup>122</sup> and mediating transcellular transport did not show an upregulation (data not shown), paracellular transport was brought into focus. Since junctions between cells are accepted as regulators for paracellular permeability, western blot for distinct junctional proteins was performed. Among them Cadherin11, and  $\beta$ -Catenin, which is a subunit of the cadherin complex in so called adherens junctions and regulates



adhesion between cells, were investigated. Immunoblots demonstrated downregulation of Cadherin11, a highly important junctional protein restricted to junctions between adjacent FRCs<sup>30</sup> (Fig 3.12A and D). Upon quantification,  $\beta$ -Catenin was also slightly downregulated at the protein level (Fig 3.12 B and D). Of note is that phosphorylation of  $\beta$ -Catenin at Serin33/37 and Threonine 41 is responsible for subsequent protein degradation<sup>123, 124</sup> and that  $\beta$ -Catenin phosphorylated on these residues was found to be upregulated (Fig 3.12 C), which is in line with the decrease in over all protein.

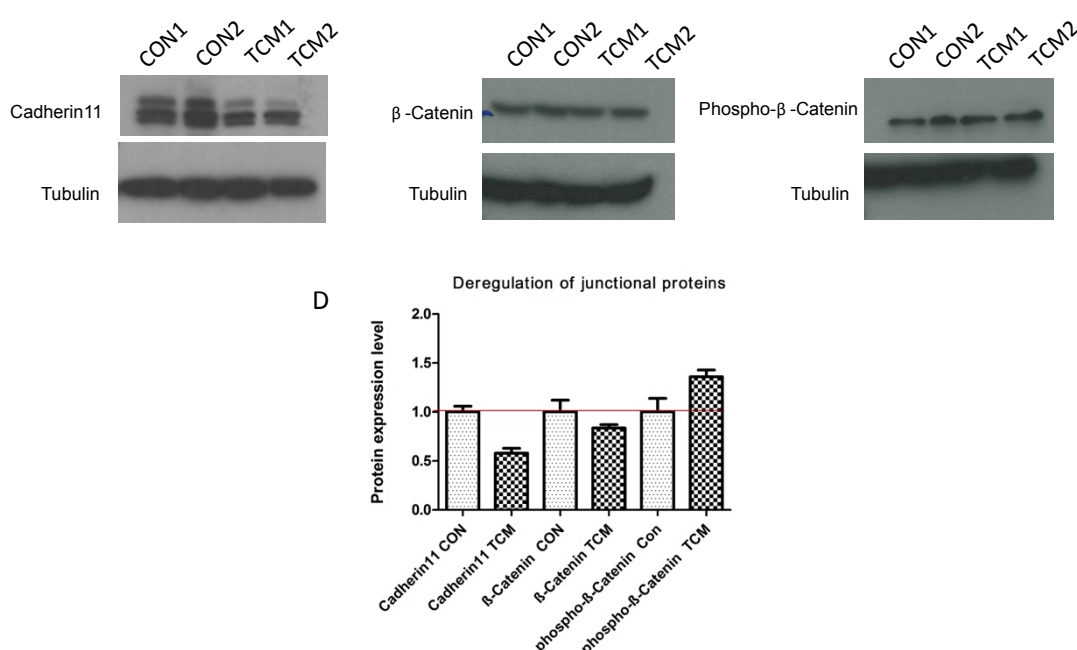


**Fig 3.12 TCM treatment influences expression levels of junctional molecules**

FRCs were treated for 7 days with CON or TCM and subsequently immunoblotting for junctional proteins was performed. A downregulation of **A** Cadherin 11 and **B**  $\beta$ -Catenin as well as an upregulation of **C** phospho- $\beta$ -Catenin could be demonstrated by immunoblotting of 40  $\mu$ g of whole cell lysate.  $\alpha$ -Tubulin, loading control. **D** Quantification of the blots represented in A, B and C was performed with ImageJ and normalized to Tubulin. Two independent biological samples were analysed per condition. Data is displayed as Mean+ SD.



This decrease in levels of junctional molecules further strengthens the hypothesis of an activation signature upon TCM treatment, as distinct studies have reported degradation of junctional molecules upon fibroblast activation<sup>119</sup>.

### **3.9 TCM treatment impacts mitochondrial dynamics and resistance to oxidative stress**

Based on a recent study reporting increase in mitochondrial mass and negative membrane potential in fibroblast activation upon TGF- $\beta$  treatment<sup>125</sup>, we next aimed to investigate whether TCM treatment is also accompanied by changes in the mitochondrial compartment.

In the study mentioned in <sup>125</sup> fibroblasts were transformed into myofibroblasts upon treatment with TGF- $\beta$ , which was accompanied by de-novo  $\alpha$ -SMA expression, morphological remodelling and increase in mitochondrial content. Based on our finding that TCM contains high levels of TGF- $\beta$ , we aimed to investigate its impact on the mitochondrial compartment, expecting to see an increase like reported in <sup>125</sup>. This would also be in line with upregulation of mitochondrial proteins like distinct subunits of ATP synthase, NADH dehydrogenase or Cytochrome C Oxidase observed in the gene array.

Therefore after 7 days of preconditioning in TCM or CON medium, cells were stained with mitotracker green to assess mitochondrial mass and analysed by flow cytometry. Quantification of fluorescence by flow cytometry demonstrated a slight, but significant increase in mitochondrial mass (~10%) (Fig 3.13.A).

To investigate whether these extra mitochondria are functional, cells were loaded with Tetramethylrhodamine- methylester (TMRM), a positively charged dye that has been reported to accumulate in active, negatively charged mitochondria, whereas inactive mitochondria fail to incorporate the dye<sup>126</sup>. We could demonstrate that the increase in mitochondrial mass correlated with an increase in mitochondrial membrane potential, indicating functionality of the mitochondria( Fig 3.13.B).

To further investigate functionality of the mitochondrial compartment, experiments investigating oxygen consumption rate (OCR) and extracellular acidification rate (ECAR) of the cells were performed (data not shown). These

studies did not reveal a significant difference between the two conditions and therefore indicated functionality, but no altered activity of mitochondria upon TCM treatment.

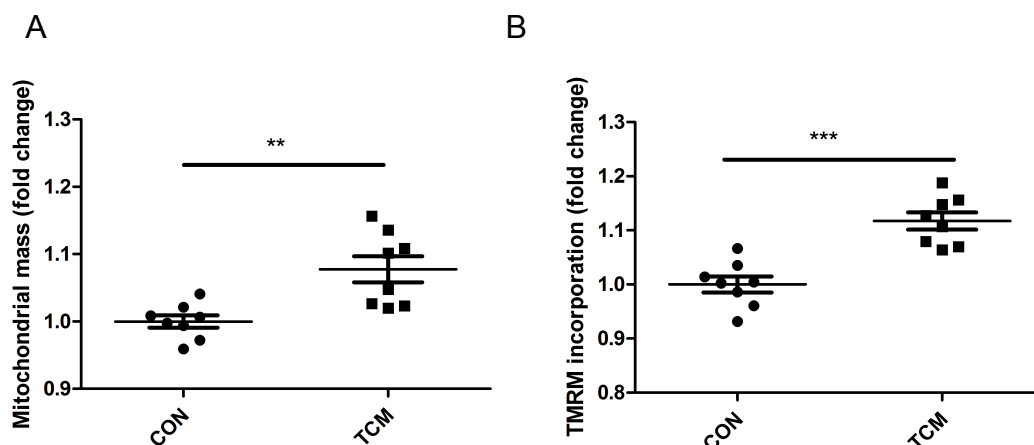


**Fig 3.13 TCM treatment increases mitochondrial mass and activity**

FRCs were treated for 7 days with TCM or CON medium and subsequently analysed for **A** mitochondrial mass by staining with Mitotracker green and **B** mitochondrial membrane potential by staining with the membrane potential sensitive dye TMRM. Flow cytometry was performed and data was analysed by use of FlowJo and gating on single cells. Data is displayed as Mean  $\pm$  SEM \*\*p<0.01, \*\*\*p<0.001 (Unpaired t-test)

As the analysis of Mitotracker green signal by flow cytometry correlates with mitochondrial mass, but does not provide information about mitochondrial morphology, confocal microscopy on cells stained with mitotracker green was performed. Interestingly this study indicated profound differences in mitochondrial structure (Fig 3.14.).

Mitochondria are known to undergo continuous fusion and fission processes, which changes their network morphology dramatically<sup>127</sup>. In FRCs treated with CON medium fused mitochondrial networks expanding throughout the cell could be observed (Fig 3.14.B). However, in TCM treated FRCs mitochondria displayed a fragmented morphology, where they could be observed as individual dots, rather than long fibrillar networks (Fig 3.14.A). This study indicated a change of mitochondrial dynamics induced by TCM treatment.

Oxidative phosphorylation, which is the metabolic pathway whereby cells produce Adenosine triphosphate (ATP) upon oxidation of nutrients in mitochondria<sup>128</sup>, has been indicated as highly up regulated in the pathway analysis of the gene array. This process is the major source of reactive oxygen species (ROS), reactive molecules containing oxygen in cells and since oxidative stress has been linked to distinct cancer types, we aimed to further investigate this topic.

Oxidative stress describes an imbalance between ROS and a system's ability to detoxify those <sup>129</sup>. Elevated levels of ROS have been reported in several different cancer types, where they might be the result of mitochondrial dysfunction, elevated metabolic rates, crosstalk with immune cells or increased peroxisome activity. Yet they are counteracted by increased amount of antioxidant proteins in cancer cells<sup>130</sup>.

Hence we aimed to investigate whether the alterations in mitochondrial dynamics are induced through the alteration of metabolic processes and the upregulation of oxidative phosphorylation. We aimed to stain the cells for endogenous ROS levels by incubating them with CellRox, a dye indicating oxidative stress by emitting fluorescence upon oxidation. The majority of the signal we could observe co-localised with mitochondria in the cell body, yet upon quantification we could not demonstrate higher basal levels of ROS in TCM treated FRCs (data not shown).

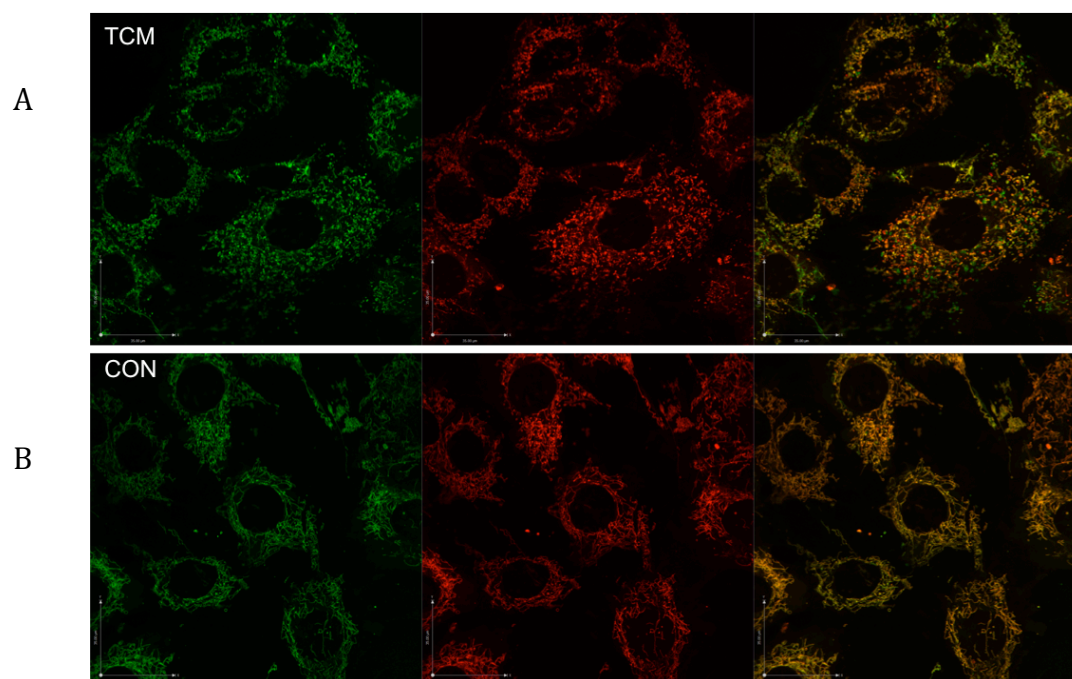


**Fig 3.14 Alterations in mitochondrial dynamics induced by TCM**

FRCs preconditioned for 7 days with **A**TCM or **B**CON medium were stained for mitochondria with Mitotracker green and ROS with Cellroxx and imaged at 100x magnification. Scale bar represents 35  $\mu$ M.

Based on the idea that mitochondrial dynamics are altered and oxidative phosphorylation processes are increased, we next aimed to investigate whether TCM treatment increases the resistance to oxidative stress and allows cells to detoxify ROS faster.

Therefore FRCs preconditioned in TCM or CON for 7 days were treated with different concentrations of  $H_2O_2$  ranging from 1.8 - 500  $\mu$ M. After 24 h the viability of the cells was investigated. On a gross scale, bright field imaging illustrated more cells surviving  $H_2O_2$  treatment when pre-treated with TCM (Fig 3.15.A). Quantification of viability based on the ability of living cells to reduce resazurin to resarufin confirmed significantly higher resistance of cells preconditioned in TCM than of those cultured in CON medium (Fig 3.15.B).

To verify reliability of the reduction based survival assay, crystal violet staining was performed and yielded similar results (data not shown).

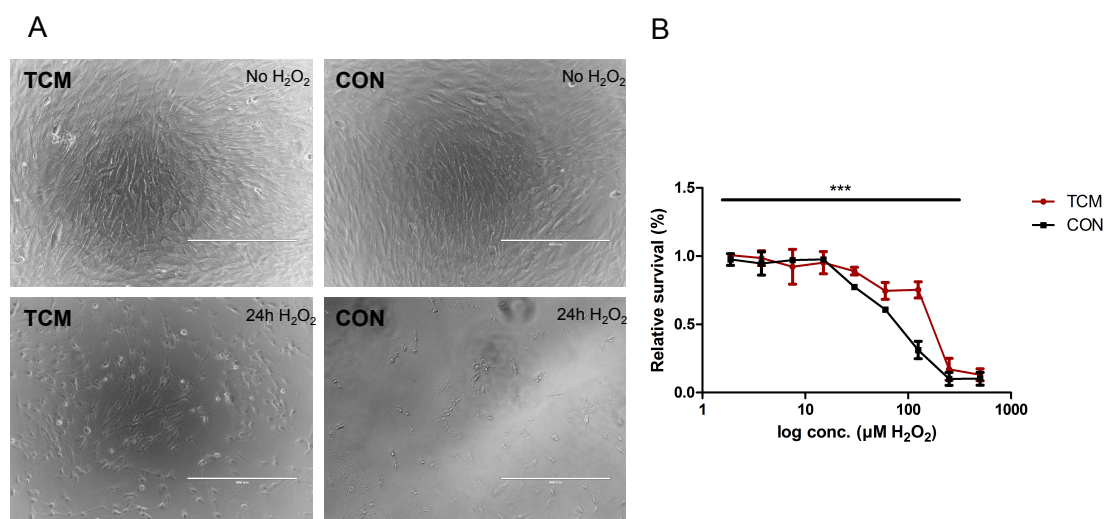


**Fig. 3.15 TCM treatment increase resistance to oxidative stress in FRCs**

Culture of FRCs preconditioned for 7 days in TCM or CON medium in different concentrations of H<sub>2</sub>O<sub>2</sub> for 24h showed significantly higher resistance in TCM treated cells. In **A** respective images of FRCs pretreated with TCM or CON as indicated and incubated without H<sub>2</sub>O<sub>2</sub> or in 150 μM H<sub>2</sub>O<sub>2</sub> for 24h are displayed. Scale bar represents 400 μm. In **B** the X-axis displays logarithmic concentration of H<sub>2</sub>O<sub>2</sub> and relative survival normalized to untreated cells is indicated on the Y-axis. The graph represents 2 independent experiments with each n=3 and a two-way analysis of variance (ANOVA) was used to determine significance. Mean ± SEM are depicted\*\*\*=p<0.001.

Whether the higher resistance is based on the altered mitochondrial dynamics investigated in 3.9 would yet still need further investigation. As mitochondria contain a high number of antioxidant enzyme systems evolved to scavenge ROS<sup>131</sup>, higher mitochondrial mass could be an indicator of the cell's better ability to detoxify them.

We need to point out that these are very preliminary results, generated towards the end of the thesis. In conclusion we could observe slight increases in mitochondrial mass, that correlated with increase in membrane potential and therefore indicated active mitochondria, but no definite differences in OCR and ECAR, despite the morphology of the mitochondria was altered dramatically. Furthermore we demonstrated higher fitness of TCM treated cells in oxidative stress, which might be correlated with the changes in mitochondrial dynamics. Overall further investigation of the mitochondrial compartment would be needed to draw final conclusions.

### **3.10 FRCs treated with TCM are not significantly diminished in their potential to support immune cells**

Earlier experiments showed a significant down regulation of the cytokine IL-7, which has been reported to be crucial for prolonged survival of naïve T cells<sup>132, 133</sup>. This raised the question whether FRCs expressing lower levels of IL-7, as may occur in tumour draining lymph nodes, would show a diminished potential of keeping T cells alive. To address this, pre-treated FRCs were incubated with freshly isolated splenocytes. After 3 days of co-culture, the immune cells were harvested and analysed by flow cytometry. Cells were stained with a live-dead dye and AnnexinV, to determine their state of survival, and for CD3ε to identify T-cells. This showed a slight, but not significantly higher level of dead T cells cultured on FRCs pretreated with TCM, which is in line with the down regulation of IL-7 (Fig 3.16A). This experiment also indicated the total dependence of immune cells on survival factors produced by FRCs, as cultured on their own without growth factors 90% of the cells were dead after 3 days (Fig 3.16A). Gating on CD62L<sup>high</sup> CD44<sup>low</sup> naïve T cells showed again a slight, but not significant decrease in the number of viable naïve T-cells, which in turn fits the hypothesis of a downregulation of IL-7 diminishing survival of naïve T cells (Fig 3.18.B). However, even with a 50% difference in IL-7 production following TCM treatment, with measured levels so low in the cultured FRCs(Fig 3.3.B), this may not be enough to recapitulate the *in vivo* situation.

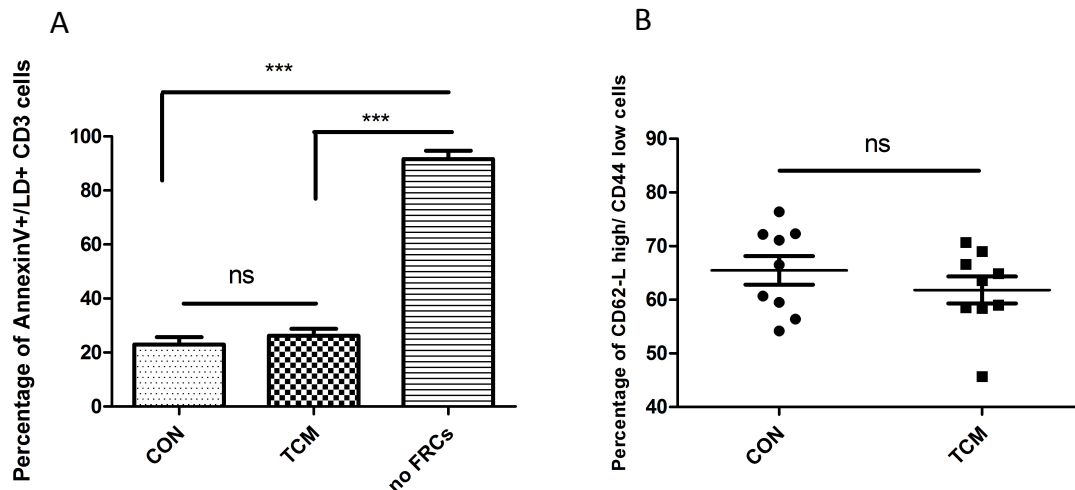


**Fig 3.16 TCM does not diminish FRC's potential to keep T cells alive**

Splenocytes were cultured for 3 days on a confluent monolayer of FRC pre treated with TCM or CON medium or on their own without FRCs and subsequently stained for **A** survival in CD3 T-cells or in **B** for numbers of CD62-L<sup>high</sup> CD44<sup>low</sup> naïve T cells. Data represents three independent experiments with  $n \geq 3$  and is displayed as Mean  $\pm$  SEM., ns not significant, \*\*\* $p < 0.001$ . (t-test)

### 3.11 FRCs take up exosomes secreted by B16 F10 melanoma cells

As the experiments performed in 3.2 indicated that the tumour cell secretome alone is capable of inducing gene expression changes in FRCs, investigation of the components in the TCM triggering the changes was the next aim. Potential candidates are exosomes, small (30-100 nm), cell derived vesicles carrying proteins, lipids, RNA and metabolites<sup>134</sup>. The first key question to ask was whether FRCs take up exosomes secreted by B16F10 melanoma cells at all and if they do, whether exosomes alone are capable of changing PDPN and IL-7 levels. To answer these questions, B16F10 cells secreting fluorescently tagged exosomes were generated. As CD9, CD63 and CD81 are commonly known as exosomal markers<sup>135, 136</sup>, three different constructs tagging each of them with green fluorescent protein (GFP) were generated. All three constructs were successfully cloned, confirmed by sequencing, and upon transfection into B16F10 melanoma cells produced green exosomes as detected by confocal imaging (Fig.3.17). CD63-GFP was subsequently used for further experiments.

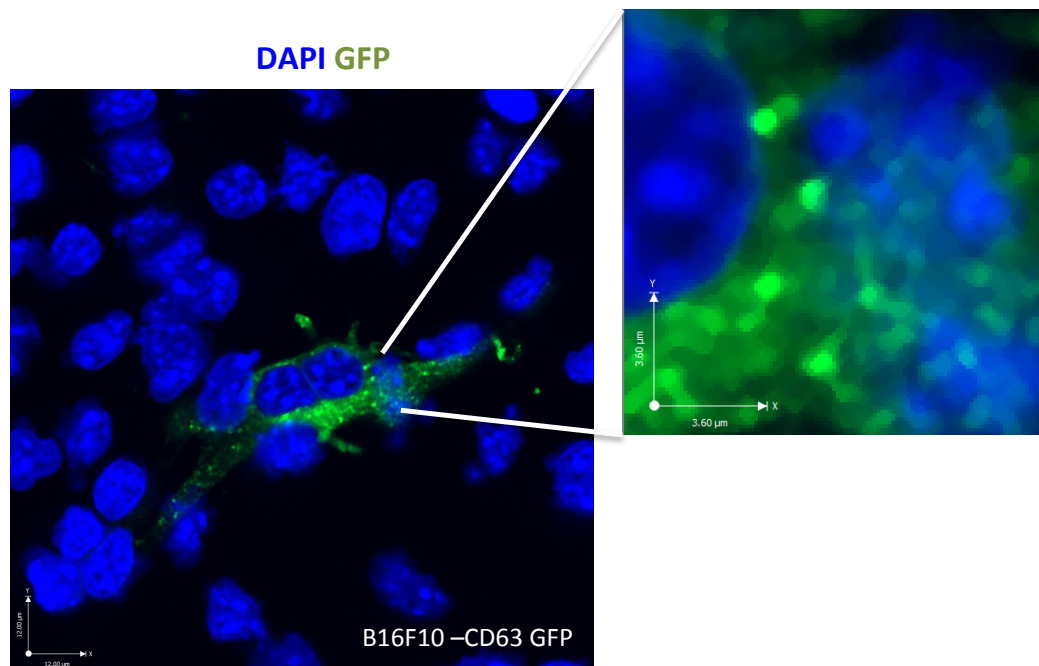


**Fig 3.17 Melanoma cells generate fluorescent exosomes in culture.**

Representative image illustrating B16F10 melanoma cells transfected with the CD63-GFP constructs and fixed 48 h after transfection. Green exosomes in the cell body are detectable as green dots in the cell body. Scale bars represent 12  $\mu\text{m}$  and 3.6  $\mu\text{m}$ . Nuclei are labelled in blue.

To address whether FRCs take up exosomes secreted by melanoma cells, exosomes from a pool of CD63-GFP transfected B16F10s were purified according to 5.5 and subsequently added to FRCs in culture. FRCs remained in the presence of exosomes for 24, 48 and 72h prior to analysis. Confocal imaging identified the presence of green exosomes in the cell body of FRCs (Fig 3.18.A). As a control B16F10 cells were transfected with the empty vector, their exosomes were purified and added to FRCs (Fig 3.18.B). When these were fed to FRCs, no green vesicles in the cell body should be visible, as the empty vector is incapable of tagging exosomes.



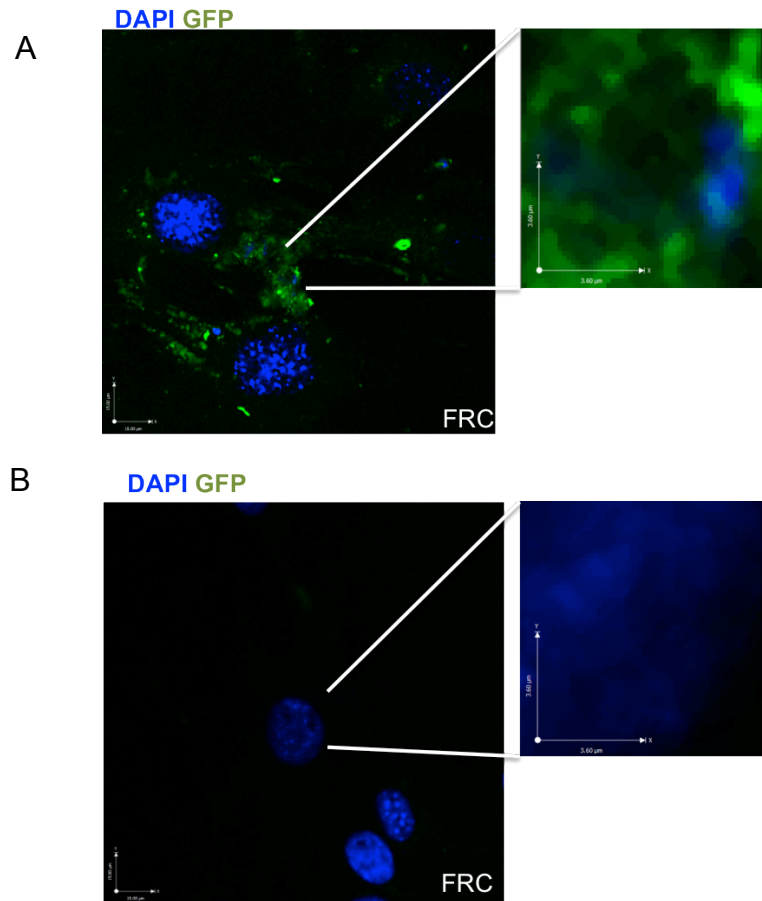


**Fig 3.18 FRCs take up exosomes secreted by melanoma cells**

Exosomes were purified from B16F10 transfected with **A** the CD63-GFP construct or **B** the empty tGFP vector and added to FRCs. 24h post adding FRCs were fixed and imaged at 100x magnification. Scale bars represent 15 µm and 3.6 µm, nuclei are labelled in blue.

FRCs engulfed GFP tagged exosomes as early as 24h after addition but processed them rapidly, as after 48h exosomes were no longer detectable (data not shown). Given that FRCs indeed take up exosomes secreted by tumour cells, it was therefore possible that these biologically active vesicles could be responsible for the changes in gene expression.

### 3.12 Exosomes do not induce changes in PDPN and IL-7 mRNA levels

The confirmation that FRCs take up exosomes secreted by melanoma cells led to the question of whether the effects of TCM treatment on PDPN and IL-7 levels was mediated by exosomes rather than other media components. Therefore purified exosomes were added to FRCs for a period of 7 days and replaced every 48 h. Serving as a control, supernatant from the exosome purification (i.e. exosome depleted media) was collected and added to the cells in the same manner. As with previous TCM experiments, RNA was extracted after 7 days, and two targets IL-7 and PDPN were assessed by qPCR (Fig 3.19.A and B, depleted media and exosomes respectively).

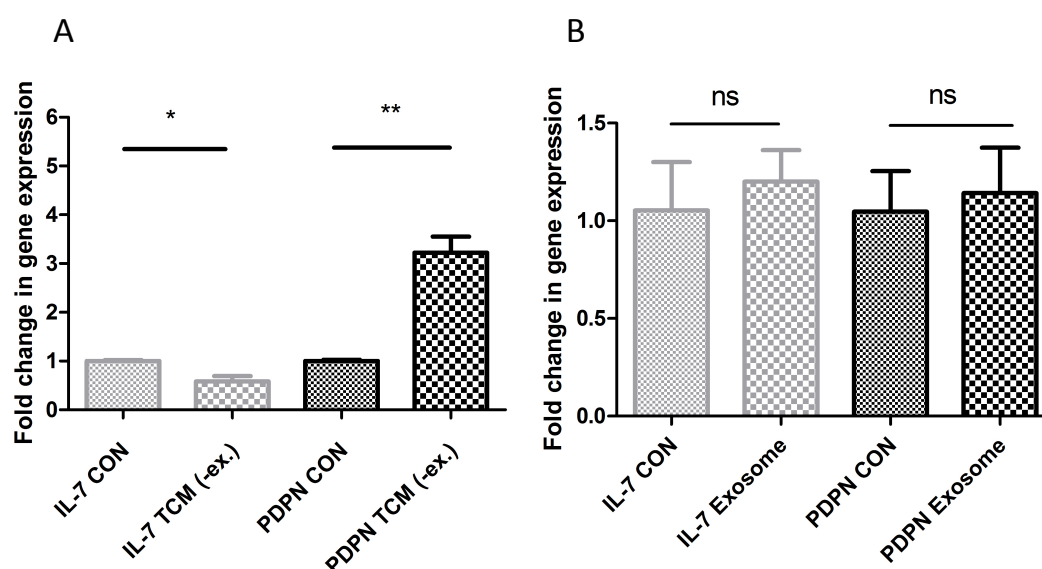


**Fig. 3.19 Changes in PDPN and IL-7 are mediated by soluble factors in TCM**

mRNA expression was analysed from **A** FRCs fed with the supernatant of the exosome purification containing soluble factors but lacking exosomes or **B** FRCs fed with the exosomal pellet over 7 days and normalized to two housekeeping genes. Data is representative of two independent experiments with each  $n \geq 2$  biological replicates and indicated as Mean  $\pm$  SEM. ns not significant; \*  $p < 0.05$ ; \*\*  $p < 0.01$  (Unpaired t-test)

As with complete TCM, changes in IL-7 and PDPN mRNA levels were again induced by the exosomes depleted supernatant, but not by the exosome pellet alone. This implies that changes to PDPN and IL-7 level are mediated by soluble factors found in the TCM rather than the result of factors delivered within exosomes. Yet it is necessary to point out that this study only focused on two targets and even if these were not deregulated by exosomes, others

may be. Hence further investigation on different target genes would need to be performed to fully conclude upon the effect of exosomes on FRCs.

### **3.13 Cytokine expression profiles of TCM and tumour lysates are highly different**

Applying the simplified model of TCM treatment to FRCs enabled us to reproduce some changes reported in the gene array of FRCs out of a TDLN, yet others could not be recapitulated merely through conditioned medium treatment. This could be due to a number of reasons, e.g physical changes induced by the tumour like increased fluid flow or size expansion which are missing in our *in vitro* model. Another potential reason could be that *in vivo* a tumour does not consist only out of tumour cells, but comprises a microenvironment containing several other cell types like CAFs or infiltrating immune cells<sup>137</sup>.

Therefore we aimed to address the complexity of the TCM and compare its protein expression profile to the lysates of tumours excised from mice injected with B16F10 melanoma cells.

For this purpose another variant of TCM was generated which may begin to more closely resemble the milieu present in the tumour microenvironment. This was termed microenvironment conditioned medium (MCM) and was derived from 60% tumour cells cultured with 20% CAFs and 20% freshly isolated immune cells. The secretome of tumour cells on their own and of the generated “microenvironment” was compared to *in vivo* tumour lysates using a proteome profiler array. The array, containing 111 cytokines, clearly indicated an increase in complexity from TCM to MCM, as well as from MCM to actual tumour lysates (Fig 3.20, full size images in appendix 8.5). As expected, tumour lysates contained many different growth factors and immune modulatory cytokines, of which several could be found in TCM. High expression levels of CCL5, Thrombopoietin, Cystatin C, Osteopontin and WISP-1 (CCN4; WNT inducible signalling pathway protein 1) could be detected in both TCM and MCM. Differences between MCM and TCM implied expression of CCL2, IGFBP6 (Insulin like growth factor binding protein 6),

VCAM-1 and Serpin E-1, which were visible in MCM, but could not be detected in the secretome of tumour cells on their own.

Both tumour lysates were highly comparable in their cytokine expression profile with only marginal differences, yet striking differences between tumour lysates and conditioned medium could be detected. These differences comprise the expression of IL-1a, IL-1ra, FGF-1, CCL6, CCL12, CXCL9 and CXCL10 in tumour lysates but not conditioned medium. In conclusion this array supports the hypothesis that the diminished complexity of TCM when compared to tumour lysates might display another reason why several changes indicated in the gene array were not reproducible by TCM treatment alone. These differences in the cytokine profile will also be the focus of the following discussion. The intensity of spots on the cytokine array was thereafter quantified using ImageJ and a detailed list of expression levels of all cytokines can be found in Fig 3.21.

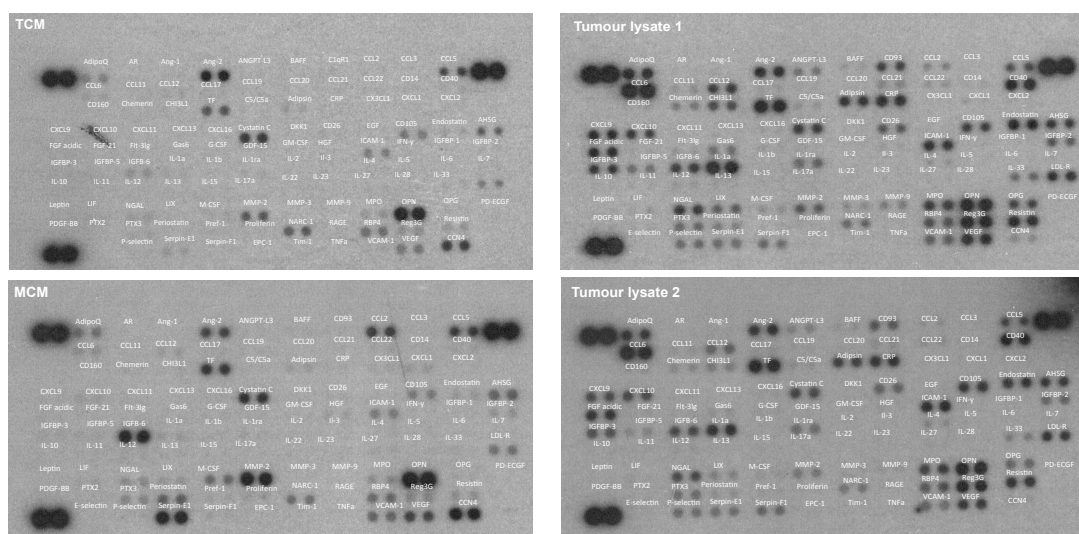


**Fig 3.20 Complexity of TCM is diminished compared to tumour lysates**

1 ml of TCM or MCM and each 1 mg of two different tumour lysates was analysed in a Proteome Profiler Cytokine array detecting 111 cytokines. The spots in the upper left, lower left and upper right corner function as positive controls and the clear space in the lower right corner indicates the negative control.



## 4. Discussion

Since metastasis remains the leading cause of cancer-associated mortality, a better understanding of this exceedingly complex, multi-step process is crucial for the improvement of therapeutic strategies<sup>138</sup>. Recent studies have increased our knowledge about cancer cells spreading through the blood stream, yet the process of metastasis throughout lymphatic vessels is less understood. A common feature of many cancers is the spreading through lymphatic vessels to lymph nodes, where nodal metastases are formed<sup>139</sup>. This initiates a series of events leading to further spread of tumour cells through the blood stream and ultimately to formation of further tumours at distant sites and death<sup>6, 79</sup>. A therapeutic option to block the metastatic cascade is highly sought, and the removal of the regional lymph node is considered as the primary therapeutic strategy to inhibit the chain of cancer progression<sup>79</sup>. Yet this carries complications such as the onset of lymphedema due to disruption of lymph drainage<sup>140</sup>. Therefore developing a non-surgical therapeutic strategy that could reverse this immune-dampening effects and prevent the formation of metastasis and subsequent secondary tumours, is an ultimate goal<sup>141</sup>.

However, a major unanswered question is, how these sentinel lymph nodes provide an environment capable of supporting metastatic tumour cells, given that they are one of our prime immunological hubs.

As sentinel nodes directly drain the tumour and its contents, they are likely influenced remotely and adapt to tumour-derived signals. Indeed, previous reports indicated that they may be partially immune suppressed<sup>142,79, 78</sup>. We also know from our own data, that TDLN undergo dramatic remodelling and enlargement. Therefore, the work performed in this thesis aimed to generate further knowledge regarding the TDLN towards understanding the complex metastatic cascade. In this project the focus lies on FRCs, non-hematopoietic stromal cells of the lymph node that are essential for structure, maintenance and immune function of the node.

*In vivo*, lymph nodes are difficult to study due to the anatomic locations, but also because of their complex, dynamic nature. The node is comprised of multiple, densely packed cell types that reciprocally influence each other even under resting conditions. Thus, extending this understanding to the context of events and interactions in nodes draining an upstream tumour, that does not only secrete soluble factors but also induces physical changes by increased fluid flow and size expansion, is extremely difficult. This was highlighted by work in the Shields Lab indicating that FRCs in the TDLN not only expand and remodel, but also undergo significant transcriptional reprogramming as tumours develop.

The work in this thesis attempted to develop an *in vitro* system that would help to dissect the complex *in vivo* situation, investigating the aspect of tumour secretion without the confounding effects of mechanical components or the impact of other cells types on FRCs. The model developed was able to show that medium derived from tumour cells is sufficient to induce changes in FRCs and highlights the strong influence a tumour exhibits by drainage into a downstream located node. To do this, an *in vitro* culture model was established, where FRCs were treated with TCM or CON medium over a time span of 7 days with replacement of medium every 48 hours. This was done with the purpose to simulate consistent drainage from an upstream tumour and the timespan was chosen after investigating shorter and longer treatment periods and finding the most consistent and reproducible changes after 7 days. Despite its simplicity this model could induce gene expression changes at mRNA level, which were also found translated into deregulated protein levels. This strengthens the hypothesis that soluble factors secreted by a tumour change gene expression programmes in FRCs, which in turn might influence function and structure of the lymph node.

#### **4.1 FRCs pretreated with TCM display an activated phenotype**

Having demonstrated the functionality of the experimental model by showing changes at mRNA and protein level (Fig 3.2, 3.3), functional assays to investigate proliferation, morphologic changes and migration were performed.

However these assays did not show a difference between TCM and CON treatment (Fig 3.7, 3.8). Here it is necessary to take the p53<sup>ER/ER</sup> nature of the used FRC cell line into consideration. The loss of p53 enables long-term culture of FRCs, as p53 is known to control the G2/M and G1 checkpoints in the cell cycle<sup>143</sup>. Its loss is therefore accompanied by accelerated progression through the cell cycle and increased proliferation. This might explain why no increase in proliferative capacity or migration upon TCM treatment could be observed (as it was *in vivo*), since minor differences could be masked by the highly increased basal proliferation rate compared to primary cells.

Although an increase in migration potential or proliferative capacity could not be demonstrated, several other signs of an “activation signature” upon TCM treatment were investigated. Collagen gel contraction assays demonstrated that FRCs pretreated with TCM exhibit faster contraction of collagen gels (Fig 3.9) using a “floating contraction model”. After 24 hours, contracted gels were stained to visualize the developed FRC networks and thereby it became obvious that TCM treated cells expanded faster throughout the gel (Fig 3.10). We subsequently hypothesized that the higher contraction level of collagen gels might be the outcome of a pre-activated state in TCM-exposed FRCs, which allows them to expand faster, inhabit larger areas of the gel and increase contraction. Interestingly other studies reported an increase in gel contraction by fibroblasts upon TGFβ treatment, as they convert into an activated phenotype<sup>144</sup>. Fibroblast activation is a crucial process in wound healing; moreover recent studies indicated activated fibroblasts as critical for tumour progression. The activation of fibroblasts is a process induced by TGFβ (which is also produced by B16F10 melanoma cells, as shown in the Shields lab), FGF and several other growth factors and leads to a conversion from a fibroblastic to a myofibroblastic phenotype. This is accompanied by increased deposition of ECM molecules, loss of cell-cell junctions through degradation of junctional proteins and morphological remodelling<sup>119</sup>.

As FRCs are myofibroblasts of mesenchymal origin they already display partial activation, which is characterized by their expression of α-SMA (Fig 3.14.C)<sup>145</sup>. Yet we hypothesize that in a lymph node located downstream of a draining tumour, FRCs obtain an even more activated phenotype.



We therefore suggest a model where, upon drainage by a tumour, FRCs adapt to tumour derived signals and convert into a special subtype of “cancer associated FRCs”.

To adhere, extravasate, survive and subsequently proliferate to form a secondary tumour in “foreign soil”, the tumour requires a receptive microenvironment<sup>146</sup>. Distinct studies have reported a “priming” of the destination site before arrival of the first cancer cells into a favourable environment for cancer cell adhesion and invasion<sup>147, 148</sup>.

In our model support for this hypothesis could be found by immunoblotting on 7 day TCM treated FRCs, where we demonstrated an upregulation of Col1 $\alpha$ 2 (forming the pro-  $\alpha$ 2 chain of Collagen I, a crucial ECM component of FRCs).

Strikingly melanoma cells have specifically been reported to attach to Collagen type I and Laminin via Integrin  $\alpha$ 2 $\beta$ 1<sup>149</sup>, therefore an upregulation of Collagen I on FRCs in the lymph nodes induced by the tumour secretome might represent an advantage for the attachment process of cancer cells. In general the composition and stiffness of the ECM at the premetastatic niche has been recognized to directly influence tumourigenesis<sup>150</sup>.

We could also detect further signs of a fibroblast activation process happening in FRCs, like the downregulation of junctional molecules like  $\beta$ -Catenin and Cadherin 11. To demonstrate that the upregulation of Col1 $\alpha$ 2 and the decrease in  $\beta$ -Catenin are mediated through factors inducing fibroblast activation, we performed immunoblots for TGF $\beta$  treated FRCs and could recapitulate the changes seen upon TCM treatment (Fig 3.15).

Moreover a recently published study showed that TGF $\beta$  mediated fibroblast activation is accompanied by an increase in mitochondrial mass and membrane potential. Hence both parameters were investigated and a slight, but significant increase (~10%) in membrane potential and mitochondrial mass was noted (Fig 3.16).

We see these as further pillars for the hypothesis of an activation of FRCs in the draining node.

## 4.2 Permeability of FRCs increases upon TCM treatment

Studies performed to investigate changes in permeability of FRCs upon TCM treatment demonstrated an increase in permeability, which we believe is because of the degradation of junctional molecules between cells (Fig 3.12).

The lymph node is a shielded region into which cells can only enter via active movement over a layer of cells lining the sinus region. Moreover fluid can only enter deeper into the node via small tubules forming a so-called conduit system. This system is mainly formed by FRCs and works as a molecular sieve<sup>151</sup> with a tightly regulated size limit of 70 kDA. This size limit allows the rapid transportation of chemokines produced at inflammation sites, as well as the transport of low molecular weight antigens but inhibits entry of pathogens (bacteria and viruses) deeper into the node. Conduit- associated dendritic cells that cross the membrane barrier with their extensions, can pick up low molecular weight antigens in conduits and subsequently present them to T cells<sup>152</sup>. However bigger particles arriving via the lymph are unable to enter conduits and instead get caught by macrophages or dendritic cells lining the sinus.

A degradation of junctional molecules located between adjacent FRCs and the disruption of the microvasculature prior to arrival of cancer cells would increase the permeability of the conduits and might allow larger debris or proteins to enter, thereby disrupting normal immune surveillance functions.

The neat size limit usually prevents larger particles from entering into the conduit system and thus ensures that macrophages residing within the sinus catch them<sup>151, 153</sup>. By increasing the permeability of conduits tumour cells might have developed a strategy to avoid the processing of tumour derived antigens carried within the lymph in the sinus and instead leaking into the inner region, where less macrophages are localized. There they might get picked up by other cell types, which could alter the kinetics of immune surveillance. Moreover, if the conduit system is more permeable, cytokines produced by FCRs might on the other side leak out of the system, thus not being transported to the region where they usually belong. The initiation of subsequent immune responses, as well as the under resting conditions tightly controlled localisation of distinct immune cell types might therefore be

disrupted. Overall the loss of the tightly regulated sieve system may therefore severely impair the node in inducing an immune response against tumour-derived antigens and represent a crucial advantage for the tumour.

The physiological relevance of this *in vitro* generated results is supported by studies performed in the Shields Lab, whereby fluorescent dextran molecules of different sizes were injected into the footpad of tumour bearing mice and leaked further into the lymph node than in non tumour bearing animals (unpublished data).

#### **4.3 TCM treatment reduces IL-7 secretion by FRCs**

IL-7, a regulatory cytokine produced by FRCs and influencing development of T cells, DCs and B cells, was found to be downregulated after TCM treatment at mRNA and protein level (Fig 3.3, 3.4). This supported the results generated in the gene array conducted on FRCs out of a TDLN that showed decreased gene expression for IL-7 *in vivo*. As IL-7 has a profound impact on homeostasis and survival of naïve and CD8 T-cells, function of dendritic cells and development of T cells, B cells and DCs, a decrease in expression might represent an advantage for the tumour<sup>108, 106, 105</sup>. Distinct studies have reported IL-7 as a non-redundant cytokine<sup>105</sup> and its reduction to below 50% of usual secretion levels by the tumour secretome might severely impair survival and development of immune cells.

This theory is strongly supported by independent studies, showing increased survival after administration of exogenous IL-7 in multiple cancer models due to expansion of CD4<sup>+</sup> and CD8<sup>+</sup> T cells<sup>154,155,156</sup>. In an approach to investigate this hypothesis in our *in vitro* model, splenocytes were isolated out of mice and cultured on FRCs preconditioned with TCM or CON medium. After three days of culture the survival of CD3ε cells as well as the number of naïve T cells was investigated by flow cytometry. Although this experiment indicated the absolute dependence of immune cells on FRCs *in vitro*, we could not detect significant increases in numbers of dead CD3 cells or decreases in number of naïve T cells after conditioning FRCs with TCM as hypothesized. Even though the trend in the experiments pointed in the right direction, with an increase of dead CD3ε cells from ~20 to 25% and a

decrease of naïve T cells from ~ 65% to 60% of all T cells, variability between different repeats was high and significance could not be reached (Fig 3.18). Here we would like to point out that the secreted levels of IL-7 by the FRC cell line used were extremely low, ranging for 5-10 pg/ml as investigated by ELISA studies (Fig 3.3). As all *in vivo* studies we could refer to only measure mRNA<sup>7,157</sup>, but no protein levels, we did not have a reference to compare this secretion levels to primary cells. The fact that no studies reporting IL-7 *in vivo* secreted by FRCs on protein level could be found, might indicate that doing so is technically demanding and IL-7 might e.g have a short half live time. Another potential mechanism why IL-7 levels *in vitro* might be reduced is a study from 2009 referring to the cytokine CCL21. This study shows that under two-dimensional and static conditions, these cells do not secrete CCL21, whereas primary cells or those cultured under flow or in 3D do<sup>115</sup>. If this theory applies for other cytokines like IL-7, this might display another reason for the marginal phenotype observed.

Moreover *in vivo* the situation is so much more complex and survival of immune cells in the tumour-draining node might be the result of a cumulative effect, as other non-hematopoietic cell types might as well influence immune cell populations. Further we should consider that the immune cells in this study have not been exposed the tumour secretome itself, but only to the altered secretome of FRCs after conditioning with tumour cell medium. Tumour cells are known to secrete a variety of immunosuppressive cytokines<sup>79</sup>, which will clearly alter the immune cell composition in the node and might in turn influence survival.

Despite not detecting a significant alteration in survival, we believe that the 50% reduction of secreted IL-7 levels we could induce with TCM treatment has an impact in the *in vivo* model, where secreted levels of IL-7 might be higher and act together with other cytokines secreted by stromal cells.

#### **4.4 Model advantages and limitations**

The p53<sup>ER/ER</sup> genotype of the used cell line might be limiting in certain aspects like investigating subtle proliferative effects of TCM treatment, yet allows to

perform large numbers of experiments in short time, which would not be possible with primary cells. We tried primary cells but had significant batch to batch variation in terms of yield and purity, and to get enough to perform all the assays described would have involved harvesting nodes from large numbers of mice. We strongly believe that the p53<sup>ER/ER</sup> cell line is a good model system, as we could investigate several significant changes with this experimental model, many of which also reflected the results gained in the gene array of primary cells. Furthermore the p53<sup>ER/ER</sup> model is commonly used in research work dealing with FRCs and therefore a well-established system<sup>115</sup>.

As mentioned before, the biggest advantage, and yet the biggest drawback, of our *in vitro* based treatment model is its simplicity. Establishing an experimental model is always a compromise of getting close to the *in vivo* situation and simplifying the model to gain understandable and traceable results. The tumour draining lymph node is exceedingly complex as it contains tremendous numbers of cells and many different cell types. Also a tumour *in vivo* does not only consist of a sheer bulk of tumour cells, but contains several distinct cell types in its microenvironment, that contribute to the tumour secretome. Our model simplified the interactions between tumour and TDLN to two cell types, namely B16F10 tumour cells and FRCs. This allowed us to conclude, that all the changes we saw in the FRCs upon TCM treatment were induced by the B16F10 secretome alone. It would not be possible to draw this conclusion easily based on the results gained *in vivo*, as so many cell types are involved.

Albeit we could reproduce some changes found in the gene array, others (e.g CCL21, CD44 or Vinculin deregulation) could not be recapitulated, which might be a reflection of the system's simplicity. Firstly FRCs in the lymph node might be exposed to other factors from the tumour microenvironment, which might not be found in the simple tumour conditioned medium.

To address this question, we decided to perform proteome profiler arrays comparing TCM with lysates from tumours excised from mice injected with B16F10 cells, which will be the focus of the following paragraph.

Moreover we also investigated the impact of exosomes, which might be secreted by the tumour and transported to FRCs within in the lymph, but did not find these as responsible for changes investigated.

To include a further degree of complexity we aimed to investigate the enhanced fluid flow induced by the tumour by culturing FRCs in flow systems. These very preliminary studies indicated that upon exposure to flow FRCs increased levels of secreted CCL21, yet were due to time limitations not taken further.

Performing a cytokine array on tumour conditioned medium and comparing it to lysates generated from *in vivo* tumours helped us to trace the difference between the TCM and an actual tumour and indicated factors that were missing in the medium and might explain the changes we couldn't reproduce from the gene array. This experiment also included conditioned medium from a mixture of tumour cells, CAFs and immune cells and thereby provided an interstage between our simple model and the highly complex tumour (Fig 3.19).

This proteome profiler investigating 111 cytokines indicated a variety of differences between TCM and tumour lysates. TCM contained about 20 cytokines detected on the array, among them the highest expressed ones were Angiopoietin-2, Thromboplastin, Cystatin C, Metalloproteinase 2 , Osteopontin and CCN4 (Wnt induced secreted protein 1). Angiopoietins are growth factors involved in angiogenesis<sup>158</sup> , whereas Thromboplastin plays a role in blood coagulation<sup>159</sup> and Osteopontin fulfils a diverse set of functions, ranging from recruitment of immune cells to cell attachment and wound healing<sup>160</sup>. All the factors expressed in TCM could be found in tumour lysates at similar or higher levels, except for CCN4 which is more abundant in TCM and MCM. Interestingly CCN4 is known to bind ECM molecules<sup>161</sup> and might therefore be altered due to differences in matrix stiffness between culture flasks *in vitro* and connective tissue *in vivo*. The differences between TCM and MCM were quite subtle, yet two additional proteins in MCM were highly abundant. These two factors were IGFBP-6 and Serpin-E1; the former regulating proliferation and differentiation via binding insulin like growth factors (IGF)<sup>162</sup> and the latter a major inhibitor of fibrinolysis, a process inhibiting blood clotting and a marker of poor prognosis in melanoma<sup>163</sup>.

Interestingly CCL2 was found to be expressed in the MCM, but only present at minor levels in tumour lysates. As CCL2 is expressed by macrophages, dendritic cells and monocytes, we therefore hypothesize that higher levels of these cells were present in our MCM model, than in a tumour *in vivo*.

Tumour lysates contained a broad spectrum of about 50 cytokines displayed in the gene array, among them a variety of factors that couldn't be found in TCM. Several of these proteins were immune-modulatory cytokines like CCL6, CXCL9, CXCL10, and IL-1a. Strikingly these factors are highly secreted by activated macrophages<sup>164</sup> or involved in the attraction of these cells and several studies have indicated that tumour associated macrophages (TAMs) play a crucial role in cancer progression<sup>165</sup>. We therefore hypothesize that several of these factors were secreted by TAMs and were missing in our TCM model. Moreover several proteins of the complement system were noted, like Adipsin or C5/C5a. The complement system has long been seen as an effective way of the immune system to kill tumour cells, but has now been reported to be of advantage for cancer growth by promoting chronic inflammation and angiogenesis<sup>166</sup>. Rather surprisingly, TGF $\beta$  was not on the panel of the array, but has previously been reported to be secreted by B16F10 cells based on an ELISA conducted in the lab. This experiment indicated a variety of differences between our used TCM model and tumour lysates, but also showed that the complexity of our simple model is already quite high. The results gained also indicated that factors expressed in TCM are also found *in vivo* in tumours and are therefore not artefacts of *in vitro* cell culture, but have physiological relevance.

#### **4.5 Conclusions and future directions**

The work performed in this thesis shows that some aspects of lymph node stromal functions can be modelled in very simple systems *in vitro*. Here we have been able to show on multiple platforms that FRCs adapt to tumour derived factors with alteration in key factors like upregulation of PDPN, or decrease in secreted levels of IL-7. Moreover we could demonstrate that the alteration status of cells is altered and we think that, considering the adapting environment, these changes have the potential to impact localisation of

survival of immune cells in the lymph node. Furthermore we believe that some occurring alterations might represent an advantage for the tumour, like the observed alterations in ECM, which could improve attachment of tumour cells. The noted increase in permeability might disrupt immune surveillance and allow tumour derived antigens to escape detection mechanisms.

For future work it would be important to step-by-step increase the complexity of the simple model and thereby approach the complex *in vivo* situation. As a next step mechanical cues like fluid flow and shear stress could be included into the model, potentially highlighting changes that could not be detected under static conditions. Including CAFs and infiltrating immune cells into the model could increase the complexity of the tumour-conditioned medium, thereby more closely resembling the tumour lysates investigated in the cytokine array (Fig 3.20). Moreover further work on the results generated so far could be performed, to dissect the molecular mechanisms behind the changes. Oxidative stress resistance and mitochondrial dynamics could be brought more into focus, to investigate the factors causing these alterations. Another interesting point for the future would be to perform co-cultures of melanoma cells with FRCs, that have either been preconditioned with TCM or CON medium, to investigate the effect of “priming” of FRCs in the premetastatic niche on the later arrival and invasion of tumour cells.



## **5. Material and Methods**

### **5.1 Cell culture**

#### **5.1.1 Melanoma cell lines**

Mouse B16F10 melanoma cells were cultured in Dulbecco's Modified Eagle Medium (DMEM; 61965-026, Life Technologies) supplemented with 100 U/ml Penicillin-Streptomycin (PS; 15140-122, Life Technologies) and 10% foetal bovine serum (FBS; Sigma Aldrich). B16F10 melanoma cell line was purchased from ATCC® (CLR-6475).

#### **5.1.2 Fibroblastic reticular cells**

Mouse C57BL/6 p53<sup>ER/ER</sup> FRCs were maintained in RPMI -1640 (R875, SIGMA) supplemented with 100 U/ml PS, 10 % FBS, 2 mM HEPES (15630106, Life Technologies) and 0.5 µl β-Mercaptoethanol (β-ME; 444203, Calbiochem). These cells are deficient for the tumour suppressor p53 and can therefore be maintained in long-term culture.

#### **5.1.3 Isolation and culture of mouse derived lymph node stromal cells**

Lymph nodes were removed from sacrificed C57BL/6 mice (female, 10 weeks), placed in sterile phosphate buffered saline (PBS) and broken apart with 19-gauge needles. Nodes were subsequently digested for 30 min at 37°C in PBS containing 1 mg/ml Collagenase A (10103586001, Roche) and 0.4 mg/ml DNaseI (11284932001, Roche) while shaking gently. After the 30 min incubation step 1 mg/ml Collagenase D (11088866001, Roche) and 0.4 mg/ml DNaseI were added, followed by another 30 min incubation at 37 °C. To inhibit collagenase EDTA was added to a final conc. of 5 mM. To ensure single cell suspensions, cells were passed through a 70 µm cell strainer, counted and plated at a density of 500 000 cells/cm<sup>2</sup> in FRC growth media. Cells in suspension (immune cells) were removed over the following days by subsequent washes and media changes.

#### **5.1.4 Isolation of mouse derived splenocytes**

The spleen was removed from a sacrificed C57BL/6 mouse (female, 10 weeks), placed in PBS, mechanically disrupted with 19- gauge needles and passed through a 70  $\mu$ m cell strainer. Erythrocytes were lysed in red blood cell lysis buffer (150 mM  $\text{NH}_4\text{Cl}$ , 10 mM  $\text{NaHCO}_3$ , 0.4 % EDTA, pH= 7.4) for 5 min on room temperature. Blood cell lysis buffer was inhibited with 10 ml of splenocyte medium (IMDM (21980-032, Life Technologies) supplemented with 10 % FBS, 100 U/ml Pen/Strep and 0.5  $\mu$ l  $\beta$ -ME) and the cell suspension was centrifuged for 4 min at 500 g. The remaining pellet was re-suspended in medium, counted and plated at a density of  $10^6$  cells/ ml in 6 well plates.

#### **5.1.5 Cell passage**

##### **5.1.5.1 B16-F10 and FRCs**

Cells were cultured in a humidified incubator with 5%  $\text{CO}_2$  at 37 °C and passaged at 60-90% confluence. Therefore culture medium was aspirated, cells were washed twice in PBS and detached with 0.25% Trypsin-EDTA (25200-072, Life Technologies). To allow detachment, cells were incubated for 5 min in trypsin at 37 °C. Trypsin was neutralized by addition of full medium and cells were re-suspended at 1:10 dilutions in fresh culture medium.

##### **5.1.5.2 Splenocytes**

Cells in suspension were re-suspended in culture medium and transferred into 50 ml polystyrene tubes. Cells were counted, centrifuged for 4 min at 500 g and re-suspended at a density of 1 Mio/ml in fresh medium.

#### **5.1.6 Cryopreservation**

For cryopreservation cells were detached following 5.1.5.2, re-suspended in freezing medium (60% full growth medium, 30% FBS, 10% DMSO) at a density of 1 Mio/ml, aliquoted into cryovials (Corning) and frozen in a freezing container (Nalgene). Subsequently cells were stored in liquid nitrogen.

Thawing was performed by rapidly thawing frozen vials at 37 °C, re-suspension in full growth medium and transfer into 75  $\text{cm}^3$  flasks. Media was exchanged following attachment of cells.

#### **5.1.7 Tumour conditioned medium (TCM) and control medium (CON) production**

B16F10 cells for TCM and FRC cells for CON production were seeded into 75 cm<sup>3</sup> flasks and grown to 40-50% confluence. Culture medium was removed; cells were washed once in PBS and RPMI-1640 containing 2% FBS was added. TCM and CON were collected after 24 h, sterile filtered and frozen at -80 °C. TCM and CON were supplemented with 50% full growth medium to restore nutrients before adding to cells.

#### **5.1.8 3D cultures of FRCs**

Preparation of collagen gels was performed according to the instruction manuals delivered with rat-tail Collagen type I (354236, CORNING) to reach a final conc. of 2 mg/ml.

FRCs were detached from plates according to 2.1.5 and counted. 75 000 cells were used for preparation of collagen gels in 24 well plates; therefore cells were centrifuged down and re-suspended in 400 µl of ice-cold collagen solution. Gels were allowed to polymerize for 20 min at 37 °C before 500 µl of medium were added drop wise on top of the gels.

#### **5.1.9 Transfection**

Cells were seeded 24h prior to transfection to reach 60% confluence on the transfection day. For transfection in 6 well plates 100 µl Opti-MEM (31985-062, Life Technologies) were mixed with 3 µl Eugene 6 Transfection reagent (E2691, Promega) and incubated for 5 min on RT. 1 µg of tGFP plasmid (see Appendix 8.4) expressing CD9, CD63 or CD81 (cloning procedure see 5.3) or 1 µg of empty tGFP control vector was added to the solution and incubated for 15 min on RT. During this incubation step cells were washed with PBS and 500 µl of Opti-MEM were added. Transfection solution was subsequently added drop-wise to the cells, cells were incubated 2 h on 37 °C and then 3 ml of full growth medium containing serum was added. 1.5 mg /ml Neomycin (G418) were used for selection and non-transfected cells were used as a control to proof efficient selection. This was performed over a timespan of 14 days with frequent media changes every 48 h.

## **5.2 RNA Work**

### **5.2.1 RNA isolation**

RNA isolation out of cells was performed using the RNeasy Mini Kit (74106, Qiagen) according to protocol with slight modifications. In brief cells were cultured until confluence, washed 2 times with PBS and subsequently lysed in 700 µl buffer RLT. The solution was snap frozen in dry ice, thawed on ice and vortexed on full speed for 1 min. After mixing with an equal volume of 70 % ethanol, solution was transferred onto the RNeasy column and centrifuged for 1 min on 10 000 g. After washing the column with 350 µl buffer RW1 genomic DNA was digested by pipetting 80 µl of DNase containing mastermix (79254, Qiagen) onto the membrane and incubation for 15 min on RT. Column was washed once with 350 µl RW1, three times with 500 µl buffer RPE and then centrifuged empty for 2 min to dry the membrane. RNA was eluted with 25 µl RNase free H<sub>2</sub>O by centrifugation at 10 000 g for 1 min, concentration was measured at Nanodrop and samples were stored at -80 °C.

### **5.2.2 cDNA synthesis**

First Strand cDNA Synthesis Kit (K1612, Thermo Scientific) was used for reverse transcription of RNA to cDNA. 1 µg of RNA was heated with 1 µl of oligo(dt) primer at 65 °C for 5 min in a final volume of 11 µl. Sample was cooled to 4 °C and 9 µl of Master mix containing dNTPs, reverse transcriptase and reaction buffer were added. Reverse transcription was performed for 1 h at 37 °C. Samples were heated to 70 °C for 5 min to stop synthesis and stored at -20 °C.

### **5.2.3 RT-qPCR**

Real time qPCR was performed using the Taqman Gene Expression Master mix (4369016, Applied Biosciences) and Taqman Gene Expression Assays (see Appendix 8.3). 10 ng of cDNA was used per well of a MicroAmp Optical 96 well reaction plate (Applied Biosciences, Life Technologies) and sample run was performed at a StepOne Plus Real-Time System (Applied Biosystems) in technical triplicates according to the cycling protocol represented in Table 5.1.

Temperature	Time	
50 °C	2 min	
95 °C	15 min	
95 °C	15 sec	} 40x
60 °C	1 min	

Table 5.1 Cycling protocol for RT-qPCR

### 5.3 DNA work

#### 5.3.1 Polymerase chain reaction (PCR)

PCR was performed using the Phusion Green High Fidelity DNA Polymerase (F-530L, Thermo Scientific). 10 ng of template DNA, 1 µl of dNTP mix (10 mM, Life Technologies), 1.5 µl of forward (fw) and reverse (rev) primer (10 mM) and 1 U of enzyme were used per reaction. The run was performed on a DNA Engine Tetrad Thermocycler and used cycling protocols can be found in 5.2. Primer sequences were designed with the online tool Primer Three Plus (<http://www.bioinformatics.nl/cgi-bin/primer3plus/primer3plus.cgi/>), purchased from Sigma and can be found in Appendix Table 8.1.

Temperature	Time	
98 °C	30 sec	
98 °C	10 sec	} 35x
see Appendix	30 sec	
72 °C	30 sec	
72 °C	5 min	

Table 5.2 Cycling Protocol for PCR

#### 5.3.2 Agarose gel electrophoresis

1% agarose gels were used for analysis of DNA products in the size range of 500 bp – 10 kbp. 1 g of Agarose was diluted in 100 ml of 1x TBE buffer and heated in the microwave until entirely dissolved. Subsequently the solution was cooled to approximately 50 °C and Ethidiumbromide was added in a 1:1000 ratio. Samples were mixed with 6x loading dye (Life Technologies)

and Gene Ruler 1 kb DNA (Life Technologies) was loaded as a size marker. Run was performed on 100 V and gels were developed in a G-Box (Syngene).

#### **5.3.3 PCR purification**

PCR purification was performed using the QIAquick PCR purification kit (28104, QIAGEN) according to the product manual. Elution of DNA was performed in 25 µl ddH<sub>2</sub>O.

#### **5.3.4 Restriction digest**

Restriction digests were performed for 2.5 h at 37 °C and subsequently analysed on a 1% agarose gel. 2 µg of vector and 1.5 µg of insert were digested with 5 U of MluI and 5 U of SgfI in Buffer C(1071A and R710B, all Clontech).

#### **5.3.5 Gel extraction**

Gel extraction was performed using the QIAGEN Gel extraction Kit (28704, QIAGEN) according to the product manual. DNA was eluted with 25 µl of ddH<sub>2</sub>O.

#### **5.3.6 Ligation**

1 U of T4 Ligase (M0202S, NewEnglandBiolabs) was used for ligation on 16 °C overnight. . A total amount of 100 ng DNA was used per reaction, whereby insert to vector was used in a ratio of 3:1. 10x ligation buffer (M0202S, NewEnglandBiolabs) was added to a final conc. of 1x.

#### **5.3.7 Transformation into chemical competent bacteria**

For transformation of plasmids into chemical competent bacteria, 5- alpha competent *E.coli* (C2987H, NewEnglandBiolabs) were thawed on ice and subsequently mixed with 10 µl of the ligation reaction. After incubation for 30 min on ice, bacteria were heat shocked for 45 sec on 42 °C and cooled on ice for 2 min. 300 µl of sterile SOC Outgrowth Medium (B9020S, NEB) were added to the cells, followed by recovery for 1 h at 37 °C shaking. Transformed DH5  $\alpha$  were plated onto LB plates containing respective antibiotics and incubated on 37°C overnight.

#### **5.3.8 Plasmid Preparations**

QIAprep Spin Mini Prep Kit (QIAGEN) and High Speed Midi Kit (QIAGEN) were used for plasmid preparations according to the product manual. 5 ml of LB containing respective antibiotics were inoculated with a single bacterial colony, incubated overnight on 37 °C shaking and used for Minipreps. 100 ml of LB were inoculated 1/1000 with this overnight culture for Midipreps.

### **5.4 Protein work**

#### **5.4.1 Fluorescent immunocytochemistry (Fluorescent- ICC)**

For fluorescent immunocytochemistry, cells were seeded onto 8 well glass Lab-Tek Chambers (Thermo Scientific) and grown until desired confluence. Cells were subsequently washed twice in PBS and fixed in 4% Paraformaldehyde in PBS for 15 min at room temperature. Slides were washed three times for 5 min in PBS and blocked for 1 h at room temperature in blocking buffer (1x PBS supplemented with 5% chicken serum and 0.3% Triton-X100). Primary antibodies were diluted 1:100 in Antibody dilution buffer (1x PBS supplemented with 1% BSA and 0.3% Triton-X100). Incubation with primary antibody was performed overnight at 4 °C. Slides were washed 3 times in PBS and stained with fluorochrome- conjugated secondary antibody diluted 1:300 in antibody dilution buffer for 1 h on RT in the dark. Incubation was followed by three washes in PBS and cells were counterstained for 10 min at RT in the dark with DAPI (1: 10 000). After 2 more washes in PBS, cells were mounted with Slowfade Gold Antifade reagent (Life Technologies). Images were collected on a Leica TCS SP5 inverted confocal microscope. A list of used antibodies can be found in Appendix Table 8.2.

For staining of collagen gels, incubation times were extended to 30 min for fixation, 3 h for blocking, overnight incubation for primary and secondary antibody and all washes were performed for 30 min each. F-Actin staining was performed with Phalloidin-647Atto (65906, SIGMA) in a 1:2000 dilution overnight and cells were permeabilised for 10 min on RT in 0.5% TritonX100 in PBS.

For mitotracker green (M-7514, Thermo Scientific) and cellrox (C10422, Thermo Scientific) stainings living cells were incubated for 30 min at growth

conditions with mitotracker green at a final conc. of 20 nM and cellrox at 5  $\mu$ M in PBS. Subsequently cells were washed twice in PBS and full growth medium was added. Image analysis was performed with the programmes Volocity and ImageJ.

#### **5.4.2 Flow cytometry analysis**

For flow cytometry analysis, cells were grown until desired confluence, washed twice in PBS and subsequently detached by use of Accutase (A11110501, Life Technologies). Cells were passed through a 70  $\mu$ m cell strainer and centrifuged on 300 g for 5 min to ensure single cell suspensions. The cell pellet was re-suspended in 100  $\mu$ l PBS containing 1/1000 live/dead violet dye (Life Technologies). Cells were incubated for 15 min in the dark on 4 °C and washed twice in FACS buffer (PBS supplemented with 0.5% BSA). Fluorochrome conjugated antibodies for flow cytometry analysis were used at 1:300 diluted in FACS buffer and incubation was performed for 45 min in the dark at 4 °C. For intracellular staining, cells were fixed for 15 min in 2% PFA and subsequently permeabilised for 15 min in 0.5% TritonX100 before staining with antibodies. Following antibody incubation, cells were washed twice in FACS buffer and analysed on a BD LSR Fortessa cell analyser. A list of antibodies used for flow cytometry studies can be found in the Appendix Table 8.2. Analysis of flow cytometry data was performed with the programme FlowJo (Treestar).

#### **5.4.3 AnnexinV staining**

Following the flow cytometry antibody staining (5.4.2), cells were re-suspended in 50  $\mu$ l AnnexinV binding buffer (422201, Biolegend) containing 2.5  $\mu$ l AnnexinV-FITC antibody. Cells were incubated for 30 min on the bench top in the dark, re-suspended in 300  $\mu$ l AnnexinV binding buffer and analysed on a BD LSR Fortessa cell analyser. Analysis of flow cytometric data was performed with FlowJo (Treestar).

#### **5.4.4 Mitochondrial Flow Cytometry staining**

To assess mitochondrial mass and membrane potential in FRCs, cells were preconditioned in TCM or CON medium for 7 days and subsequently stained with TMRM (T-668, Life Technologies) and MitoTracker green (M-7514, Life



Technologies) at a final conc. of 50 nM. After 30 min incubation in medium containing TMRM and MitoTracker on 37 °C with 5% CO<sub>2</sub>, cells were washed twice, trypsinised as indicated in 5.1.5, filtered through a 70 µM cell strainer and analysed at a BD LSR Fortessa cell analyser.

#### **5.4.5 Sodium dodecyl sulphate polyacrylamide gel electrophoresis (SDS- PAGE) and Western Blot**

Cells for SDS-PAGE were grown until desired confluence, scraped into 1 ml of PBS and centrifuged for 5 min on 300 g. For cytokine stainings cells were treated with 5 µg/ml Brefeldin A (420601, Biolegend) for 6 h before harvesting. The cell pellet was lysed in 70 µl of RIPA buffer (89900, Thermo Scientific) containing protease inhibitors (11836153001, Complete Mini, Roche) and phosphatase inhibitors (0.1 mM activated Sodiumorthovanadate (NaO), 0.1 mM PMSF) for 30 min at 4°C while gently shaking. The lysate was cleared from DNA and cell debris by centrifugation at 10 000g for 20 min at 4°C. Protein concentration in the supernatant was determined by Pierce BCA Protein Assay Kit (23225, Life Technologies) according to product manual, and 30 µg of whole cell lysate were used for subsequent immunoblotting. Gel-electrophoresis was performed on 12% SDS-PAGE gels. Gels were prepared in Biorad apertures according to well-established protocols. Transfer was performed onto PVDF membranes (IPVH00010, Millipore), which had been pre-activated in Methanol for 5 min. A sandwich system was used for wet transfer on 90 V and 250 mAMP for 1.5 h. (Sandwich assembly as follows: Sponge, Whatman Paper, SDS-PAGE Gel, Membrane, Whatman Paper, Sponge, all soaked in transfer buffer). Membranes were blocked in 5% milk (Marvel) in TBST (0.5%) for 1 h before incubation with primary antibodies overnight. Membranes were washed 3 times for 5 min in TBST and incubated with secondary antibody conjugated to horseradish peroxidase (HRP) for 45 min at room temperature. Membranes were washed 3 times for 10 min in TBST and subsequently developed using Pierce ECL Western Blotting substrate (32106, Pierce). Antibodies used for immunoblotting can be found in the appendix table 8.2. ImageJ was used to quantify band intensity.

#### **5.4.6 Enzyme-linked-immunosorbent assay (ELISA)**

Protein quantification per ELISA was performed according to the R&D System Quantikine IL-7 ELISA Kit (M70000, R&D Systems) product manuals.

#### **5.4.7 Cytokine Array**

Cytokine Arrays were performed according to the R&D System Proteome Profiler Mouse XL Cytokine Array Kit (ARY028, R&D Systems) product manuals. B16F10 tumour cells were seeded at a density of 3 000 000 cells in a 75cm<sup>3</sup> flask in 8 ml medium containing 2% FBS and medium was collected 24 h after seeding. For microenvironment conditioned medium 60% B16F10 cells were mixed with 20% cancer associated fibroblasts (TF7) and 20% freshly isolated splenocytes (see 5.1.4) and seeded at a density of 5 000 000 cells in a 75cm<sup>3</sup> in 8 ml medium containing 2% FBS. Medium was collected 24 h post seeding. Both media were subsequently centrifuged at 300 g to exclude cell debris, aliquoted and stored at -20°C. 1 ml medium was used per membrane of the cytokine array. For analysis of tumour lysates tumours were excised from mice (under Authority of Home Office PPL 80/2574), homogenized in 1 ml of RIPA buffer using a tissue grinder and subsequently spun at 13000 rpm for 10 min. A BCA assay of the supernatant was performed to quantify protein content and 1 mg of tumour lysate was used per membrane of the cytokine array. Analysis of the cytokine array was performed by use of ImageJ with the “Protein Array Analyser” Macro.

### **5.5 Exosome purification**

Collection medium for the production of exosomes had to be depleted of exosomes contained in the serum prior to the collection. Therefore FBS was centrifuged for 16 h on 100 000 g in a SW28 rotor in a Beckman Coulter Optimal XL 80 K centrifuge and the supernatant was collected. After sterile filtration FBS was added to DMEM in a final conc. of 10%. B16F10 Melanoma cells for the production of exosomes were seeded at 50% density into 175 cm<sup>3</sup> tissue culture flasks. 24 h post seeding the medium was exchanged for exosome production medium and collected 48 h later. Medium was

centrifuged for 10 min at 300 g and subsequently for 20 min at 2000 g to remove cellular debris and dead cells. The supernatant was centrifuged for 30 min on 10 000g, transferred into a fresh tube without disturbing the pellet and thereafter centrifuged for 70 min at 100 000 g. The supernatant was subsequently discarded and the remaining pellet re-suspended in 40 ml of PBS to wash the exosomal pellet. The suspension was centrifuged for another 60 min at 100 000 g, the supernatant carefully removed and the remaining exosome pellet re-suspended in 50 µl of PBS.

## **5.6 Functional assays**

### **5.6.1 Cell titre blue proliferation assay**

Cells were seeded into 96 well plates at densities of 200, 500 or 1000 cells per well in 50% TCM or 50% CON, mixed with 50% RPMI containing 2% FBS. For the first time point (Day 0) 20 µl of cell titre blue viability assay reagent (G8080, Promega) were added 1h post seeding and fluorescence was measured 3 h later at a TECAN plate reader (Excitation: 550 nm, Emission: 600 nm). In the first measurement a calibration curve with different cell numbers was included, all subsequent measurements were performed in exactly the same way. Media without cells was included for blank measurements.

### **5.6.2 Permeability assay**

For in vitro permeability assays, 0.4 µm pore PCF cell culture inserts were coated for 1 h with collagen coating solution containing 50 µg/ml Type I rat-tail collagen. Coated insets were washed 3 times in PBS, 65 000 cells were seeded into the insets and allowed to settle for 24 h. To demonstrate a completely confluent and intact monolayer of cells, one insert was sacrificed per condition, stained with cell mask dye (Life Technologies) and imaged.

The media was removed from the insert, the insert was transferred into a new plate and 500 µl of basal medium were added to the bottom well. A solution containing FITC-Dextran (500 000 MW; D-7136, Life Technologies) and Cascade Blue- Dextran (3000 MW; D-7132, Life Technologies) at a final conc. of 1 mg/ml was prepared and 200 µl were added to the upper layer of

the insert. Hourly readings were performed, whereby 2 times 150 µl of media from the lower chamber were removed, fluorescence measured at an excitation wavelength of 494 nm and an emission wavelength on 521 nm and subsequently returned to the plate. A standard curve containing Dextran in concentrations of 0.1 – 50 µg/ml was included in the first measurement.

#### **5.6.3 Adhesion assay**

For performance of adhesion assays an Xcelligence RTCA DP Instrument (ACEA Biosciences) was used. 5000 cells were seeded per well of an E Plate 16 (ACEA Biosciences) and the assay was performed over a time course of 120 min with measurements every 10 min.

#### **5.6.4 Scratch assay**

A pipette tip was used to produce 3 scratches per well in a 6 well plate containing a completely confluent monolayer of cells in the culture medium of interest. Images were taken at a Zeiss Lifecell Imaging Microscope over a time course of 48 h with measurements every 30 min at 37°C and 5% CO<sub>2</sub>. Data was analysed by use of Zen Blue Software and velocity of gap closure was calculated as µm/h.

#### **5.6.5 Splenocyte survival assay**

7 days prior to the assay FRCs were seeded into 24 well plates at a density of 20 000 cells per well. Cells were treated with TCM over a time course of 7 days, whereby they were split once on day 4 according to 5.1.5. On day 7 splenocytes were isolated from the spleen of female C57BL/6 mice (10 weeks) according to 5.1.4. and 100 000 splenocytes were seeded in 0.5 ml of splenocyte medium on top of the FRCs. 3 days later splenocytes were collected from the FRCs and stained for flow cytometry according to 5.4.2 including an AnnexinV stain according to 5.4.3.

#### **5.6.6 Contractility assay**

FRCs were pretreated with TCM or CON for 7 days and 150 000 cells were seeded in triplicates in a collagen gel at a final conc. of 2 mg/ml according to 5.1.8. in 24 well plates. The gel was allowed to polymerize for 30 min and

detached from the wall of the plate with a tip. Medium was added on top and the gels were incubated at 37 °C and 5% CO<sub>2</sub>. Pictures were taken after 6 h and 24 h and the gel area was measured with ImageJ.

#### **5.6.7 Oxidative stress assay**

FRCs were pre-treated with TCM or CON for a timespan of 6 days. On day 6 1500 FRCs were seeded per well into 96 well plates in technical triplicates in 50 µl of CON or TCM. 24h after seeding H<sub>2</sub>O<sub>2</sub> was added to final concentrations of 1.8 µM, 3.75 µM, 7.5 µM, 15 µM, 30 µM, 60 µM, 125 µM, 250 µM and 500 µM and cells were incubated for 24 h in growth conditions. Subsequently the number of living cells was determined by use of cell titre blue assay as explained in 5.6.1. Crystal violet stainings were performed to confirm reliability of cell titre blue assay. Therefore cells were washed in PBS, incubated for 10 min in Crystal Violet staining solution (1% Formaldehyde (v/v), 0.05% (w/v) Crystal Violet, 1% Methanol (v/v) in 1x PBS) and washed another 3 times in PBS. Subsequently plates were allowed to dry overnight, crystal violet was solubilized in 10% Acetic Acid and absorbance was measured at 590 nm.

#### **5.7 Statistics**

All statistics were performed with use of the program GraphpadPrism. Unpaired t-tests were performed to investigate whether two sets of data are significantly different from each other and p-values below 0.05 were considered significant. Two-way analysis of variance was used to determine the response to two different factors, e.g comparison of viability in TCM or CON treated FRCs in response to drug treatment. p<0.05 was considered significant.

#### **5.8 Mice**

All experiments were performed by lab members holding an approved personal licence in accordance with the institutional guidelines for animal care and under the authority of UK Home Office Project Licence 80/2574.

## 6. References

1. Ruddle NH, Akirav EM. Secondary lymphoid organs: responding to genetic and environmental cues in ontogeny and the immune response. *J Immunol.* 2009;183(4):2205-2212. doi:10.4049/jimmunol.0804324.
2. Vittet D. Lymphatic collecting vessel maturation and valve morphogenesis. *Microvasc Res.* 2014;96:31-37. doi:10.1016/j.mvr.2014.07.001.
3. Mallick A, Bodenham AR. Disorders of the lymph circulation: Their relevance to anaesthesia and intensive care. *Br J Anaesth.* 2003;91(2):265-272. doi:10.1093/bja/aeg155.
4. Datta K, Muders M, Zhang H TD. Mechanism of lymph node metastasis in prostate cancer. *Futur Oncol.* 2010;6(5):823-836. doi:10.2217/fon.10.33.Mechanism.
5. Wada N, Duh Q-Y, Sugino K, et al. Lymph node metastasis from 259 papillary thyroid microcarcinomas: frequency, pattern of occurrence and recurrence, and optimal strategy for neck dissection. *Ann Surg.* 2003;237(3):399-407. doi:10.1097/01.SLA.0000055273.58908.19.
6. Pereira ER, Jones D, Jung K, Padera TP. The lymph node microenvironment and its role in the progression of metastatic cancer. *Semin Cell Dev Biol.* 2015;38:98-105. doi:10.1016/j.semcdb.2015.01.008.
7. Yang C-Y, Vogt TK, Favre S, et al. Trapping of naive lymphocytes triggers rapid growth and remodeling of the fibroblast network in reactive murine lymph nodes. doi:10.1073/pnas.1312585111.
8. Chyou S, Ekland EH, Carpenter AC, et al. Fibroblast-Type Reticular Stromal Cells Regulate the Lymph Node Vasculature. 2015. doi:10.4049/jimmunol.181.6.3887.
9. Malhotra D, Fletcher AL, Turley SJ. Stromal and hematopoietic cells in secondary lymphoid organs: Partners in immunity. *Immunol Rev.* 2013;251(1):160-176. doi:10.1111/imr.12023.
10. Mueller SN, Germain RN. Stromal cell contributions to the homeostasis and functionality of the Immune System. *Nat Rev Immunol.* 2009;9(9):618-629. doi:10.1038/nri2588.Stromal.
11. Turley SJ, Fletcher AL, Elpek KG. The stromal and haematopoietic antigen-presenting cells that reside in secondary lymphoid organs. *Nat Rev Immunol.* 2010;10:813-825.

12. Willard-Mack CL. Normal structure, function, and histology of lymph nodes. *Toxicol Pathol.* 2006;34(5):409-424. doi:10.1080/01926230600867727.
13. Link A, Vogt TK, Favre S, et al. Fibroblastic reticular cells in lymph nodes regulate the homeostasis of naive T cells. *Nat Immunol.* 2007;8(11):1255-1265. doi:10.1038/ni1513.
14. Katakai T. Marginal reticular cells: A stromal subset directly descended from the lymphoid tissue organizer. *Front Immunol.* 2012;3(JUL):1-6. doi:10.3389/fimmu.2012.00200.
15. Lukacs-Kornek V, Malhotra D, Fletcher AL, et al. Regulated release of nitric oxide by nonhematopoietic stroma controls expansion of the activated T cell pool in lymph nodes. *Nat Immunol.* 2012;12(11):1096-1104. doi:10.1038/ni.2112.
16. Suzuki K, Maruya M, Kawamoto S, et al. The sensing of environmental stimuli by follicular dendritic cells promotes immunoglobulin A generation in the gut. *Immunity.* 2010;33(1):71-83. doi:10.1016/j.immuni.2010.07.003.
17. Stranford S, Ruddle NH. Follicular dendritic cells, conduits, lymphatic vessels, and high endothelial venules in tertiary lymphoid organs: Parallels with lymph node stroma. *Front Immunol.* 2012;3(NOV):1-6. doi:10.3389/fimmu.2012.00350.
18. Gonzalez SF, Pitcher L a, Mempel T, Schuerpf F, Carroll MC. B cell aquisition of antigen in vivo. *Curr Opin Immunol.* 2010;21(3):251-257. doi:10.1016/j.coi.2009.05.013.B.
19. Anderson a O, Anderson ND. Studies on the structure and permeability of the microvasculature in normal rat lymph nodes. *Am J Pathol.* 1975;80(3):387-418.
20. Gretz JE, Norbury CC, Anderson a O, Proudfoot a E, Shaw S. Lymph-borne chemokines and other low molecular weight molecules reach high endothelial venules via specialized conduits while a functional barrier limits access to the lymphocyte microenvironments in lymph node cortex. *J Exp Med.* 2000;192(10):1425-1440. doi:10.1084/jem.192.10.1425.
21. Gowans , J.L., Knight EJ. The route of re-circulation of lymphocytes in the rat. *Proc R Soc Lond B.* 1964;(159):257-282.
22. Weninger W, Crowley M a, Manjunath N, von Andrian UH. Migratory properties of naive, effector, and memory CD8(+) T cells. *J Exp Med.* 2001;194(7):953-966.

23. Von Andrian UH, Mempel TR. Homing and cellular traffic in lymph nodes. *Nat Rev Immunol*. 2003;3(11):867-878. doi:10.1038/nri1222.
24. Förster R, Davalos-Misslitz AC, Rot A. CCR7 and its ligands: balancing immunity and tolerance. *Nat Rev Immunol*. 2008;8(5):362-371. doi:10.1038/nri2297.
25. Bajénoff M, Egen J, Koo LY, et al. Stromal cell networks regulate lymphocyte entry, migration and territoriality in lymph nodes. 2009;25(6):989-1001. doi:10.1016/j.immuni.2006.10.011.Stromal.
26. Mionnet C, Sanos SL, Mondor I, et al. High endothelial venules as traffic control points maintaining lymphocyte population homeostasis in lymph nodes. 2012;118(23):6115-6122. doi:10.1182/blood-2011-07-367409.
27. Alvarez D, Vollmann E, Andrian U Von. Mechanisms and Consequences of Dendritic Cell migration. *Immunity*. 2008;29(3). doi:10.1016/j.immuni.2008.08.006.Mechanisms.
28. Braun A, Worbs T, Moschovakis GL, et al. Afferent lymph-derived T cells and DCs use different chemokine receptor CCR7-dependent routes for entry into the lymph node and intranodal migration. *Nat Immunol*. 2011;12(9):879-887. doi:10.1038/ni.2085.
29. Girard J-P, Moussion C, Foerster R. HEVs, lymphatics and homeostatic immune cell trafficking in lymph nodes. *Nat Rev Immunol*. 2012;12:762-773.
30. Malhotra D, Fletcher AL, Astarita J, et al. Transcriptional profiling of stroma from inflamed and resting lymph nodes defines immunological hallmarks. *Nat Immunol*. 2012. doi:10.1038/ni.2262.
31. Kaldjian EP, Gretz JE, Anderson a O, Shi Y, Shaw S. Spatial and molecular organization of lymph node T cell cortex: a labyrinthine cavity bounded by an epithelium-like monolayer of fibroblastic reticular cells anchored to basement membrane-like extracellular matrix. *Int Immunol*. 2001;13(10):1243-1253. doi:10.1093/intimm/13.10.1243.
32. Fletcher AL, Lukacs-Kornek V, Reynoso ED, et al. Lymph node fibroblastic reticular cells directly present peripheral tissue antigen under steady-state and inflammatory conditions. *J Exp Med*. 2010;207(4):689-697. doi:10.1084/jem.20092642.
33. Siegert S, Huang HY, Yang CY, et al. Fibroblastic reticular cells from lymph nodes attenuate T cell expansion by producing nitric oxide. *PLoS One*. 2011;6(11). doi:10.1371/journal.pone.0027618.
34. Cyster JG, Ansel KM, Reif K, et al. Follicular stromal cells and lymphocyte homing to follicles. *Immunol Rev*. 2000;176:181-193. doi:10.1034/j.1600-065X.2000.00618.x.



35. Lund AW, Duraes F V., Hirose S, et al. VEGF-C Promotes Immune Tolerance in B16 Melanomas and Cross-Presentation of Tumor Antigen by Lymph Node Lymphatics. *Cell Rep.* 2012;1(3):191-199. doi:10.1016/j.celrep.2012.01.005.
36. Card CM, Yu SS, Swartz M a. Emerging roles of lymphatic endothelium in regulating adaptive immunity. *J Clin Invest.* 2014;124(3):943-952. doi:10.1172/JCI73316.
37. Denton AE, Roberts EW, Linterman M a, Fearon DT. Fibroblastic reticular cells of the lymph node are required for retention of resting but not activated CD8+ T cells. *Proc Natl Acad Sci U S A.* 2014;111(33):12139-12144. doi:10.1073/pnas.1412910111.
38. Mionnet C, Mondor I, Jorquera A, et al. Identification of a New Stromal Cell Type Involved in the Regulation of Inflamed B Cell Follicles. *PLoS Biol.* 2013;11(10). doi:10.1371/journal.pbio.1001672.
39. Cremasco V, et.al. B cell homeostasis and follicle confines are governed by fibroblastic reticular cells. *Nat Immunol.* 2014;15:973-981.
40. Acton SE, Astarita JL, Malhotra D, et al. Podoplanin-Rich Stromal Networks Induce Dendritic Cell Motility via Activation of the C-type Lectin Receptor CLEC-2. *Immunity.* 2012;37(2):276-289. doi:10.1016/j.immuni.2012.05.022.
41. Herzog BH, Fu J, Wilson SJ, et al. Podoplanin maintains high endothelial venule integrity by interacting with platelet CLEC-2. *Nature.* 2013;502(1476-4687 (Electronic)):105-109. doi:10.1038/nature12501.
42. Siegert S, Luther S a. Positive and negative regulation of T cell responses by fibroblastic reticular cells within paracortical regions of lymph nodes. *Front Immunol.* 2012;3(SEP):1-10. doi:10.3389/fimmu.2012.00285.
43. Lee J-W, Epardaud M, Sun J, et al. Peripheral antigen display by lymph node stroma promotes T cell tolerance to intestinal self. *Nat Immunol.* 2007;8(2):181-190. doi:10.1038/ni1427.
44. Magnusson FC, Liblau RS, von Boehmer H, et al. Direct Presentation of Antigen by Lymph Node Stromal Cells Protects Against CD8 T-Cell-Mediated Intestinal Autoimmunity. *Gastroenterology.* 2008;134(4):1028-1037. doi:10.1053/j.gastro.2008.01.070.
45. Baptista AP, Roozendaal R, Reijmers RM, et al. Lymph node stromal cells constrain immunity via MHC class II self-antigen presentation. *Elife.* 2014;3.
46. Cording S, Wahl B, Kulkarni D, et al. The intestinal micro-environment imprints stromal cells to promote efficient Treg induction in gut-draining

- lymph nodes. *Mucosal Immunol.* 2014;7(2):359-368. doi:10.1038/mi.2013.54.
47. Chai Q, Onder L, Scandella E, et al. Maturation of Lymph Node Fibroblastic Reticular Cells from Myofibroblastic Precursors Is Critical for Antiviral Immunity. *Immunity.* 2013;38(5):1013-1024. doi:10.1016/j.immuni.2013.03.012.
  48. Klein CA. The Metastasis Cascade. *Science (80- ).* 2008;321:1785-1787. doi:10.1029/2007GC001696.
  49. Tuttle TM. Technical advances in sentinel lymph node biopsy for cancer. *Am Sur.* 2004;70:407-413. doi:10.1002/cncr.20794.
  50. Qian CN, Berghuis B, Tsarfaty G, et al. Preparing the “soil”: The primary tumor induces vasculature reorganization in the sentinel lymph node before the arrival of metastatic cancer cells. *Cancer Res.* 2006;66(21):10365-10376. doi:10.1158/0008-5472.CAN-06-2977.
  51. Björndahl M a., Cao R, Burton JB, et al. Vascular endothelial growth factor-A promotes peritumoral lymphangiogenesis and lymphatic metastasis. *Cancer Res.* 2005;65(20):9261-9268. doi:10.1158/0008-5472.CAN-04-2345.
  52. Tammela T, Alitalo K. Lymphangiogenesis: Molecular Mechanisms and Future Promise. *Cell.* 2010;140(4):460-476. doi:10.1016/j.cell.2010.01.045.
  53. Cao R, Ji H, Feng N, et al. Collaborative interplay between FGF-2 and VEGF-C promotes lymphangiogenesis and metastasis. *Proc Natl Acad Sci.* 2012;109(39):15894-15899. doi:10.1073/pnas.1208324109.
  54. Cao R, Björndahl M a., Religa P, et al. PDGF-BB induces intratumoral lymphangiogenesis and promotes lymphatic metastasis. *Cancer Cell.* 2004;6(4):333-345. doi:10.1016/j.ccr.2004.08.034.
  55. Bracher A, Cardona AS, Tauber S, et al. Epidermal Growth Factor Facilitates Melanoma Lymph Node Metastasis by Influencing Tumor Lymphangiogenesis. *J Invest Dermatol.* 2012;133. doi:10.1038/jid.2012.272.
  56. Shayan R, Inder R, Karnezis T, et al. Tumor location and nature of lymphatic vessels are key determinants of cancer metastasis. *Clin Exp Metastasis.* 2013;30(3):345-356. doi:10.1007/s10585-012-9541-x.
  57. Leu AJ, Berk D a, Lymboussaki A, Alitalo K, Jain RK. Absence of Functional Lymphatics within a Murine Sarcoma : A Molecular and Functional Evaluation Advances in Brief. *Cancer Res.* 2000:4324-4327.

58. Padera TP, Kadambi A, di Tomaso E, et al. Lymphatic metastasis in the absence of functional intratumor lymphatics. *Science*. 2002;296(5574):1883-1886. doi:10.1126/science.1071420.
59. Wong SY, Haack H, Crowley D, Barry M, Bronson RT, Hynes RO. Tumor-secreted vascular endothelial growth factor-C is necessary for prostate cancer lymphangiogenesis, but lymphangiogenesis is unnecessary for lymph node metastasis. *Cancer Res*. 2005;65(21):9789-9798. doi:10.1158/0008-5472.CAN-05-0901.
60. Karpanen T, Alitalo K. Lymphatic vessels as targets of tumor therapy? *J Exp Med*. 2001;194(6):F37-F42. doi:10.1084/jem.194.6.F37.
61. Wong SY, Hynes RO. Tumor-lymphatic interactions in an activated stromal microenvironment. *J Cell Biochem*. 2007;101(4):840-850. doi:10.1002/jcb.21146.
62. Stacker S a, Caesar C, Baldwin ME, et al. VEGF-D promotes the metastatic spread of tumor cells via the lymphatics. *Nat Med*. 2001;7(2):186-191. doi:10.1038/84635.
63. Mandriota SJ, Jussila L, Jeltsch M, et al. Vascular endothelial growth factor-C-mediated lymphangiogenesis promotes tumour metastasis. *EMBO J*. 2001;20(4):672-682. doi:10.1093/emboj/20.4.672.
64. Skobe M, Hawighorst T, Jackson DG, et al. Induction of tumor lymphangiogenesis by VEGF-C promotes breast cancer metastasis. *Nat Med*. 2001;7(2):192-198. doi:10.1038/84643.
65. He Y, Rajantie I, Pajusola K, et al. Vascular Endothelial Cell Growth Factor Receptor 3 – Mediated Activation of Lymphatic Endothelium Is Crucial for Tumor Cell Entry and Spread via Lymphatic Vessels  
Vascular Endothelial Cell Growth Factor Receptor 3 – Mediated Cell Entry and Spread via Lymph. 2005;(11):4739-4746.
66. Hoshida T, Isaka N, Hagendoorn J, et al. Imaging steps of lymphatic metastasis reveals that vascular endothelial growth factor-C increases metastasis by increasing delivery of cancer cells to lymph nodes: Therapeutic implications. *Cancer Res*. 2006;66(16):8065-8075. doi:10.1158/0008-5472.CAN-06-1392.
67. Karnezis T, Shayan R, Caesar C, et al. VEGF-D Promotes Tumor Metastasis by Regulating Prostaglandins Produced by the Collecting Lymphatic Endothelium. *Cancer Cell*. 2012;21(2):181-195. doi:10.1016/j.ccr.2011.12.026.
68. Hirakawa S. From tumor lymphangiogenesis to lymphovascular niche. *Cancer Sci*. 2009;100(6):983-989. doi:10.1111/j.1349-7006.2009.01142.x.

69. Hirakawa S, Brown LF, Kodama S, Paavonen K, Alitalo K, Detmar M. VEGF-C – induced lymphangiogenesis in sentinel lymph nodes promotes tumor metastasis to distant sites. *Blood*. 2007;109(3):1010-1017. doi:10.1182/blood-2006-05-021758.The.
70. Farnsworth RH, Karnezis T, Shayan R, et al. A role for bone morphogenetic protein-4 in lymph node vascular remodeling and primary tumor growth. *Cancer Res*. 2011;71(20):6547-6557. doi:10.1158/0008-5472.CAN-11-0200.
71. Lyden D, Hattori K, Dias S, et al. Impaired recruitment of bone-marrow-derived endothelial and hematopoietic precursor cells blocks tumor angiogenesis and growth. *Nat Med*. 2001;7(11):1194-1201. doi:10.1038/nm1101-1194.
72. Wagner JD, Gordon MS, Chuang TY, Coleman JJ. Current therapy of cutaneous melanoma. *Plast Reconstr Surg*. 2000;105(5):1774-1799; quiz 1800-1801.
73. Tas F. Metastatic behavior in melanoma: Timing, pattern, survival, and influencing factors. *J Oncol*. 2012;2012. doi:10.1155/2012/647684.
74. Christianson DR, Dobroff AS, Proneth B, et al. Ligand-directed targeting of lymphatic vessels uncovers mechanistic insights in melanoma metastasis. *Proc Natl Acad Sci*. 2015;112(8):201424994. doi:10.1073/pnas.1424994112.
75. Kaufman HL, Disis ML. Immune system versus tumor: Shifting the balance in favor of DCs and effective immunity. *J Clin Invest*. 2004;113(5):664-667. doi:10.1172/JCI200421148.
76. Cao X, Cai SF, Fehniger T a., et al. Granzyme B and Perforin Are Important for Regulatory T Cell-Mediated Suppression of Tumor Clearance. *Immunity*. 2007;27(4):635-646. doi:10.1016/j.immuni.2007.08.014.
77. Sharma MD, Hou DY, Liu Y, et al. Indoleamine 2,3-dioxygenase controls conversion of Foxp3+ Tregs to TH17-like cells in tumor-draining lymph nodes. *Blood*. 2009;113(24):6102-6111. doi:10.1182/blood-2008-12-195354.
78. Munn DH, Mellor AL. The tumor-draining lymph node as an immune-privileged site. *Immunol Rev*. 2006;213(1):146-158. doi:10.1111/j.1600-065X.2006.00444.x.
79. Cochran AJ, Huang R-R, Lee J, Itakura E, Leong SPL, Essner R. Tumour-induced immune modulation of sentinel lymph nodes. *Nat Rev Immunol*. 2006;6(9):659-670. doi:10.1038/nri1919.

80. Melief CJM. Cancer immunotherapy by dendritic cells. *Immunity*. 2008;29(3):372-383. doi:10.1016/j.immuni.2008.08.004.
81. Matsuura K, Yamaguchi Y, Ueno H, Osaki A, Arihiro K, Toge T. Maturation of dendritic cells and T-cell responses in sentinel lymph nodes from patients with breast carcinoma. *Cancer*. 2006;106(6):1227-1236. doi:10.1002/cncr.21729.
82. Huang RR, Wen DR, Guo J, et al. Selective modulation of paracortical dendritic cells and T-lymphocytes in breast cancer sentinel lymph nodes. *Breast J*. 2000;6(4):225-232. doi:10.1046/j.1524-4741.2000.98114.x.
83. Macián F, García-Cózar F, Im SH, Horton HF, Byrne MC, Rao A. Transcriptional mechanisms underlying lymphocyte tolerance. *Cell*. 2002;109(6):719-731. doi:10.1016/S0092-8674(02)00767-5.
84. Wetterwald a., Hofstetter W, Cecchini MG, et al. Characterization and cloning of the E11 antigen, a marker expressed by rat osteoblasts and osteocytes. *Bone*. 1996;18(2):125-132. doi:10.1016/8756-3282(95)00457-2.
85. Farr AG, Berry ML, Kim A, Nelson AJ, Welch MP, Aruffo A. Characterization and cloning of a novel glycoprotein expressed by stromal cells in T-dependent areas of peripheral lymphoid tissues. *J Exp Med*. 1992;176(5):1477-1482. doi:10.1084/jem.176.5.1477.
86. Wicki A, Christofori G. The potential role of podoplanin in tumour invasion. 2007;(December 2006):1-5. doi:10.1038/sj.bjc.6603518.
87. Astarita JL, Acton SE, Turley SJ. Podoplanin: emerging functions in development, the immune system, and cancer. *Front Immunol*. 2012;3:283. doi:10.3389/fimmu.2012.00283.
88. Ramirez MI, Millien G, Hinds A, Cao YX, Seldin DC, Williams MC. T1a, a lung type I cell differentiation gene, is required for normal lung cell proliferation and alveolus formation at birth. *Dev Biol*. 2003;256(1):61-72. doi:10.1016/S0012-1606(02)00098-2.
89. Martín-Villar E, Scholl FG, Gamallo C, et al. Characterization of human PA2.26 antigen (T1 $\alpha$ -2, podoplanin), a small membrane mucin induced in oral squamous cell carcinomas. *Int J Cancer*. 2005;113(6):899-910. doi:10.1002/ijc.20656.
90. Martín-Villar E, Megías D, Castel S, Yurrita MM, Vilaró S, Quintanilla M. Podoplanin binds ERM proteins to activate RhoA and promote epithelial-mesenchymal transition. *J Cell Sci*. 2006;119(Pt 21):4541-4553. doi:10.1242/jcs.03218.

91. E. M-V, Fernandez-Munoz B, Et.al. Podoplanin associates with CD44 to promote directional cell migration. *Mol Biol Cell*. 2010;21(24):4387-4399. doi:10.1091/mbc.E10.
92. Nakazawa Y, Sato S, Naito M, et al. Tetraspanin family member CD9 inhibits Aggrus/podoplanin-induced platelet aggregation and suppresses pulmonary metastasis. *Blood*. 2008;112(5):1730-1739. doi:10.1182/blood-2007-11-124693.
93. Colonna M, Samaridis J, Angman L. Molecular characterization of two novel C-type lectin-like receptors, one of which is selectively expressed in human dendritic cells. *Eur J Immunol*. 2000;30(2):697-704. doi:10.1002/1521-4141(200002)30:2<697::AID-IMMU697>3.0.CO;2-M.
94. Sobanov Y, Bernreiter A, Derdak S, et al. A novel cluster of lectin-like receptor genes expressed in monocytic, dendritic and endothelial cells maps close to the NK receptor genes in the human NK gene complex. *Eur J Immunol*. 2001;31(12):3493-3503. doi:10.1002/1521-4141(200112)31:12<3493::AID-IMMU3493>3.0.CO;2-9.
95. Astarita JL, Cremasco V, Fu J, et al. The CLEC-2–podoplanin axis controls the contractility of fibroblastic reticular cells and lymph node microarchitecture. *Nat Immunol*. 2014;16(1):75-84. doi:10.1038/ni.3035.
96. Hou TZ, Bystrom J, Sherlock JP, et al. A distinct subset of podoplanin (gp38) expressing F4/80+ macrophages mediate phagocytosis and are induced following zymosan peritonitis. *FEBS Lett*. 2010;584(18):3955-3961. doi:10.1016/j.febslet.2010.07.053.
97. Swartz MA, Lund AW. Lymphatic and interstitial flow in the tumour microenvironment: linking mechanobiology with immunity. *Nat Rev Cancer*. 2012;12(3):210-219.
98. Breiteneder-Geleff S, Matsui K, Soleiman a, et al. Podoplanin, novel 43-kd membrane protein of glomerular epithelial cells, is down-regulated in puromycin nephrosis. *Am J Pathol*. 1997;151(4):1141-1152.
99. Kato Y, Fujita N, Kunita A, et al. Molecular Identification of Aggrus/T1 $\alpha$  as a Platelet Aggregation-inducing Factor Expressed in Colorectal Tumors. *J Biol Chem*. 2003;278(51):51599-51605. doi:10.1074/jbc.M309935200.
100. Wicki A, Lehembre F, Wick N, Hantusch B, Kerjaschki D, Christofori G. Tumor invasion in the absence of epithelial-mesenchymal transition: Podoplanin-mediated remodeling of the actin cytoskeleton. *Cancer Cell*. 2006;9(4):261-272. doi:10.1016/j.ccr.2006.03.010.
101. Durum SK, Mazzucchelli RI. Live from the Liver: Hepatocyte IL-7. *Immunity*. 2009;30(3):320-321. doi:10.1016/j.immuni.2009.03.001.

102. Watanabe M, Ueno Y, Yajima T, et al. Interleukin 7 is produced by human intestinal epithelial cells and regulates the proliferation of intestinal mucosal lymphocytes. *J Clin Invest*. 1995;95(6):2945-2953. doi:10.1172/JCI118002.
103. Kröncke R, Loppnow H, Flad HD, Gerdes J. Human follicular dendritic cells and vascular cells produce interleukin-7: a potential role for interleukin-7 in the germinal center reaction. *Eur J Immunol*. 1996;26(10):2541-2544. doi:10.1002/eji.1830261040.
104. Fry TJ, Mackall CL. Interleukin-7 : from bench to clinic. 2009;99(11):3892-3904. doi:10.1182/blood.V99.11.3892.
105. Von Freeden-Jeffry U, Vieira P, Lucian L a, McNeil T, Burdach SE, Murray R. Lymphopenia in interleukin (IL)-7 gene-deleted mice identifies IL-7 as a nonredundant cytokine. *J Exp Med*. 1995;181(4):1519-1526. doi:10.1084/jem.181.4.1519.
106. Watson JD, Morrissey PJ, Namen AE, Conlon PJ, Widmer MB. Effect of IL-7 on the growth of fetal thymocytes in culture. *J Immunol*. 1989;143(4):1215-1222.
107. Candéias S, Muegge K, Durum SK. IL-7 Receptor and VDJ recombination: Trophic versus mechanistic actions. *Immunity*. 1997;6(5):501-508. doi:10.1016/S1074-7613(00)80338-6.
108. Schluns KS, Kieper WC, Jameson SC, Lefrançois L. Interleukin-7 mediates the homeostasis of naïve and memory CD8 T cells in vivo. *Nat Immunol*. 2000;1(5):426-432. doi:10.1038/80868.
109. Varas a, Vicente a, Sacedón R, Zapata a G. Interleukin-7 influences the development of thymic dendritic cells. *Blood*. 1998;92(1):93-100.
110. Peschon JJ, Morrissey PJ, Grabstein KH, et al. Early lymphocyte expansion is severely impaired in interleukin 7 receptor-deficient mice. *J Exp Med*. 1994;180(5):1955-1960. doi:10.1084/jem.180.5.1955.
111. Foss HD, Hummel M, Gottstein S, et al. Frequent expression of IL-7 gene transcripts in tumor cells of classical Hodgkin's disease. *Am J Pathol*. 1995;146(1):33-39.
112. Tang JC, Shen GB, Wang SM, Wan YS, Wei YQ. IL-7 inhibits tumor growth by promoting T cell-mediated antitumor immunity in Meth A model. *Immunol Lett*. 2014;158(1-2):159-166. doi:10.1016/j.imlet.2013.12.019.
113. Roato I, Brunetti G, Gorassini E, et al. IL-7 up-regulates TNF- $\alpha$ -dependent osteoclastogenesis in patients affected by solid tumor. *PLoS One*. 2006;1(1):1-9. doi:10.1371/journal.pone.0000124.

114. Li B, VanRoey MJ, Jooss K. Recombinant IL-7 enhances the potency of GM-CSF-secreting tumor cell immunotherapy. *Clin Immunol*. 2007;123(2):155-165. doi:10.1016/j.clim.2007.01.002.
115. Tomei AA, Siegert S, Britschgi MR, Luther SA, Swartz MA. Fluid flow regulates stromal cell organization and CCL21 expression in a tissue-engineered lymph node microenvironment. *J Immunol*. 2009. doi:10.4049/jimmunol.0900835.
116. Klausner RD, Donaldson JG, Lippincott-Schwartz J. Brefeldin A: Insights into the control of membrane traffic and organelle structure. *J Cell Biol*. 1992;116(5):1071-1080. doi:10.1083/jcb.116.5.1071.
117. Tsuneki M, Yamazaki M, Maruyama S, Cheng J, Saku T. Podoplanin-mediated cell adhesion through extracellular matrix in oral squamous cell carcinoma. *Lab Invest*. 2013;93(8):921-932. doi:10.1038/labinvest.2013.86.
118. Acton SE, Farrugia AJ, Astarita JL, et al. Dendritic cells control fibroblastic reticular network tension and lymph node expansion. doi:10.1038/nature13814.
119. Kalluri R, Zeisberg M. Fibroblasts in cancer. *Nat Rev Cancer*. 2006;6(5):392-401. doi:10.1038/nrc1877.
120. Grande MT, López-Novoa JM. Fibroblast activation and myofibroblast generation in obstructive nephropathy. *Nat Rev Nephrol*. 2009;5(6):319-328. doi:10.1038/nrneph.2009.74.
121. Anderson JM. Molecular structure of tight junctions and their role in epithelial transport. *News Physiol Sci*. 2001;16:126-130.
122. Kruse E, Uehlein N, Kaldenhoff R. The aquaporins. *Genome Biol*. 2006;7(2):206. doi:10.1186/gb-2006-7-2-206.
123. Yost C, Torres M, Miller JR, Huang E, Kimelman D, Moon RT. The axis-inducing activity, stability, and subcellular distribution of beta-catenin is regulated in *Xenopus* embryos by glycogen synthase kinase 3. *Genes Dev*. 1996;10(12):1443-1454. doi:10.1101/gad.10.12.1443.
124. Lee M-H, Koria P, Qu J, Andreadis ST. JNK phosphorylates beta-catenin and regulates adherens junctions. *FASEB J*. 2009;23(11):3874-3883. doi:10.1096/fj.08-117804.
125. Negmadjanov U, Godic Z, Rizvi F, et al. TGF- $\beta$ 1-Mediated Differentiation of Fibroblasts Is Associated with Increased Mitochondrial Content and Cellular Respiration. *PLoS One*. 2015;10(4):e0123046. doi:10.1371/journal.pone.0123046.



126. Joshi DC, Bakowska JC. Determination of mitochondrial membrane potential and reactive oxygen species in live rat cortical neurons. *J Vis Exp*. 2011;(51):2-5. doi:10.3791/2704.
127. Blik A Van Der. Mechanisms of Mitochondrial Fission and Fusion. *Cold Spring Harb Perspect Biol*. 2013;5(6):1-16. doi:10.1101/cshperspect.a011072.
128. Mitchell P, Moyle J. Chemiosmotic Hypothesis of Oxidative Phosphorylation. *Nature*. 1967:137-139.
129. Simone Reuter BBA. Oxidative stress, inflammation and cancer: How are they linked? *Free Radic Biol Med*. 2011;49(11):1603-1616. doi:10.1016/j.freeradbiomed.2010.09.006.Oxidative.
130. Sosa V, Moliné T, Somoza R, Paciucci R, Kondoh H, LLeonart ME. Oxidative stress and cancer: An overview. *Ageing Res Rev*. 2013;12(1):376-390. doi:10.1016/j.arr.2012.10.004.
131. Li X, Fang P, Mai J, Choi ET, Wang H, Yang X. Targeting mitochondrial reactive oxygen species as novel therapy for inflammatory diseases and cancers. *J Hematol Oncol*. 2013;6(1):19. doi:10.1186/1756-8722-6-19.
132. Rathmell JC, Farkash E a, Gao W, Thompson CB. IL-7 enhances the survival and maintains the size of naive T cells. *J Immunol*. 2001;167(12):6869-6876. doi:10.4049/jimmunol.167.12.6869.
133. Tan JT, Dudl E, LeRoy E, et al. IL-7 is critical for homeostatic proliferation and survival of naive T cells. *Proc Natl Acad Sci U S A*. 2001;98(15):8732-8737. doi:10.1073/pnas.161126098.
134. Van der Pol E, Böing AN, Harrison P, Sturk A, Nieuwland R. Classification, functions, and clinical relevance of extracellular vesicles. *Pharmacol Rev*. 2012;64(3):676-705. doi:10.1124/pr.112.005983.
135. Escola JM, Kleijmeer MJ, Stoorvogel W, Griffith JM, Yoshie O, Geuze HJ. Selective enrichment of tetraspan proteins on the internal vesicles of multivesicular endosomes and on exosomes secreted by human B-lymphocytes. *J Biol Chem*. 1998;273(32):20121-20127. doi:10.1074/jbc.273.32.20121.
136. Bard MP, Hegmans JP, Hemmes A, et al. Proteomic analysis of exosomes isolated from human malignant pleural effusions. *Am J Respir Cell Mol Biol*. 2004;31(1):114-121. doi:10.1165/rcmb.2003-0238OC.
137. Chen F, Zhuang X, Lin L, et al. New horizons in tumor microenvironment biology: challenges and opportunities. *BMC Med*. 2015;13(1). doi:10.1186/s12916-015-0278-7.

138. Mehlen P, Puisieux A. Metastasis: a question of life or death. *Nat Rev Cancer*. 2006;6(6):449-458. doi:10.1038/nrc1886.
139. Podgrabinska S, Skobe M. Role of lymphatic vasculature in regional and distant metastases. *Microvasc Res*. 2014;95:46-52. doi:10.1016/j.mvr.2014.07.004.
140. Hayes SC, Janda M, Cornish B, Battistutta D, Newman B. Lymphedema after breast cancer: Incidence, risk factors, and effect on upper body function. *J Clin Oncol*. 2008;26(21):3536-3542. doi:10.1200/JCO.2007.14.4899.
141. Lee JH, Torisu-itakara H, Cochran AJ, et al. Quantitative Analysis of Melanoma-Induced Cytokine-Mediated Immunosuppression in Melanoma Sentinel Nodes. 2005;11:107-112.
142. Swann JB, Smyth MJ. Immune surveillance of tumors. *J Clin Invest*. 2007;117(5):1137-1146. doi:10.1172/JCI31405.antigens.
143. Agarwal ML, Agarwal a, Taylor WR, Stark GR. p53 controls both the G2/M and the G1 cell cycle checkpoints and mediates reversible growth arrest in human fibroblasts. *Proc Natl Acad Sci U S A*. 1995;92(18):8493-8497. doi:10.1073/pnas.92.18.8493.
144. Sever P. Transforming growth factor-b1-mediated collagen gel contraction by cardiac fibroblasts. *J Hypertens*. 2006;(June):8-10. doi:10.3317/jraas.2008.002.
145. Fletcher AL, Acton SE, Knoblich K. Lymph node fibroblastic reticular cells in health and disease. *Nat Rev Immunol*. 2015. doi:10.1038/nri3846.
146. Psaila B, Lyden D. The metastatic niche: adapting the foreign soil. *Nat Rev Cancer*. 2009;9(4):285-293. doi:10.1038/nrc2621.
147. Kaplan RN, Riba RD, Zacharoulis S, et al. VEGFR1-positive haematopoietic bone marrow progenitors initiate the pre-metastatic niche. *Nature*. 2005;438(7069):820-827. doi:10.1038/nature04186.
148. Hiratsuka S, Watanabe A, Aburatani H, Maru Y. Tumour-mediated upregulation of chemoattractants and recruitment of myeloid cells predetermines lung metastasis. *Nat Cell Biol*. 2006;8(12):1369-1375. doi:10.1038/ncb1507.
149. Eguchi H, Horikoshi T. The expression of integrin alpha 2 beta 1 and attachment to type I collagen of melanoma cells are preferentially induced by tumour promoter, TPA (12-O-tetradecanoyl phorbol-13-acetate). *Br J Dermatol*. 1996;134(1):33-39. doi:10.1046/j.1365-2133.1996.d01-749.x.

150. Alcaraz J, Xu R, Mori H, et al. Laminin and biomimetic extracellular elasticity enhance functional differentiation in mammary epithelia. *EMBO J*. 2008;27(21):2829-2838. doi:10.1038/emboj.2008.206.
151. Roozendaal R, Mebius RE, Kraal G. The conduit system of the lymph node. *Int Immunol*. 2008;20(12):1483-1487. doi:10.1093/intimm/dxn110.
152. Sixt M, Kanazawa N, Selg M, et al. The conduit system transports soluble antigens from the afferent lymph to resident dendritic cells in the T cell area of the lymph node. *Immunity*. 2005;22(1):19-29. doi:10.1016/j.immuni.2004.11.013.
153. Gray EE, Cyster JG. Lymph Node Macrophages. 2013;4:424-436. doi:10.1159/000337007.Lymph.
154. Zarogoulidis P, Lampaki S, Yarmus L, et al. Interleukin-7 and Interleukin-15 for Cancer. *J Cancer*. 2014;5(9):765-773. doi:10.7150/jca.10471.
155. Morre M, Beq S. Interleukin-7 and immune reconstitution in cancer patients: A new paradigm for dramatically increasing overall survival. *Target Oncol*. 2012;7(1):55-68. doi:10.1007/s11523-012-0210-4.
156. Fritzell S, Eberstål S, Sandén E, Visse E, Darabi A, Siesjö P. IFN $\gamma$  in combination with IL-7 enhances immunotherapy in two rat glioma models. *J Neuroimmunol*. 2013;258(1-2):91-95. doi:10.1016/j.jneuroim.2013.02.017.
157. Onder L, Narang P, Scandella E, et al. Plenary paper IL-7 – producing stromal cells are critical for lymph node remodeling. *Blood*. 2012;120(24):4675-4683. doi:10.1182/blood-2012-03-416859.The.
158. Felcht M, Luck R, Schering A, et al. Angiopoietin-2 differentially regulates angiogenesis through TIE2 and integrin signaling. *J Clin Invest*. 2012;122(6):1991-2005. doi:10.1172/JCI58832.
159. Biggs R, Douglas a S, Macfarlane RG. The formation of thromboplastin in human blood. *J Physiol*. 1953;119(1):89-101.
160. Denhardt DT, Guo X. Osteopontin: a protein with diverse functions. *FASEB J*. 1993;7(15):1475-1482. doi:10.1016/S0378-4347(00)84195-X.
161. Gurbuz I, Chiquet-Ehrismann R. CCN4/WISP1 (WNT1 inducible signaling pathway protein 1): A focus on its role in cancer. *Int J Biochem Cell Biol*. 2015;62:142-146. doi:10.1016/j.biocel.2015.03.007.
162. Bach LA, Fu P, Yang Z. Insulin-like growth factor-binding protein-6 and cancer. *Clin Sci*. 2012;124(4):215-229. doi:10.1042/CS20120343.

163. Klein RM, Bernstein D, Higgins SP, Higgins CE, Higgins PJ. SERPINE1 expression discriminates site-specific metastasis in human melanoma. *Exp Dermatol*. 2012;21(7):551-554. doi:10.1111/j.1600-0625.2012.01523.x.
164. Hao NB, Lü MH, Fan YH, Cao YL, Zhang ZR, Yang SM. Macrophages in tumor microenvironments and the progression of tumors. *Clin Dev Immunol*. 2012;2012. doi:10.1155/2012/948098.
165. Noy R, Pollard JW. Tumor-Associated Macrophages: From Mechanisms to Therapy. *Immunity*. 2014;41(1):49-61. doi:10.1016/j.immuni.2014.06.010.
166. Pio R, Ajona D, Lambris JD. Complement inhibition: a promising concept for cancer treatment. *Changes*. 2012;29(6):997-1003. doi:10.1016/j.biotechadv.2011.08.021.Secreted.

## **7. Abbreviations**

ANOVA= Analysis of variance

ATP= Adenosine triphosphate

BAFF= B cell-activating factor

BEC= Blood endothelial cell

CAD11= Cadherin 11

CCL= Chemokine (C-C motif) ligand

CLEC-2= C-type lectin domain family 1 member B

CON= Control medium

DC= Dendritic cell

DMSO= Dimethyl sulfoxide

DNA= Deoxy ribonucleic acid

ECAR= Extracellular acidification rate

EGF=Epidermal growth factor

EMT= Epithelial mesenchymal transition

FACS= Fluorescence activated cell sorting

FBS= Foetal bovine serum

FDC= Follicular dendritic cells

FGF= Fibroblast growth factor

FRC= Fibroblastic reticular cell

GFP= Green fluorescent protein

HEV= High endothelial venule

IFN= Interferon

IGF= Insulin like growth factor

IGFBP= Insulin like growth factor binding protein

IL= Interleukin

ILC= Innate lymphoid cells

IS= Immune System

LEC= Lymphatic endothelial cell

LCMV= Lymphocytic choriomeningitis virus

MCM= Microenvironment conditioned medium

MDSC= Myeloid derived suppressor cell

OCR= Oxygen consumption rate

PBS= Phosphate buffered saline  
PCR= Polymerase chain reaction  
pDC= Plasmacytoid dendritic cell  
PDGFR= Platelet derived growth factor receptor  
PDPN= Podoplanin  
PLO= Primary lymphoid organ  
RNA= Ribonucleic acid  
ROS= Reactive oxygen species  
SD= Standard deviation  
SEM= Standard error of mean  
SLO= Secondary lymphoid organ  
SMA= Smooth muscle actin  
S1P= Sphingosine 1 phosphate  
TCM= Tumour conditioned medium  
TCR= T cell receptor  
TDLN= Tumour draining lymph node  
TGF= Transforming growth factor  
TLO= Tertiary lymphoid organ  
TMRM= Tetramethylrhodamine methyl ester  
Treg= Regulatory T cells  
VEGF= Vascular endothelial growth factor

## 8. Appendix

### 8.1 Primer sequences

Name	Sequence	Annealing Temp.
CD9 fw	5' GGGCGATCGCATGCCGGTCAAAGGAG	72 °C
CD9 rev	5' CCACGCGTGACCATTTCTCGGCTCCTGC	72 °C
CD63fw	5' GGGCGATCGCATGGCGGTGGAAGG	72 °C
CD63 rev	5' CCACGCGTCATTACTTCATAGCCACTTC	72 °C
CD81 fw	5' GGGCGATCGCATGGGGGTGGAGG	72 °C
CD81 rev	5' CCACGCGTGTACACGGAGCTGTTCCGGA	72 °C

### 8.2 Antibodies

#### 1.1.1 Immunofluorescence

Antigen	Supplier	Clone	Cat. Number	Conjugation	Species	Working Dilution
Podoplanin	eBiosciences	8.1.1	sc-23564	None	Hamster	1:100
VCAM-1	Biolegend	429	105702	None	Rat	1:100
Anti-rat Sec	Invitrogen	-	A-21470	Alexa Fluor 488	Chicken	1:300
Anti-ham Sec	Invitrogen	-	A-21451	Alexa Fluor 647	Goat	1:300
Col1	AbD serotec		2150-1410	None	rabbit	1:50

#### 1.1.2 Flow Cytometer

Antigen	Supplier	Clone	Cat. Number	Conjugation	Species	Working Dilution
AnnexinV	BD Pharmagen	-	556547	FITC	-	1:25
CD3ε	Biolegend	144-2C11	100205	PE	Hamster	1:300
CD11b	Biolegend	M1/70	101211	APC	Rat	1:300
CD31	eBioscience	MEC13.3	11-0311-81	FITC	Rat	1:300
CD44	eBioscience	IM7	47-0441-80	780	Rat	1:300
CD45	Biolegend	30-F11	103115	APC-Cy7	Rat	1:300
CD62L	Biolegend	Mel-14	104411	APC	Rat	1:300
Podoplanin	Biolegend	8.1.1	127409	APC	Hamster	1:300
VCAM	Biolegend	429	105705	FITC	Rat	1:300

### 1.1.3 Western Blotting

Antigen	Supplier	Clone	Cat. Number	Conjugation	Species	Working Dilution
Alpha-Tubulin	Sigma	B-5-1-2	T6074	none	mouse	1:2000
Interleukin 7	R&D systems	-	M7000	HRP	-	1:5
Cadherin 11	Invitrogen	WTID1	71-7600	none	rabbit	1:500
Beta-Catenin	Cell Signalling	D10A8	8480	none	rabbit	1:1000
Phospho-beta-catenin	Cell Signalling		9561	none	rabbit	1:1000
Col1α2	Santa Cruz		sc-8788	none	goat	1:500
N-Cadherin	R&D		AF6426	none	sheep	1:1000
α-SMA	Abcam		ab5694	none	rabbit	1:1000
Anti-rat	DAKO		P045001-8	HRP	rabbit	1:2000
Anti-mouse	DAKO		Z0420	HRP	goat	1:2000
Anti-rabbit	DAKO		Z0196	HRP	swine	1:2000
Anti-sheep	DAKO		P0163	HRP	rabbit	1:2000
Anti-goat	DAKO		E0466	HRP	rabbit	1:2000

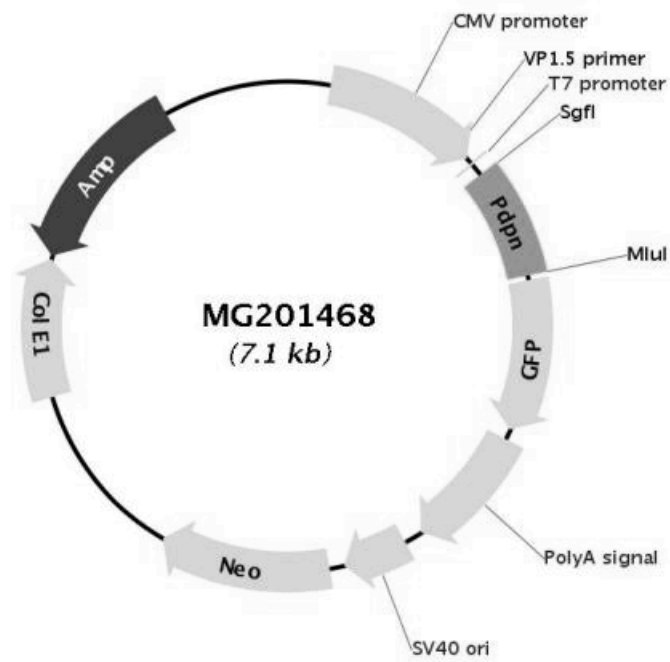
### 8.3 TaqMan Assays

Assay	Cat. Number	Dye
ActB	Mm00607939_s1	FAM
GAPDH	Mm99999915_g1	FAM
IL-7	Mm01295803_m1	FAM
PDPN	Mm01348912_g1	FAM

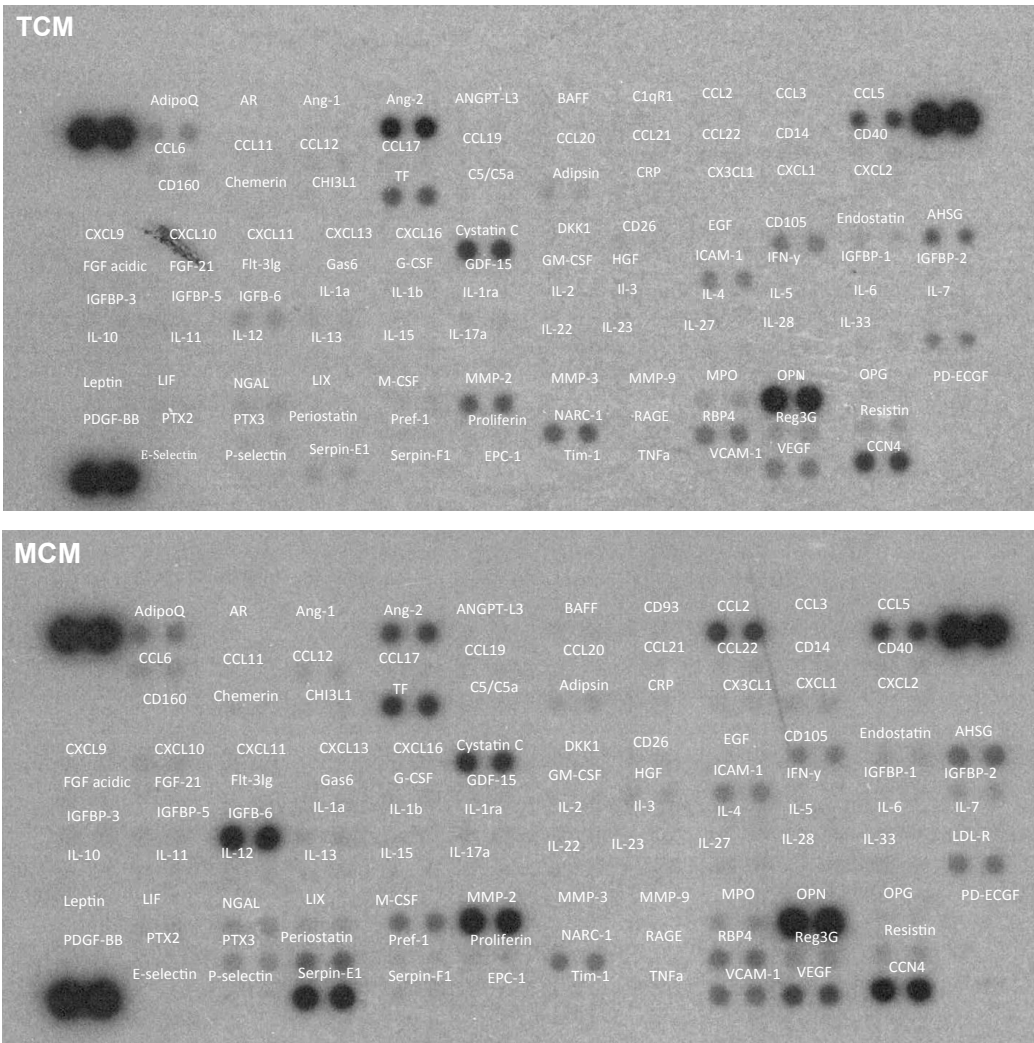


## 8.4 Plasmid Maps

### 8.4.1 Pdpn (BC026551) Mouse cDNA ORF Clone



8.5 Cytokine array





## 9. Curriculum Vitae

### Lisa Haas, BSc

#### Personal Information

---

**Birth Place:** Steyr, Austria  
**Nationality:** Austrian  
**Telephone:** +43/650 580 36 30  
**E-Mail:** haas.lisa@gmx.at

#### Education

---

**Since 10/2013:** MSc in Molecular Biology with emphasis on Molecular Medicine  
University of Vienna, Austria

**10/2010-06/2013:** BSc in Biology with emphasis on Microbiology and Genetics (graduated with honours)  
University of Vienna, Austria

**9/2002-6/2010:** Secondary school finished with Matura, graduated with honours  
BG Steyr Werndlpark, Austria

**9/1998-6/2002:** Primary school  
VS Steyr Tabor, Austria

#### Work experience

---

**1/2015-9/2015:** MSc Thesis in Dr. Jacqueline Shield's laboratory "The role of fibroblastic reticular cells in the tumour draining lymph node and their contribution to tumour progression"  
MRC Cancer Unit, Cambridge, United Kingdom

**9/2014-1/2015:** Research placement in Dr. Brian Ferguson's laboratory "The role of a previously uncharacterized protein in non-homologous end joining and the innate immune system"  
Department of Pathology, Cambridge, United Kingdom

**3/2014-4/2014:** Research internship in Prof. Johannes Huppa's group "Super resolution microscopy of the immunological synapse with emphasis on CD80 in mouse dendritic cells"  
Institute of Applied Immunology, Vienna, Austria

**10/2013-11/2013:** Research placement in Dipl. Ing. Dr. Hannes Stockinger's laboratory "Characterization of CD87 swap mutants carrying different GPI anchors in T lymphocytes"

Department of Molecular Immunology, Vienna, Austria

**6/2013 – 8/2013:** Research internship in Dr. Michael Nodine's group "Generation of pDRN transgenic Arabidopsis thaliana"

Gregor Mendel Institute, Vienna, Austria

**3/2013-5/2013:** BSc Thesis in Prof. Dieter Blaas' laboratory "Investigating early interaction between host cell and the Human Rhinovirus C"

Max F. Perutz Laboratories, Vienna, Austria

#### **Honours and awards**

---

**10/2013-9/2014:** Performance Scholarship for exceptional curricular achievements  
1<sup>st</sup> place in ranking for Molecular Biology  
University of Vienna, Austria

**10/2012- 9/2013:** Performance Scholarship for exceptional curricular achievements  
University of Vienna, Austria

**10/2011- 9/2012:** Performance Scholarship for exceptional curricular achievements  
University of Vienna, Austria

**10/2010- 9/2011:** Performance Scholarship for exceptional curricular achievements  
University of Vienna, Austria

#### **Skills**

---

**Laboratory skills:** Basic laboratory skills (Handling of chemicals, handling of micropipettes, aseptic techniques..), Cell culture techniques (human and murine cells), Retroviral and lentiviral infections, handling of different model systems (Arabidopsis Thaliana, C. elegans..), Cloning, RNA extractions, qRT-PCR, ELISA, Western Blot, Immunoprecipitation, Flow Cytometry, Immunohistochemistry, Light Microscopy, Confocal Imaging...

**IT skills:** Office, Graphpad, Photoshop, ImageJ, Volocity, FlowJo, FACSDiva, Leica Imaging Software, Zeiss Imaging Software

**Languages:** German (mother tongue), English (fluently), Spanish (basic knowledge), Italian (basic knowledge)

**Personal skills:** -Readiness to help others  
-Ability to decide calmly in stressful situations, deepened by a paramedical education

- Ambition and motivation
- High interest in scientific research
- Full commitment to science
- Willingness to support others in research, strengthened by teaching at immunology practical courses at the University of Cambridge
- Interest in foreign countries and cultures, reinforced by performing a master thesis in the United Kingdom
- Independence and self-confidence

**Additional skills:** Paramedical education

#### **Attended conferences**

---

- |                 |   |
|-----------------|---|
| <b>3/2015:</b>  | CRUK Symposium 2015: Unanswered Questions in Cancer and the Immune System |
| <b>10/2014:</b> | Symposium for Biology and Life Science Students 2014                      |
| <b>9/2014:</b>  | Cambridge Immunology Forum 2014: Immunometabolism                         |
| <b>10/2013:</b> | Platform for Advanced Cellular Therapies Symposium Vienna                 |